Diazotrophic behaviour in a non-sterile bioreactor: the effect of O_2-availability

Dissertation submission in the partial fulfilment of the requirements
for the degree of Magister Scientiae in Chemical Engineering

By Amber Yasemin Shirin de Zoete

Department of Chemical Engineering
Faculty of Engineering, the Built Environment, and Information Technology
University of Pretoria
Pretoria, South Africa

CVD800

2022-01-27

Diazotrophic behaviour in a non-sterile bioreactor: the effect of O_2-availability

Amber Yasemin Shirin de Zoete

Dissertation submission in the partial fulfilment of the requirements
for the degree of Magister Scientiae in Chemical Engineering

Department of Chemical Engineering
Faculty of Engineering, the Built Environment, and Information Technology
University of Pretoria
Pretoria, South Africa

Supervisor: Prof. Willie Nicol
Co-supervisor: Dr. Hendrik G. Brink

CVD800

2022-01-27

Declaration

I, Amber Yasemin Shirin de Zoete, do hereby declare that this research is my own, unassisted work. In addition, I declare that all references have been acknowledged. Lastly, I declare that to the best of my knowledge this dissertation has not been submitted, in its entirety or in parts, to other universities or similar institution for the purpose of examination.

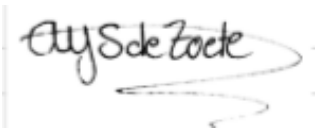

Candidate signature

Signed on the 6^{th} of December, 2021 in Silver Lakes, Pretoria

Abstract

Current agricultural practices have proven unsustainable due to high reliance on chemical fertilizers. Several environmental problems such as leaching of nitrogen into water bodies and the release of NOx gasses emerge from conventional agriculture. This poses a threat to human health and the environment. Thus, there is a need to develop alternative technologies to safeguard food production in the future. The use of diazotrophic bacteria was identified as a promising route as these bacteria could aid in the nitrogen supply of crops through biological nitrogen fixation. Therefore, the behaviour of a locally isolated diazotrophic consortium was investigated with the prospect of agricultural applications in a non-sterile environment.

The behaviour of the consortium was mapped through batch experiments. Concentration profiles of the suspended biomass were obtained through spectrometry, and carbon-compound and nitrogen-compound analyses were employed. The oxygen supply to the reactor was varied to investigate the energy effect of oxygen availability. Mass-transfer limited growth was attained under all aeration conditions. In addition, metagenomic analysis was completed through next-generation sequencing to identify the dominant species in the consortium. Lastly, mass and energy balances were performed to explore mechanisms that could explain the observed behaviour.

A repeatable culture, from a process point-of-view, was obtained in a non-sterile bioreactor. Metagenomic analysis indicated *Chryseobacterium* ssp. and *Flavobacterium* ssp. were the dominant species, making up approximately 50 % of the microbial community. For each aeration condition, negligible amounts of aqueous metabolites were formed indicating a high selectivity towards biomass production. High oxygen availability resulted in decreased growth efficiencies i.e. the specific energy requirements for biomass synthesis. This was attributed to reduced electron transport chain efficiencies and nitrogenase protection mechanisms. The most efficient growth was measured at an aeration feed composition of 21 % oxygen and 79 % nitrogen. This is consistent with atmospheric conditions. An average yield of 0.20 g/g for biomass synthesis was obtained at this condition with a productivity of 6.03 mg/L.h. For all conditions, the mass and energy balances indicated that sessile biomass with a high C:N served as a carbon sink.

The study presents one of the only known investigations of operational conditions on diazotrophic growth in a non-sterile bioreactor. In addition, it provides a strong foundation for the development of a Biological Nitrogen Fixation process with scaling potential.

Acknowledgements

The author would like to thank:

- Prof W. Nicol for his guidance throughout this research and for his encouragement and support during the course of the work.
- Dr H.G. Brink for his insights during research discussions and his contribution to the research through interpretation of results and valuable advice among others.
- My fellow student, Joshua Beukes, for his hard work and assistance in the laboratory.
- My research group members at the University of Pretoria for challenging my ideas and asking questions.
- My family for their encouragement and support.
- The Devroop family for their support and for providing a safe place to stay when working late nights in the laboratory.
- Lastly, I would like to thank my fellow engineer and soulmate, Devesh, for his advise, mental support, and assistance with electronics.

Publication of work

The author has already published the major findings of the study in a peer-reviewed journal. The following link redirects the reader to the paper: de Zoete, A.Y.S., Brink, H.G., Beukes, J.C. van Rooyen, I.L. and Nicol, W. (2021) "Diazotrophic Behaviour in a Non-Sterile Bioreactor: The Effect of O2-Availability" *Processes, 9*, (11): 2039. https://doi.org/10.3390/pr9112039

Contents

1 Introduction **1**

2 Literature **3**

2.1 The nitrogen cycle . . . 3

2.2 Modern agriculture and nitrogen pollution . . . 4

2.3 State-of-the-art agriculture: hydroponics . . . 5

2.4 Identification of the research gap . . . 5

2.5 Diazotrophs . . . 6

2.5.1 Environmental factors - O_2 availability . . . 9

2.5.2 Environmental factors - C availability . . . 9

2.5.3 Environmental factors - N_2 availability . . . 10

2.5.4 Environmental factors - other . . . 10

2.5.5 Nitrogen fixation rates . . . 10

2.6 Previously studied diazotrophs - pure culture experiments . . . 11

2.6.1 Trichodesmium IMS101 . . . 12

2.6.2 Azotobacter . . . 12

2.6.3 Azospirillium brasilense . . . 13

2.7 Byproduct formation . . . 13

2.8 Biofilm formation . . . 13

2.9 Applications of diazotrophic cultures . . . 14

2.9.1 Bio-augmentation . . . 14

2.9.2 Bio-fertilizer . . . 14

2.9.3 Lignocellulose breakdown . . . 15

2.9.4 Land reclamation . . . 15

2.9.5 Effluent treatment . . . 15

2.9.6 Bioelectrochemical nitrogen fixation . . . 16

3 Experimental **16**

3.1 Materials . . . 16

3.2 Equipment . . . 17

3.2.1 Reactor setup . . . 17

3.2.2 Monitoring and control system . . . 18

3.2.3 Analysis . . . 18

3.2.4 Statistical Analysis . . . 19

3.3 Operating procedure . . . 20

3.3.1 Inoculum procurement and development . . . 20

3.3.2 Experimental runs . . . 20

3.3.3 Mass-transfer experiments . . . 21

4 Results and discussion **21**

4.1 Mass-transfer properties of the experimental setup . . . 21

4.2 Aeration with atmospheric air . . . 22

4.2.1 Dissolved oxygen and pH control . . . 22

4.2.2 Concentration profiles . . . 24

4.3 Aeration with oxygen-rich air . . . 25

4.3.1 Dissolved oxygen and pH control . . . 25

4.3.2 Concentration profiles . . . 27

4.4 Aeration with oxygen-poor air . . . 28

4.4.1 Dissolved oxygen and pH control . . . 28

4.4.2 Concentration profiles . . . 29

4.4.3 Comparison of conditions . . . 31

4.5 Culture properties . . . 33

4.5.1 C:N ratio . . . 33

4.5.2 Next-generation DNA sequencing results . . . 35

5 Modelling **38**

5.1 Mass balance 38

5.1.1 Approach 1: Biofilm as a carbon-sink 38

5.1.2 Approach 2: PHB as a carbon-sink 39

5.1.3 Comparison between approaches 40

5.2 Energy balance 41

5.3 Model limitations and intention 43

6 Conclusion and recommendations **44**

A Appendix A: Test kit and instrument calibration **A.52**

B Appendix B: Carbon analysis verification **B.53**

B.1 HPLC analysis B.54

B.2 TOC analysis C.55

B.3 Conclusion C.55

C Appendix C: ngDNA sequencing reports **C.55**

List of Figures

1 Nitrogen cycle . . . 3

2 Main keywords in bibliometric data . . . 7

3 Chronological bibliometric data map . . . 8

4 Experimental setup . . . 17

5 Mass-transfer coefficient data . . . 22

6 Filtered dissolved oxygen data at condition O2_21 . . . 23

7 Time-shifted dissolved oxygen data at condition O2_21 . . . 23

8 Raw pH data indicates sufficiently tight pH control . . . 23

9 Cumulative base addition at condition O2_21 . . . 23

10 Growth curve at condition O2_21 . . . 25

11 Glucose profile at condition O2_21 . . . 25

12 Malic acid profile at condition O2_21 . . . 25

13 Filtered dissolved oxygen data at condition O2_35 . . . 26

14 Time-shifted dissolved oxygen data at condition O2_35 . . . 26

15 Raw pH data at condition O2_35 . . . 26

16 Base addition data at condition O2_35 . . . 26

17 Growth profile at condition O2_35 . . . 27

18 Glucose profile at condition O2_35 . . . 28

19 Malic acid profile at condition O2_35 . . . 28

20 Filtered dissolved oxygen data at condition O2_7 . . . 29

21 Time-shifted dissolved oxygen data at condition O2_7 . . . 29

22 pH data for condition O2_7 . . . 29

23 Base addition data for condition O2_7 . . . 29

24 Biomass concentration profiles at condition O2_7 . . . 30

25 Glucose trends at condition $O2_7$ . . . 31

26 Malic acid profiles at condition O2_7 . . . 31

27 Comparison of growth curves . . . 32

28 Cell-based glucose uptake rate comparison . . . 32

29 C:N ratio comparison . . . 35

30 Overview of species under condition O2_21 . . . 36

31 Overview of species under condition O2_35 . . . 36

32 Overview of species under condition O2_7 . . . 36

33 Oxygen uptake rate profiles at each condition . . . 42

A.34 Calibration curve for the ammonia test kit . . . A.52

A.35 Calibration curve for Brooks flow controller - Nitrogen . . . B.53

A.36 Calibration curve for Brooks flow controller - Oxygen . . . B.53

B.37 An exponential curve was fit against the HPLC measured data and the theoretical malic acid values. . . . B.54

List of Tables

1 Bibliometric data 6

2 N_2-fixation rates 11

3 Comparison of yields and maximum growth rates for various nitrogen-fixing bacteria 12

4 Summary of utilised aeration feed compositions. 21

5 Yield and productivity at condition O2_21 24

6 Yield and productivity at condition O2_35 28

7 Yield and productivity at condition O2_7 30

8 Yield and productivity comparison 32

9 NPOC data 33

10 Total nitrogen data 34

11 Estimated supernatent C:N 34

12 Bacterial species summary 37

13 Mass-balance approach 1: specifications 39

14 Mass-balance approach 1: results 39

15 Mass-balance approach 2: specifications 40

16 Mass-balance approach 2: results 40

17 Modelled P/O-ratios 43

18 Result comparison of malic acid measuremensts B.54

19 TOC: malic acid calibration C.55

20 TOC: spiked malic acid results C.55

1 Introduction

Nitrogen is a crucial element to life on Earth as it forms a substantial part of amino acids which can be found in all living things (Pankievicz *et al*, 2019). Nitrogen's role in food production is vital as it is the most important nutrient for plant growth (Mahanty *et al*, 2018). Prior to industrialisation, nitrogen was supplied to the soil by nitrogen-fixing prokaryotes. The need for synthetic nitrogen arose from rapid population growth in the late nineteenth century. At the start of the twentieth century, the Haber-Bosch process was invented (OECD, 2018). This process allowed for synthetic nitrogen production under high temperatures and high pressure (Haber Transport, 2018). This led to an exponential increase in fertilizer availability and thus, food production. Anthropogenic activity has, however, caused the nitrogen input to the environment to double over the last century, which has resulted in an imbalance in the nitrogen cycle (OECD, 2018). The addition of synthetic nitrogen to crops has led to leaching of nitrogen into groundwater, rivers, lakes, and estuarine zones. This has offset hydrospheric nitrogen which results in phenomena such as aquatic biodiversity loss and eutrophication. Nitrogen pollution in soil results in reduced soil fertility and increased salinity among others (Mahanty *et al*, 2018). In addition, the release of nitrogen as nitrous oxides has a detrimental effect on our climate due to their high global warming potential (OECD, 2018).

Population growth and urbanisation have been catalysed in the past decade by the rapid industrialisation of developing countries and technological advancements. Population Action International (2011) predicts a 200 % population increase with reference to 2011 by 2050. Since economic growth is proportional to food demand, food security is one of the main challenges of the future (Hester & Harrison, 2012). The challenge lies mostly in the developing countries as they are expected to experience the largest growth (Hester & Harrison, 2012). These regions face the additional challenge of inferior infrastructure for transportation and storage which makes them more susceptible to food scarcity (Pankievicz *et al*, 2019). Therefore, it is of paramount importance to develop sustainable agricultural systems that can be implemented locally. To accommodate the rapid population growth, crop production should exponentially increase (Kozai, Niu & Takagaki, 2015). This implies a steep increase in fertilizer usage.

Furthermore, the need for arable land poses a threat to food security (Hester & Harrison, 2012). Deforestation and desertification are major environmental issues arising from modern agriculture (Kozai *et al*, 2015). There are two main solutions to this problem: increased productivity of existing farming land or reduction of land usage through vertical farming (Kozai *et al*, 2015). Vertical farming through hydroponic crop cultivation is a promising method of safeguarding food security in the future when arable land is of concern as it allows crops to be grown at the source of the food demand (Kozai *et al*, 2015). This would result in more efficient use of land and decreased transportation costs. The downsides of hydroponic systems are their equipment costs and their dependence on fertilizers, which generate a nutrient-dense effluent (Kumar & Cho, 2014). Thus, alternative "green" fertilizers for hydroponic systems to reduce pollution are imperative for this solution to be sustainable.

There is a need to reevaluate current agricultural practices, soilless and conventional, and to consider a more sustainable approach. The development of a green, effective nitrogen-source which supports the natural nitrogen cycle and minimally disturbes the microbial community is essential. Biological nitrogen fixation (BNF) might be the solution. BNF is the process in which nitrogenase-bearing prokaryotes reduce atmospheric nitrogen to a more bio-available form of nitrogen (Oelze, 2000). These nitrogenase-containing prokaryotes

naturally occur in soil and accounted for 58 million tonnes of nitrogen per year prior to industrialisation (OECD, 2018). The free-living variety of nitrogen-fixers are called diazotrophs (Mahanty *et al*, 2018). Diazotrophs show much promise in aiding the development of sustainable agriculture, as they could live in a mutually beneficial relationship with crops. This relationship is set up such that diazotrophs provide plants with nitrogen, while consuming plant exudates as their carbon-source (Pankievicz *et al*, 2019). In addition, these microbial communities release several plant-growth hormones, aid in nutrient cycling, and combat pathogens. Thus, utilising naturally occurring diazotrophs as bio-fertilizer for crops could significantly ameliorate soil fertility and plant growth Mahanty *et al* (2018). Bio-fertilizers are already in use, however, there is a need for improved formulations for commercialisation. Several desirable characteristics, including: easily adjustable pH and nutrient addition, non-toxic, simple application, and biodegradable, were described by Mahanty *et al* (2018). Liquid bio-fertilizers from a diazotrophic culture broth could be the solution to this need as culture broths are measurable and controllable. In addition, they are easy to apply and compatible with agricultural machinery Mahanty *et al* (2018). This study investigated a consortium in non-sterile conditions to facilitate more realistic soil microbial interactions as compared to pure culture studies. The cultivation of a diazotrophic consortium in a liquid medium allowed for the mapping of its behaviour in terms of concentration profiles and the evaluation of its energy response to varying environmental conditions. A system was envisioned where independent bio-reactors supply biofertilizer to crops, soil or soilless. The benefit of this separation is the measurability and control of the microbial community.

This study aimed to investigate the behaviour of a non-sterile diazotrophic consortium with the prospect agricultural applications. The main objectives of the investigation were: to obtain a repeatable, non-sterile diazotrophic culture; to study the behaviour of the consortium under various aeration conditions; and to investigate the energy effect of varying aeration conditions on the microbial culture. The study presents one of the only known investigations of operational conditions on diazotrophic growth in a non-sterile bioreactor. In addition, it provides a strong foundation for the development of a Biological Nitrogen Fixation process with scaling potential.

The growth behaviour of the microbial culture was studied through biomass quantification. Nitrogen-lean soil samples were collected and used for inoculum extraction. A bench-scale reactor with a high gas-liquid mass transfer efficiency was constructed and commissioned. A monitoring and control system was implemented with continuous pH and dissolved oxygen data collection. This was supplemented with periodic absorbance readings, carbon-compound analyses, total nitrogen measurements, and organic acid analyses. Lastly, next-generation DNA sequencing was performed to determine the active species in the consortium. Two modelling approaches were used to investigate the energy effect of varying experimental conditions. These models were applied in an exploratory manner and not considered definitive. This study investigated the consortium in non-sterile conditions to mimic a natural soil environment. Thus, exact metabolic pathways were not determined due to the complexity of the consortium. The carbon feed consisted of glucose as it is a simple model compound and would be suitable to determine the potential for nitrogen fixation.

2 Literature

The following section serves to inform the reader about previously conducted studies in the field of diazotrophs, as well as, the existing understanding of diazotrophs in terms of their metabolism and growth behaviour under various conditions. A brief overview of their current application was also included.

2.1 The nitrogen cycle

Nitrogen is an essential compound to sustain life. It plays a vital part in physiological and metabolic processes. Nitrogen constitutes amino acids and DNA in all living organisms (BYJU's, 2021). The largest nitrogen reserve is in the atmosphere, however, this nitrogen is not directly bio-available to all life forms (Kuypers, Marchant & Kartal, 2018). Atmospheric nitrogen, therefore, undergoes a series of reactions to become more bio-available. This series of reactions is called the nitrogen cycle. The nitrogen-cycling process constitutes fourteen reactions which affect the oxidation state of nitrogen.

According to G Gupta *et al* (2012), nitrogen is the most limiting growth factor for plants. The fixation and conversion of atmospheric nitrogen to ammonia, nitrates, and nitrites is required to provide plants with sufficient nitrogen. The fixation step (Equation 1) entails the conversion of atmospheric di-nitrogen to ammonia. Nitrogen fixation is facilitated by prokaryotic and archaic organisms, called diazotrophs, with the aid of the nitrogenase enzyme. This nitrogenase enzyme reduces nitrogen gas over one of three metals: vanadium, iron, or molybdenum (G Gupta *et al*, 2012). The conversion step (nitrification) facilitates the oxidation of ammonia to nitrites and nitrates (Equation 2 and 3). These nitrogen-containing compounds are more easily assimilated by plants (Kuypers *et al*, 2018). To complete the cycle, nitrogen is released into the atmosphere again by denitrification (Equation 4). Figure 1 shows a summary of the nitrogen cycle.

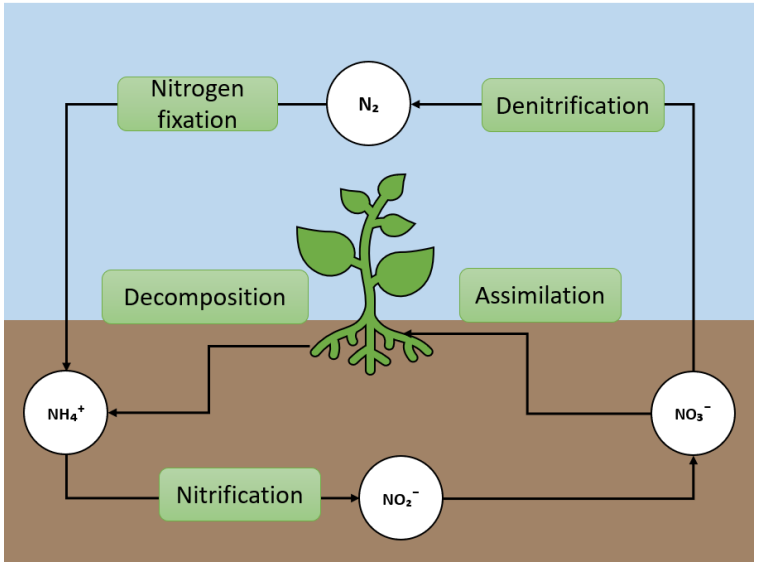

Figure 1: The nitrogen cycle consists of three major steps: nitrogen fixation, nitrification, and denitrification

$$N_2(g) + 8H^+ + 8e^- \rightarrow 2NH_3(g) + H_2(g) \quad (1)$$

$$NH_4^+ + 1.5O_2(g) \rightarrow NO_2^- + 2H^+(g) + H_2O(l) \quad (2)$$

$$NO_2^- + 0.5O_2(g) \rightarrow NO_3^- \quad (3)$$

$$NO_3^- \rightarrow NO_2^- \rightarrow NO \rightarrow N_2O \rightarrow N_2 \quad (4)$$

2.2 Modern agriculture and nitrogen pollution

OECD (2018) stated that the rapid population growth in the late nineteenth century gave rise to the need for industrialised nitrogen fixation. This led to the invention of nitrogen-fixing processes in the early twentieth century. The Haber-Bosch process for synthetic nitrogen production became the most prevalent in modern agriculture. Nowadays, 450 million tonnes of nitrogen fertilizer are produced through this process each year (Haber Transport, 2018). Even though synthetic nitrogen has enabled an exponential increase in crop production, the Haber-Bosch process has two major drawbacks. Firstly, the process is energy-intensive as it relies on fossil fuels (1 % - 2 % of world's annual energy supply) (Haber Transport, 2018) and secondly, it has a negative impact on the environment (Kuypers *et al*, 2018) as it contributes to greenhouse gas emissions. Altieri & Nicholls (2012) claim that 25 % - 30 % of greenhouse gas emissions arise from agriculture.

The application of synthetic fertilizer also has detrimental effects on the environment. The addition of synthetic nitrogen to crops has led to leaching of nitrogen into groundwater, rivers, lakes, and estuarine zones. This has created an offset in hydrospheric nitrogen which results in phenomena such as aquatic biodiversity loss and eutrophication (Mahanty *et al*, 2018). OECD (2018) claims that nitrate release into groundwater poses a direct health concern for humans and animals alike. In addition, the release of nitrogen as nitrous oxides has a detrimental effect on the global climate due to its high global warming potential. Nitrous oxides also have a direct effect on human health by increasing the likelihood of respiratory disease. Furthermore, release of N_2O into the atmosphere exacerbates the depletion of the ozone layer (OECD, 2018). Since the invention of artificial nitrogen fixation, 413 million tonnes of nitrogen have been fixed each year, where pre-industrial nitrogen fixation accounted for only 58 million tonnes of nitrogen per year. Thus, anthropogenic nitrogen fixation has caused an imbalance in the natural nitrogen cycle (OECD, 2018). Therefore, the Academy of Engineers has deemed nitrogen-cycle management as a pressing challenge for engineers in the near future (Pappu *et al*, 2017).

According to Altieri & Nicholls (2012), modern agriculture is heavily dependent on fertilizers, pesticides, and fossil fuels. As environmental damage and climate change are predicted to pose an increasingly large threat to food security, an alternative method of fertilizing plants should be explored (Mahanty *et al*, 2018). Sustainable ecosystems which benefit from naturally occurring processes are being explored to increase agricultural viability in the future (Altieri & Nicholls, 2012). A myriad of alternatives to modern agricultural

setups is available. These include: polycultures, crop rotations, and agroforestry (Altieri & Nicholls, 2012). Nevertheless, the need for arable land poses an additional threat to food security. Deforestation and desertification are major environmental issues arising from modern agriculture. Besides, logistical difficulties often result in large food wastes. A possible solution to safeguard future food production is soilless agriculture.

2.3 State-of-the-art agriculture: hydroponics

Hydroponics are a form of soilless agriculture which use aqueous solutions as the growth medium. Hydroponics allow crops to be grown vertically and at the source of food demand, which results in more efficient use of land and decreased transportation costs. The few disadvantages of hydroponics include rapid disease transmission between plants, high capital investment (Dreschel, 2018), and nitrogen-rich waste streams. On the other hand, due to its liquid medium, the system is much more controllable and waste stream compositions can be measured. According to Dreschel (2018), hydroponic systems reduce abiotic stress caused by pH and nutrients. In addition, hydroponic systems allow for a deeper understanding of plant-nutrient exchange and favourable plant growth conditions. Lastly, hydroponic systems are suitable for localized agriculture in developing countries and less season dependent.

This project focused on a non-sterile bio-reactor which yielded an aqueous product. If the aqueous state would be maintained during subsequent processing steps, the use of this product in hydroponics could bypass the use of soil throughout the food production process.

2.4 Identification of the research gap

A literature search was completed in three major databases: Scopus, Web of Science, and Science Direct. Bibliometric data was collected in order to map out the main themes throughout literature relating to diazotrophs. Table 1 shows a disproportionately small amount of research focused on bioreactors in parallel with diazotrophs. Various research papers have been published on the use of diazotrophs to improve plant growth by inoculating plant roots, but little to no research has focused on development of large-scale processes. The behaviour of diazotrophic cultures in liquid bioreactors for agricultural applications was identified as a research gap. In addition, minimal research was done on diazotrophic cultures in bioreactors as opposed to pure cultures. Among the existing studies on cultured diazotrophs, little to no investigations of operational conditions on diazotrophic growth in a non-sterile bioreactor were presented.

Bibliometric mapping was completed using the software tool VosViewer using a bibliometric database from Web of Science. Figure 2 shows the main keywords linking to diazotrophs throughout papers. The bulk of papers focused on the ability of bacteria to fixate nitrogen, the effect of nitrogen on plants, and microbial diversity. Keywords such as biofertilizer and bioreactor were not mapped out which confirmed the lack of research in these fields. The chronology of bibliometric data is shown in Figure 3. It is clear that most papers were published before 2010 and there is a lack of recent research in this field.

Table 1: Bibliometric data (04/07/2021) shows a fairly low amount of research has focused on the cultivation of diazotrophs in bioreactors.

Keywords		Scopus		Web of Science		Science Direct		Average
		#	(%)	#	(%)	#	(%)	(%)
Diazotrophs		1428	100.00	1401	100.00	2074	100.00	100.00
Diazotrophs	free-living	552	38.66	141	10.06	858	41.37	30.03
Diazotrophs	aerobic	271	18.98	38	2.71	674	32.50	18.06
Diazotrophs	batch	80	5.60	10	0.71	265	12.78	6.36
Diazotrophs	bio-fertilizer	16	1.12	7	0.50	214	10.32	3.98
Diazotrophs	bioreactor	25	1.75	2	0.14	95	4.58	2.16
Diazotrophs	chemostat	19	1.33	2	0.14	62	2.99	1.49
Bioreactor		90865	100.00	41397	100.00	79249	100.00	100.00
Bioreactor	fertilizer	2381	2.62	189	0.46	5652	7.13	3.40
Bioreactor	nitrogen fixation	1207	1.33	47	0.11	3719	4.69	2.04

2.5 Diazotrophs

The classification of diazotrophs is determined by their relationship with plants and consists of three categories: symbiotic, rhizospheric, and free-living (Wang *et al*, 2017). Rhizospheric microbes inhabit the soil region near plant roots by forming nodule-like structures. These structures are referred to as rhizospheres and act as a barrier against environmental stresses. This category of microbes has been studied thoroughly as these microbes are ubiquitous and highly adaptable (Wang *et al*, 2017). To intrude the intracellular space of the plant, the rhizospheric microbes infect the root hairs of the plant by excreting a signal molecule, the Nod factor. The plant distinguishes between pathogens and nitrogen-fixers through the analysis of the Nod factor and the extracellular polymeric substances (EPS) of the microbes (Terpolilli, Hood & Poole, 2012). Symbiotic diazotrophs refer to microbes that live in symbiosis with a plant, but do not necessarily nodulate in their roots. These species provide nitrogen for the plant, while the plant provides a carbon source for the microbes. Free-living diazotrophs can be autotrophic or heterotrophic and do not require a symbiotic relationship to survive. These bacteria could, therefore, theoretically, be cultured in a bioreactor. Examples of free-living diazotrophs are *Azotobacter* ssp. and *Cyanobacteria* ssp.. Recent studies on free-living diazotrophs focused on non-cyanobacterial biomass from pelagic waters as it grows in diverse environments. However, according to Bentzon-Tilia *et al* (2014), there is still a lack of research regarding cultivated aquatic diazotrophs. This might be due to the large range of conditions in which these organisms are able to survive and thus, the many variables that come in play when determining reactor conditions (Smercina *et al*, 2019). Several studies have been completed on aerobic diazotrophs, *Azotobacter* ssp., to study their growth curves in liquid, pure cultures. In these studies, wild type and genetically modified microbes were compared in their ammonia excretion ability (Bali *et al*, 1992; Barney *et al*, 2017; Brewin, Woodley & Drummond, 1999).

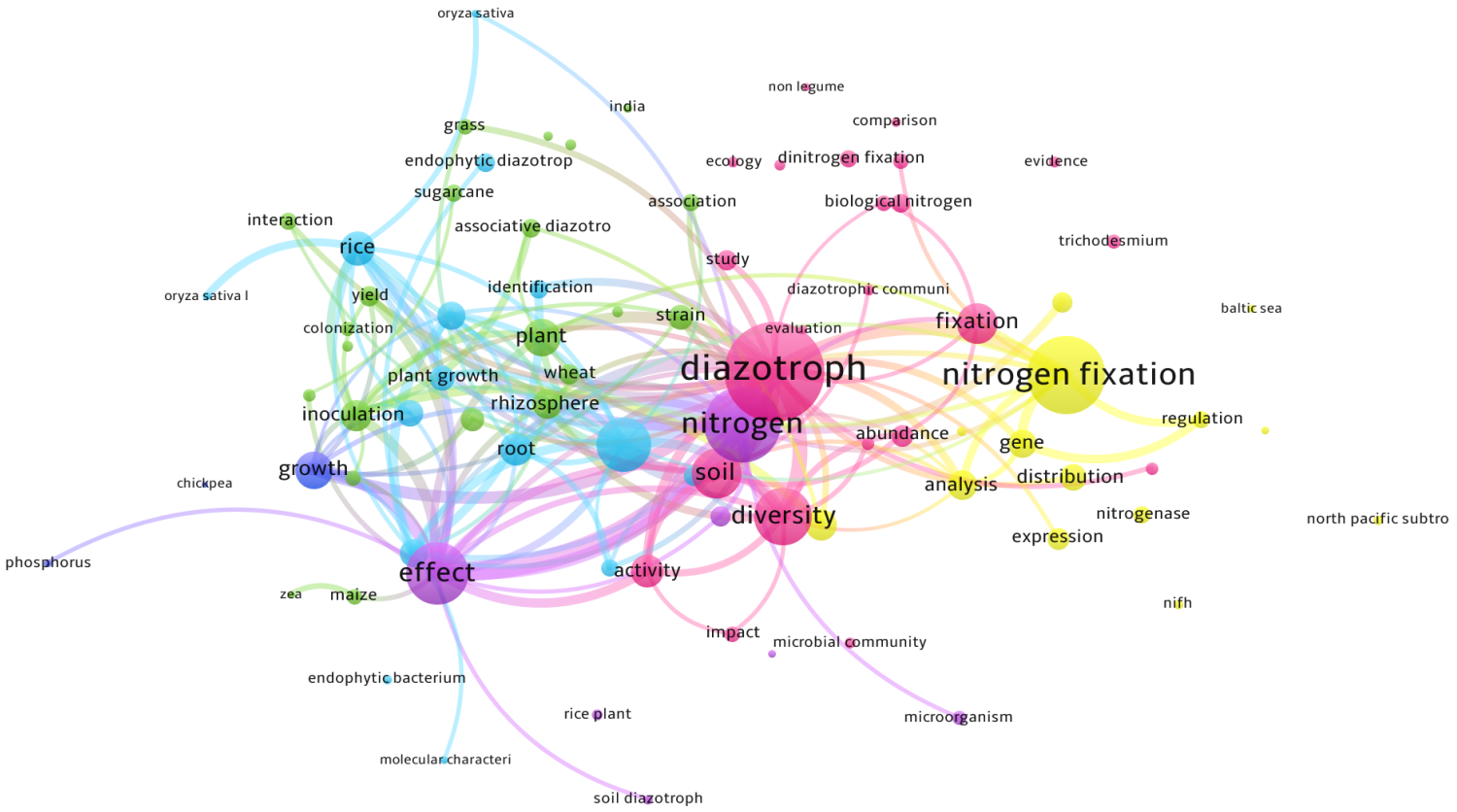

Figure 2: Bibliometric data was mapped to show the main keyword linkages. The overarching themes did not include bioreactor cultivation of diazotrophs or the use of diazotrophs for biofertilizer.

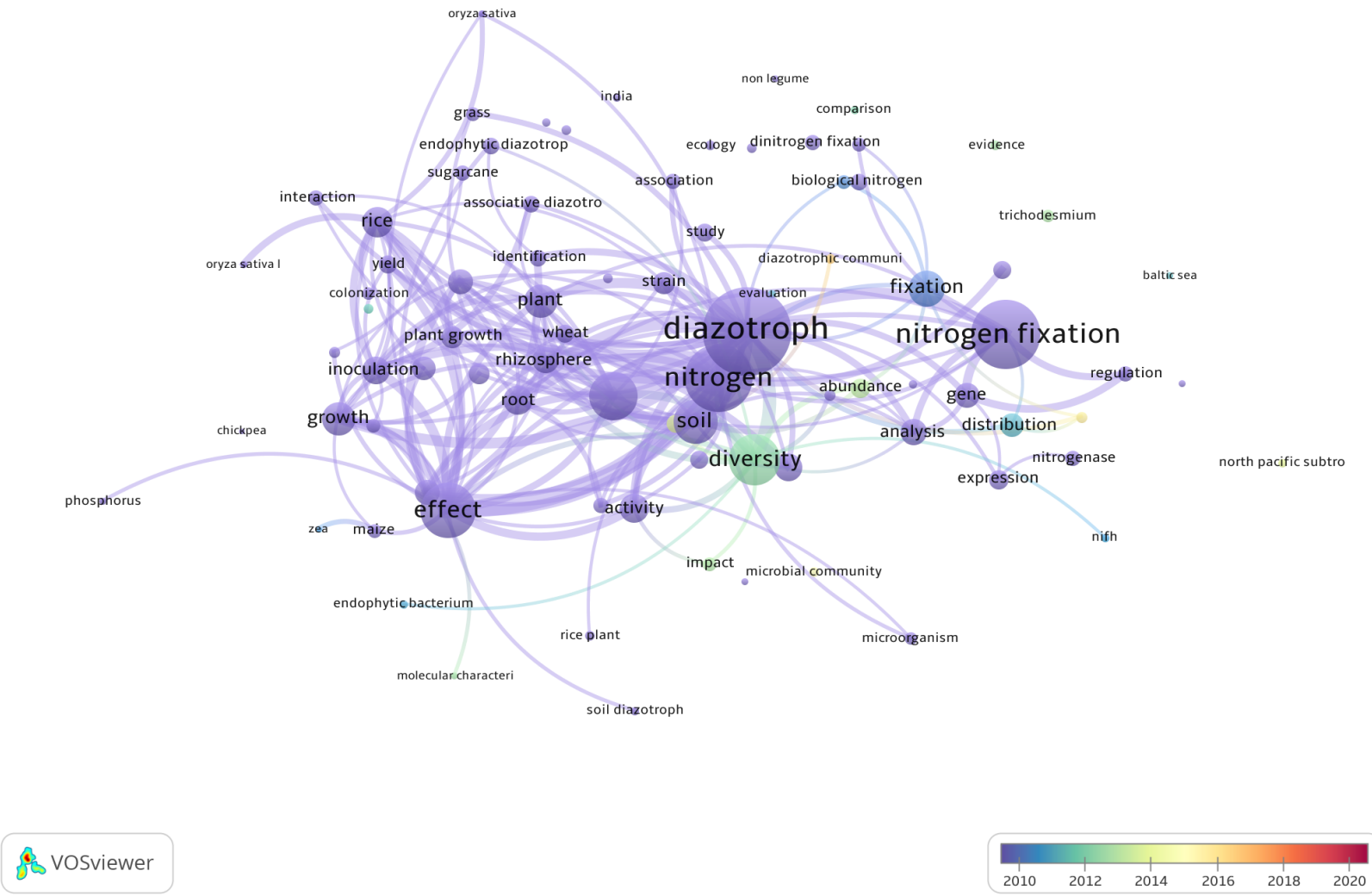

Figure 3: Bibliometric data was mapped chronologically and showed most research was performed before 2010.

2.5.1 Environmental factors - O_2 availability

Identification of nitrogen-fixing bacteria in the environment is performed by staining samples with the NifH gene-marker. This gene-marker indicates the presence of a nitrogenase enzyme. The nitrogenase enzyme facilitates nitrogen fixation and exists in three pairing variations: iron-iron, iron-vanadium, or iron-molybdenum. This enzyme is irreversibly deactivated by oxygen, thus aeration control is of paramount importance to diazotrophic growth (Kuypers *et al*, 2018). Protection against highly aerobic conditions is achieved in various ways. Rhizospheric species employ their EPS matrix to control oxygen concentrations (Wang *et al*, 2017), whereas other species, such as *Cyanobacteria*, use segmentation of photosynthesis and nitrogen fixation to maintain anaerobic conditions. This is done through the formation of heterocysts (Mahanty *et al*, 2018). According to Oelze (2000), the scavenging of oxygen at the peripheral cytoplasmic membrane level is a widely accepted nitrogenase protection mechanism hypothesis for free-living diazotrophs.

It was observed by Oelze (2000) that nitrogenase activity in *Azotobacter vinelandii* remained uncompromised up to dissolved oxygen concentrations of 7.36 mg/L oxygen. In addition, the oxygen consumption of the *A. vinelandii* was observed to largely exceed the energy requirements for growth if conventional electron transport chain (ETC) mechanisms were at play. A down-regulation mechanism of the ETC was proposed to prevent energy (ATP) build-up. The reduction of hydrogen-ions released during oxygen consumption would result in a smaller chemical gradient over the ATP complex. This would, in turn, result in less ATP produced per oxygen consumed. Thus, oxygen stress has a direct effect on the efficiency of oxidative phosphorylation.

According to Oelze (2000), ambient oxygen levels affect cellular respiration activity in aerobic diazotrophs such as *A. vinelandii*. The cellular respiration and thus, the oxygen consumption was found to be dependent on the C:N ratio of the microbial biomass. The C:N ratio, in turn, was affected by ambient oxygen. In addition, Oelze (2000) stated that the C:N ratio of diazotrophic biomass remained constant when a surplus of carbon was supplied and the excess carbon was either stored as poly-β-hydroxybutyrate (PHB) or dissimilated.

Arashida *et al* (2019) studied the effect of co-culturing purple non-sulfur bacteria (PNBS) with *Bacillus subtilis*. Under aerobic conditions, PNBS did not fix nitrogen in single culture. However, when they were co-cultured, nitrogenase was actively fixing nitrogen. This was probably due to a decrease in dissolved oxygen due to the *B. subtilis*. This implies that using consortia or co-cultures might be beneficial to the bacteria when mitigating nitrogenase inhibition due to oxygen.

2.5.2 Environmental factors - C availability

The availability of sufficient carbon is paramount to grow diazotrophs. In addition, the type of carbon source could influence growth rates significantly. Plant exudates contain a variety of low-molecular-weight carbon compounds. This is a natural carbon source for bacteria. Diazotroph cultures exposed to acetate have shown a complete deactivation of nitrogenase, whereas citrate was found to be able to both increase and reduce nitrogenase activity in autonomous studies (Smercina *et al*, 2019). Haury & Spillert (1981) investigated growth rates of a cyanobacteria, *Anabaena variabilis*, using different carbon substrates. Fructose showed the

fastest growth rate. After six days of growth, the optical density measurement of the fructose culture was ten-fold higher than that of sucrose. Oelze (2000) claims that the maximum growth rates of *A. vinelandii* were higher when malate and lactate were used as carbon sources than when glucose was used.

2.5.3 Environmental factors - N_2 availability

A nitrogen devoid liquid and solid environment, with sufficient nitrogen gas, is required to enable nitrogen fixation. This is due to the fact that the organisms are selective towards readily available nitrogen in the soil and therefore, do not fix nitrogen if sufficient nitrogen is already available. In addition, ammonia inhibits nitrogenase synthesis (Smercina *et al*, 2019). This implies that combined nitrogen in a bioreactor growth environment should ideally be removed (continuous reactor set-up).

2.5.4 Environmental factors - other

Other environmental factors, such as mineral availability, temperature, and photon flux, also affect nitrogenase activity. According to Iwata *et al* (2010), the presence of Mn^{+2}, Fe^{+2}, and Mo^{+2} is essential for ammonia accumulation in solution. In addition, slightly acidic and neutral conditions were shown to be most favourable for most diazotrophs. Evans *et al* (2000) investigated the effect of irradiance on Cyanobacteria strains from the Baltic Sea. It was found that nitrogenase activity was optimal during light periods (photon flux = 600 $\mu mol\ m^{-2}\ s^{-1}$) as opposed to darkness. However, photo-inhibition of nitrogenase was observed at a photon flux of 1000 μ mol $m^{-2}\ s^{-1}$. Hill, Patriquin & Sircom (1990) investigated the effect of temperature on nitrogenase activity. The hypothesis was that nitrogenase activity would be higher at elevated temperatures as this would increase respiration and therefore, decrease inhibition by oxygen. Experiments were performed under atmospheric oxygen conditions and temperatures were varied between 5 °C and 45 °C. The highest nitrogenase activity was measured between 24 °C and 27 °C.

2.5.5 Nitrogen fixation rates

Various field trials in the supplementation of plants with diazotrophic nitrogen have been performed. In addition, environmental conditions affecting nitrogen fixation rates have been studied. This has provided estimated nitrogen fixation rates for a few bacteria as shown in Table 2.

Table 2: N_2-fixation rates show a high variety depending on the species and conditions of cultivation.

Microbe	Conditions	N2-fixation rate	Reference
Cyanobacteria	Submerged rice paddy	2.83 - 4.28 nmol N/L d*	(Welz *et al*, 2018)
Azotobacter vinelandii	Bahiagrass	2.14 – 13.28 nmol N/L d*	(Welz *et al*, 2018)
	Culture	9300 nmol N/L	(Iwata *et al*, 2010)
Eustarine consortium	Sea water filtrate	1.70 nmol N /L d	(Pedersen *et al*, 2018)
	Enriched sea water	4.90 nmol N/L d	(Pedersen *et al*, 2018)
	Sediment addition	217 nmol N/L d	(Pedersen *et al*, 2018)
Pelagic consortium	Indian ocean	92.4 nmol N/L d	(McInnes *et al*, 2014)
Lysobacter	Culture	1800 nmol N/L d**	(Iwata *et al*, 2010)
Microaerophilic		1857 nnmol N/g C	(Smercina *et al*, 2019)
Anaerobic		786 nmol N/g C	(Smercina *et al*, 2019)
Aerobic		500 nmol N/g C	(Smercina *et al*, 2019)

* Units of nmol N/ha.d were converted to nmol N/L d by assuming the soil depth of the plot was 0.5 m.
** This value was calculated using the slope of an ammonia accumulation graph provided by the authors.

2.6 Previously studied diazotrophs - pure culture experiments

To investigate the physiological and growth parameters of diazotrophs, a substantial amount of pure culture experiments were performed over the past decades. These include batch runs (B) and continuous runs, with the aid of chemostats (C). Table 3 shows the yields (Y) and maximum growth rates (μ_{max}) for various pure cultures. The yields given by Brewin *et al* (1999), Barney *et al* (2017), and Bali *et al* (1992) were in terms of an optical density, these were converted using the assumption that Equation 5 and 6 hold. Other yields given in terms of optical density were converted with the assumption that for every 1.0 OD reading there was 0.5 g/L biomass (for any wavelength).

$$(cells/mL) = 4.9 \times 10^7 \times OD \tag{5}$$

$$(g/L) = 2.464 \times (cells/mL) + 0.023 \tag{6}$$

Table 3: Comparison of yields and maximum growth rates for various nitrogen-fixing bacteria

Culture	Set-up	T (°C)	pH	Medium	Y (g/g)	μ_{max} (h^{-1})	Reference
A. vinelandii	C	30	7	Burke	0.070	0.340	(Nagai, Nishizawa & Aiba, 1969)
	B	30	7.2	Burke	0.073	-	(Bali *et al*, 1992)
	B	30	7	Burke	0.299	-	(Brewin, Woodley & Drummond, 1999)
	B	30	7	Burke	0.337	-	(Barney *et al*, 2017)
	B	35	7	N-free	0.271	-	(Yu *et al*, n.d.)
A. beijerinckii	B	35	7	N-free	0.464	-	(Yu *et al*, n.d.)
A. brasilene	C	37	7	N-free	0.200	0.055	(Kloss, Imannek & Fendrick, 1983)
	C	30	7	Burke	-	0.035	(Cacciari *et al*, 1986)
	C	30-32	6.8	Azosp-1	-	1.790	(Romero-Perdomo *et al*, 2015)
T. erythraeum	C	26	7	N-free	-	0.028	(Holl & Montoya, 2008)
C. pasteurianum	B	30	7	N-lean	0.002	-	(Rice & Paul, 1971)

2.6.1 Trichodesmium IMS101

The diazotroph *Trichodesmium* IMS101 is an oligotrophic cyanobacterium. This species contributes largely to oceanic nitrogen-fixation. Holl & Montoya (2008) investigated this species in a batch set-up and a chemostat at 26 °C. The N_2-fixation rate during the batch run varied widely: it decreased as the biomass concentration increased; the fastest rates were during the early exponential stage. A possible explanation for this is the limitation of minerals and micro-nutrients. In a chemostat set-up, the maximum growth rate was estimated as 0.67 d^{-1}.

2.6.2 Azotobacter

The optimisation of growth conditions for *A. vinelandii* was described by Mukhtar *et al* (2018). Temperature, pH, and incubation time were optimized in batch experiments. A Burke's medium was utilised with different C-source and N-source additions. *A. vinelandii* was found to tolerate a wide range of pH (5-9), however, its growth was faster at a neutral pH. The optimal temperature was found to be 30 °C, where significantly lower growth rates occurred at temperatures past 35 °C. Manitol was found as the superior carbon source, whereas ammonium sulphate was the best performing nitrogen source. Nagai, Nishizawa & Aiba (1969) investigated *A. vinelandii* as a continuous culture under carbon-source limitation (initial glucose concentration: 5 g/L). A Burke's medium with a neutral pH was used. The experiments were run at 30 °C and the dilution rate varied between 0.1 - 0.3 h^{-1}. The reactor was sparged with air and the aeration rate was controlled tightly. The dissolved oxygen (DO) concentration was observed to decrease with an increasing growth rate. Higher yields were found under low oxygen-availability, this could point to oxygen-inhibition. The largest yield on glucose was found as 0.1 g/g at a dilution rate of 0.3 h^{-1}. Bali *et al* (1992) genetically modified a wild-type *A. vinelandii* and successfully altered its nitrogenase activity in the presence of ammonia, whereas Brewin *et al* (1999) investigated the effect of genetic manipulation on ammonia release. Barney *et al* (2017) also

looked at the ammonia excretion of *A. vinelandii* and found that higher ammonia yields might be achieved by increasing the molybdenum concentration in the standard Burke's solution.

2.6.3 Azospirillium brasilense

Kloss, Imannek & Fendrick (1983) investigated the growth parameters of *Azospirillium brasilense* in a chemostat using a neutral, nitrogen-free medium. Malic acid was used as the carbon source and the temperature was maintained at 37 °C. Dilution rates under 0.05 h^{-1} resulted in carbon limitation and the maximum growth rate was 0.055 h^{-1}. The maximum yield on malate was 0.2 g/g. Cacciari *et al* (1986) investigated *A. brasilense* at 30 °C at various dilution rates in a Burke's medium. The highest yield on glucose was found at 0.035 h^{-1}, which coincided with the highest N_2-fixing activity. The growth rate of *A. brasilense* is largely affected by pH and temperature. The fastest growth rate was observed at a pH of 6.8 by Romero-Perdomo *et al* (2015). A pH of 5.5 also yielded comparable results. However, a basic pH resulted in a significant drop in growth rate. The optimal temperature was between 30 °C - 32 °C. Sub-optimal temperatures were described to lower yield and have reduced plant-growth promoting substance production.

2.7 Byproduct formation

According to Cohen & Johnstone (1963), Azotobacter ssp. usually produce no acids. They oxidize their carbon source completely instead. There are, however, byproducts which are not organic acids. As mentioned in section 2.5.1, excess carbon supply to certain diazotrophs might result in the excretion of byproducts. The biopolymer, poly-β-hydroxybutyrate (PHB), is one such byproduct. According to Dedkova & Blatter (2014), prokaryotes produce PHB as a carbon energy storage when other nutrients are limited. The conversion of Acetyl-CoA to PHB requires NAD^+, however, no ATP is required. According to Díaz-Barrer *et al* (2016), nitrogen-limitation is a key factor in PHB accumulation for most bacterial species. Diazotrophs such as *Azotobacter* ssp., *Pseudomonas* ssp., *Brevundimonas* ssp., and *Azorhizophilus* ssp. are known PHB producers (Dedkova & Blatter, 2014; Prashad *et al*, 2001; Padilla-Córdova *et al*, 2020; Ali & Jamil, 2017; Kaminski *et al*, 1991; Jurat-Fuentes & Jackson, 2012; Naqqash *et al*, 2020; Bhuwal *et al*, 2013). Oxygen supply was deemed a bigger factor in PHB production in these species than nitrogen supply (Díaz-Barrer *et al*, 2016). Oxygen supply affects the NAD^+/NADH - ratio and thereby, carbon flux into the TCA-cycle is inhibited (lower oxygen levels) or promoted (higher oxygen levels). Carbon that does not enter the TCA-cycle results in PHB production (Díaz-Barrer *et al*, 2016).

2.8 Biofilm formation

Bacterial communities form biofilms in order to increase their resistance against environmental stress. Biofilms consist of a structure of bacteria in a matrix. This matrix is often formed from extracellular polymetric substances (EPS) (Wang *et al*, 2017). A study on physiological conditions relating to biofilm formation by Wang *et al* (2017) concluded that sufficient carbon sources and limiting nitrogen availability were the key to biofilm formation. Inorganic nitrogen concentrations were found to significantly affect the morphology, consortia, and physiology of the biofilm (Li *et al*, 2017). Another important factor was the EPS

make-up in the biofilm. The EPS structure contains nucleic acids, proteins, phospholipids, and polysaccharides. In addition, it is highly hydrated as it contains water channels for nutrient distribution (Bailey, 2011). According to Wang *et al* (2017), EPS in the biofilm matrix facilitates aeration management and generates a suitable micro-environment for the microbe. Balsanelli *et al* (2014) mentioned the ability of EPS to shield microbes against plant defence-mechanisms as another advantageous characteristic. Between 50 % and 90 % of the total organic carbon in biofilms can be attributed to EPS (Bailey, 2011). Serra & Hengge (2019) found that cellulose constituted part of the EPS in biofilms for various bacteria. The structure of bacterial cellulose is similar to plant cellulose (Augimeri, Varley & Strap, 2015). It facilities attachment and provides rigidity of the biofilm. *Proteobacteria*, such as *Agrobacterium* ssp., *Rhizobium* ssp., and *Pseudomonas* ssp., are the most prominent cellulose-synthesizers (Augimeri *et al*, 2015).

Pedersen *et al* (2018) conducted a study on the association between diazotrophic colonization of sediment and coastal nitrogen fixation. The study showed the importance of nucleation sites for biofilm formation using estuarine diazotrophs. Particle size was shown to be an important variable for successful biomass accumulation. The study also highlighted the possible importance of particle re-suspension. This implies that the attachment surface morphology might be of high importance to establish the desired consortium. In addition, depending on the nature of the bacterial culture, the pH level, and the temperature, the biofilm structure will be a different and the thickness will vary (Bailey, 2011).

2.9 Applications of diazotrophic cultures

2.9.1 Bio-augmentation

The term bio-augmentation refers to the addition of exogenous microbes to facilitate bio-remediation (Welz *et al*, 2018). Bioremedation of polluted soils is cost-effective and eco-friendly (Zhou *et al*, 2020). The accumulation of heavy metals and other compounds results in reduced plant growth and disturbance of the natural ecosystem (Mahanty *et al*, 2018). Nitrogen-fixing soil bacteria have a potential use in bio-augmentation in effluent treatment and agriculture. Zhou *et al* (2020) showed approximately 90 % promotion of polycyclic aromatic hydrocarbon (PAH) removal in 21 d through bio-stimulation of diazotrophs. This was done by increasing nitrogenase activity through the addition of molybdenum and tungsten to soil contaminated with PAH. Ullah *et al* (2015) showed the positive effect of plant-growth promoting bacteria on phytoremediation. Phytoremediation is the removal of pollutants from soil and water by plants. This remediation technique relies on the natural ability of plants to hyperaccumulate metals. Diazotrophic bacteria aid plants in phytoremediation by providing an increased metal tolerance and disease resistance. Metal toxicity is prevented by nitrogen-fixing bacteria through mechanisms such as redox reactions, soil pH changes, remediation using siderophores, and changes in metal bio-availability (Ullah *et al*, 2015).

2.9.2 Bio-fertilizer

Due to the use of chemical fertilizers, agricultural soils have suffered various problems, for example, reduced fertility and water-holding capacity. It is, therefore, necessary to reevaluate current agricultural practices. Bio-fertilizers show a promising alternative to conventional fertilisers as they support the natural ecology

of the soil (Mahanty *et al*, 2018). Bio-fertilizers are microorganism-containing substances that aid plant growth by the colonization of microorganisms in roots or seeds of plants (Mahanty *et al*, 2018). Plant-growth promoting bacteria (PGPB) have been found to enhance plant-growth through various mechanisms including, but not limited to, the following: nitrogen fixation, phosphorus stabilisation and solubization, potassium stabilisation, phytohormone release, EPS production, and heavy metal remediation (Mahanty *et al*, 2018; Ullah *et al*, 2015). In addition, diazotrophs have been shown to increase resistance to abiotic stresses in plants (Ullah *et al*, 2015). This is due to PGPB excreting antibiotics and other substances to combat pathogens (Mahanty *et al*, 2018). In addition, biofertilizers could reduce pesticide toxicity through bio-transformation or enzymatic degradation (Mahanty *et al*, 2018). Various species have been tested in greenhouse experiments and field trials. *A. vinelandii* has been shown to improve rice yields by up to 20 % and *Acetobacter diazotrophicus* has been shown to provide up to 80 % of nitrogen for sugar cane plants (Kennedy, Choudhury & Kecskes, 2004). Both species were inoculated in the seedlings of the respective plants (Kennedy *et al*, 2004).

2.9.3 Lignocellulose breakdown

Diazotrophs have been used in combination with lignocellulolytic and cellulolytic micro-organisms for the breakdown of wheat straw (Halsall, 1993; Lynch & Harper, 1985). Wheat straw, when not removed from a field after harvesting, is considered a considerable agricultural waste as it can render soil N-deficient (Lynch & Harper, 1985). This is due to a high N demand during lignocellulose breakdown, which results in soil nitrogen accumulating in microbial biomass (Lynch & Harper, 1985; Halsall, 1993). There is an opportunity to use wheat straw as a C-source for diazotrophs. Since diazotrophs require simple carbohydrates, a symbiosis between diazotrophs and lignocellulolytic and cellulolytic micro-organisms would be evident (Halsall, 1993). Diazotrophs would, in turn, provide nitrogen to the soil which would prevent N-deficiency and create an advantage for the next crops (Halsall, 1993). The combination of organisms would act as a fertilizer, soil conditioner, and bio-control agent (Lynch & Harper, 1985). Thus, diazotrophs can provide the nitrogen needed in lignocellulose breakdown while utilising the breakdown products as a carbon source.

2.9.4 Land reclamation

Diazotrophs in biofertilizers could also aid in the reclamation of mining sites. Mineral mining sites often leave behind acidified soil due to the leaching of chemicals. The pH of these soils could be altered and their microbial community could be restored to an extend through the application of biofertilizer. The success-rate of land reclamation is highly dependent on the soil microbiome and thus, the application of a suitable fertilizer is crucial. The use of biofertilizer could be paired with the cultivation of legumes or trees to recover the soil for future agro-forestry usage (Mahanty *et al*, 2018).

2.9.5 Effluent treatment

Ammonia-oxidizing, nitrite-oxidizing, and denitrifying microbes have previously been used in wastewater treatment to remove nitrogen from effluents (Pappu *et al*, 2017). According to Pappu *et al* (2017), the

pH of the effluent is an important parameter in creating a suitable environment for denitrifying bacteria. Elevated pH-values resulted in higher rates of denitrification. In addition, Huang *et al* (2013) suggested the importance of C:N ratios for the microbial metabolism in wastewater treatment using a bio-electrochemical system. Recently, diazotrophs have been shown to aid paper and pulp mill effluent treatment by decreasing the carbon to nitrogen ratio. According to Welz *et al* (2018), insufficient organic nitrogen could decrease suspended growth system efficiencies. Similarly, the addition of *Azotobacter* ssp.. to winery effluent benefits the process by balancing the C:N. Welz *et al* (2018) observed adaptation of *Azotobacter* ssp. to their environment and subsequent increases in biological sand filter performance. Thus, the nitrogen-balance in the effluent is of significant importance to increase system efficiencies and thereby, decrease negative environmental impacts.

2.9.6 Bioelectrochemical nitrogen fixation

According to Rago *et al* (2019), the biochemical pathway of nitrogen fixation is enabled by the reducing power for electron transfer and chemical energy for ATP storage. This allows for interactions with the microbial metabolism by applying currents. A consortium was grown as a biofilm on carbon-fibre cathode and a current was applied to the biomass. This resulted in simultaneous carbon and nitrogen sequestration. Rago *et al* (2019) suggest the opening of an entirely new field where microbial electrosynthesis can be utilised as an alternative to the Haber-Bosch process.

3 Experimental

Several experiments were conducted on a bench-scale setup to investigate a diazotroph culture. No sterilisation equipment was utilized as all runs where done in a non-sterile environment to mimic bacterial colonies in the soil. Open-source equipment was utilised where possible to facilitate replication.

3.1 Materials

The diazotrophic bacteria were cultured in a modified Burke's medium. This medium consists of the following minerals and carbon source added to distilled water:

- 1 g/L $KH_2PO_4 \cdot 7\ H_2O$ (Sigma-Aldrich)
- 0.2 g/L $MgSO_4 \cdot 7\ H_2O$ (Merck)
- 0.1 g/L $CaCl \cdot 2\ H_2O$ (Sigma-Aldrich)
- 0.00145 g/L $FeSO_4 \cdot 7\ H_2O$ (Merck)
- 0.0002 g/L $Na_2MoO_4 \cdot 2\ H_2O$ (Merck)
- 0.05 g/L KOH (Merck)

- 5 g/L Glucose (Sigma-Aldrich)

The pH was controlled through base addition, a 1M NaOH solution was utilised for the application. Aeration was done by mixing pure oxygen (Afrox) and pure nitrogen gas (Afrox) to the desired ratio.

3.2 Equipment

3.2.1 Reactor setup

A reactor with high liquid-gas mass transfer potential was constructed and commissioned. The reactor volume was measured as ± 400 mL and the reactor was left open to atmosphere. A recycle line was implemented for the purpose of temperature control and as a gas injection point to facilitate Taylor flow bubbles for good gas-liquid mass transfer. Taylor flow is characterised by consecutive bubbles separated by a slug, where the small diffusion paths and a large liquid-gas interface enhance mass transfer significantly compared to other flow patterns (R Gupta, Fletcher & Haynes, 2010). An overflow system was used as level control, however, no other level control was implemented as due to the relatively low working temperature (30 °C) and the short duration of runs, evaporation of the medium was considered negligible. The reactor was assumed to be well-mixed through a magnetic stirrer at 105 rpm and the cycling of liquid by the heat exchanger at 40 rpm. Figure 4 shows the experimental setup.

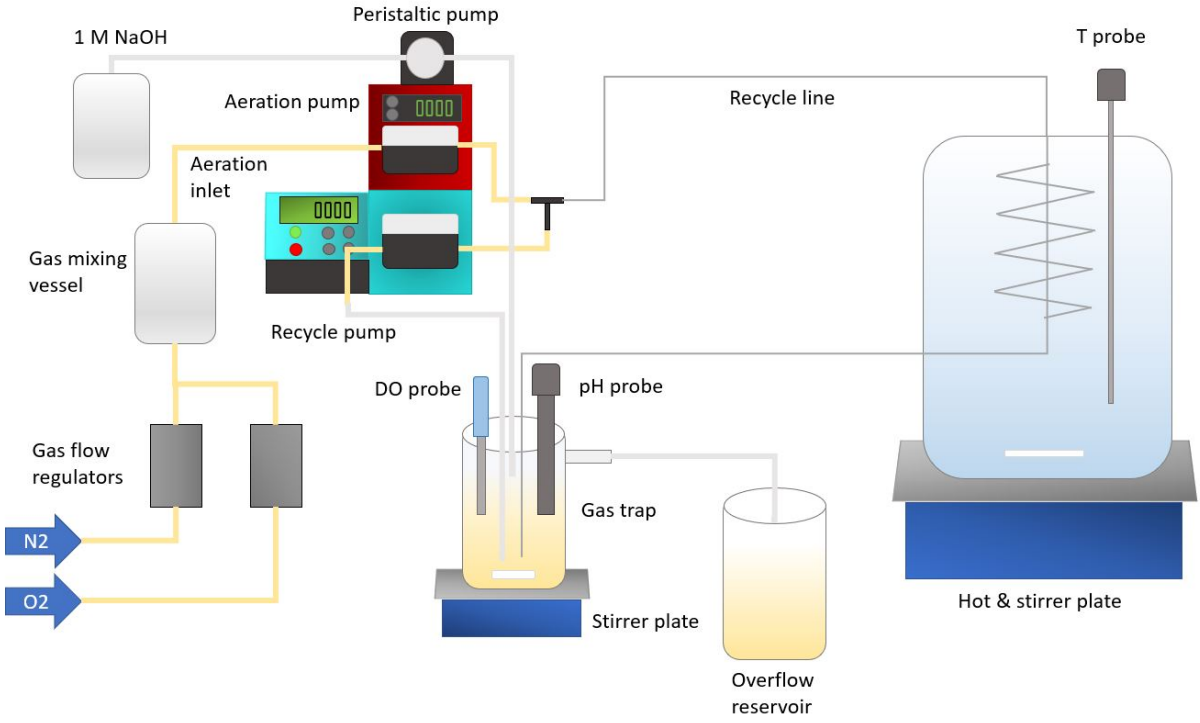

Figure 4: Experimental setup for diazotrophic culture growth

3.2.2 Monitoring and control system

A monitoring and control system was implemented to maintain a constant pH and temperature. A DFRobot Analog pH probe was used for pH measurements which were captured by an Arduino MEGA 2650 and utilised to control a peristaltic pump. This peristaltic pump was connected to a Stepper Motor Driver 4.2A (Wantai) which controlled the dosing of base solution through a proportional, piece-wise control strategy. A heat and stirrer plate with a built-in thermocouple was utilised for temperature control. The heat exchanger was setup as follows: Approximately 90 % of the recycle line (ID 3 mm) was submerged in a 5 L bottle of water. This bottle was chosen to be large to provide a capacitor for the control system and it was heated to 2 °C above the set point temperature of 30 °C to attain the desired temperature inside the reactor.

Two Brooks Delta II Smart Mass Flow Controllers were utilised for gas composition control to the aeration pump. The flow controllers were connected to a nitrogen line and an oxygen line and their valve openings were controlled by means of a changing current input. Thereby, changing the gas flow rates. The gasses would mix in a large mixing vessel, before entering the system. This mixing vessel contained an oxygen sensor which logged the oxygen % in the mixing vessel at 2 min intervals. The calibration of the flow controllers is described in Appendix A. An aeration pump was connected to the mixing vessel and manually set to the desired set point of 10 rpm (0.143 mL/s). This set point was chosen to provide sufficient gas inflow without causing excessive shear. The aeration pump would inject gas bubbles into the recycle line.

In addition, dissolved oxygen measurements were performed online and logged via the Arduino MEGA 2650. An Endress+Hauser Memosens COS81D oxygen sensor was utilised for this application. This probe also provided temperature readings, however, these were not logged online or utilised for the control strategy. Readings were logged every 2 min *via* a communication software called *TeraTerm*.

3.2.3 Analysis

Minerals and reagents were weighed off using a laboratory scale (± 0.0001 g). Samples were taken periodically and in duplicate. Absorbance (A) readings were done using 3 mL cuvettes at a wavelength of 660 nm in a spectrometer (± 0.0001) (Agilent Technologies, Johannesburg, South-Africa - Cary 60 UV-Vis). The absorbance measurements were only based on suspended biomass (Lexow, 2019) and thus, any biofilm attachment would lead to an underestimation in yield and productivity. The absorbance readings were converted to dry cell weight (DCW) according to Equation 7. This equation was obtained by determining the mass of the suspended biomass for several absorbance readings. Samples were centrifuged and washed three times and then dried in the oven overnight at 60 °C.

$$DCW = A \times 0.6 \tag{7}$$

Carbon-compound and acid concentrations were measured in a high-pressure liquid chromatographer (HPLC) (± 0.00001 g/L) (Agilent Technologies - 1260 Infinity, Johannesburg, South-Africa), after being centrifuged for 90 s at 120 rpm and filtered (0.45 μm) to separate the biomass from the liquid fraction. In addition, samples were taken at the end of each run for the total organic carbon analysis. The samples were centrifuged

at 2500 rpm for 5 min and filtered (45 μm) and then diluted to 30 mL solutions. The solutions were analyzed on a Total Organic Carbon Analyzer (Shimadzu, Kyoto, Japan). The TOC-V (liquid samples) setting was used to determine the non-purgeable organic carbon. Nitrogen was used as a carrier gas and sodium persulfate and phosphoric acid were used as oxidizers. Appendix B describes the methods used to ensure the correctness of malic acid readings under carbon-compound analysis.

To determine the presence of nitrogen compounds, ammonia concentrations were determined utilizing ammonia test kits (Spectroquant, Merck, South-Africa). Ammonia test kits were utilised as per suppliers manual and the resulting solution was analysed at 690 nm in the spectrometer (Agilent Technologies, Johannesburg, South-Africa - Cary 60 UV-Vis). At the end of a run, total nitrogen was determined for the culture (unfiltered) and its supernatent (centrifuged and filtered). The total nitrogen in biomass was calculated by difference of the two samples. A DMP Spectroquant total nitrogen test kit (Spectroquant, Merck, South-Africa) was used which determined the total nitrogen based on the sum of total Kjehldahl nitrogen, nitrate, and nitrite (Merck KGaA, 2021). Samples were prepared as per suppliers instruction (analogous to method EN ISO 11905-1) (Spectroquant, Merck, South-Africa) which included digestion of biomass-containing samples at 120 °C for 1 h (Merck KGaA, 2021). An absorbance reading at 340 nm (Agilent Technologies, Johannesburg, South-Africa - Cary 60 UV-Vis) was taken to determine the total nitrogen present in the samples (analogous to method DIN 38405-9) (Merck KGaA, 2021). The calibration of the N-compound test kits (Spectroquant, Merck, South-Africa) is described in Appendix A.

To determine which bacterial strains were responsible for the observed behaviour, samples were analysed through next-generation sequencing. At the end of each run, a sample was taken of the final solution. This sample was centrifuged (2000 rpm for 5 min) and filtered (45 μm). Next-generation DNA sequencing was outsourced to Inqaba Biotec (Pretoria, South-191Africa). A metagenomic analysis of full length 16s gene amplicons was performed on a sample from each experimental condition. A two-step PCR was performed on each sample and 16S (forward and reverse) primers (27F and 1492R) tailed with PacBio universal sequences were used (PacBio, 2018). To process raw subreads the Circular Consensus Sequences (CCS) algorithm accessible through the software *SMRTlink (v9.0)* was utilized to produce highly accurate reads (>QV40).

3.2.4 Statistical Analysis

To quantify the repeatability of experimental runs under a specific condition, standard deviations (σ) were calculated according to Equation 8, where Xm is the mean, Xi is the value of the data point, and n is the number of data points.

$$\sigma = \frac{\sqrt{(Xi - Xm)^2}}{n - 1} \tag{8}$$

In addition, the relative standard deviation (RSD) for each data point was calculated using Equation 9, where M signifies the mean.

$$RSD = \frac{\sigma}{M} \times 100 \tag{9}$$

To quantify the similarity of the culture compositions, the Bary-Curtis dissimilarity index (BC) was calculated. The BC is a number between 0 and 1, where 0 signifies that the data sets were identical and 1 signifies there was no overlap. Equation 10 was used to compute the BC, where A and B are the sum of frequencies for the two data sets and where W is sum of minimum frequencies among the data sets (Somerfield, 2008).

$$BC = 1 - \frac{2 \times W}{A + B} \tag{10}$$

3.3 Operating procedure

3.3.1 Inoculum procurement and development

Three soil samples from N-lean soil were collected at $-25,75361$ N, $28,229721$ E at 10 mm depth. The samples were suspended in equal amounts (1 g soil from each soil sample) in 200 mL distilled water. The distilled water containing the soil particles was agitated by mixing the particles thoroughly with a spatula and manually swirling the solutions. Thereafter, the sand particles were allowed to settle and a 10 mL aliquot was decanted from the supernatant and used as an initial inoculum. The bioreactor and adjacent lab space was disinfected using surfactants, distilled water, ethanol, and Virkon^{TM} prior to each run to minimize the microbes present in the bioreactor space. The system was intentionally not autoclaved as the focus of the study was to develop a robust system able to perform under non-sterile operational conditions. Several runs were performed in a 1.5 L batch reactor with stirrer and a recycle line for mixing. The inoculum was grown in a Burke's medium (5 g/L glucose) at pH 6.8 and at 25 °C. Aeration was provided by a 3 - 4 W aquarium air pump. The solution was stored when the glucose was depleted. Then, the stored solution was used to inoculate another run and the process was repeated. After several runs, a natural selection had occured as the microbial behaviour became relatively repeatable based on measured concentration profiles: suspended biomass, byproducts, and glucose concentrations. The resulting solution was stored in 10 mL vials. The contents of one 10 mL vial was used for each inoculation of further experiments on the reactor setup described in Section 3.2.1.

3.3.2 Experimental runs

To investigate diazotrophic behaviour, experimental runs were performed at the following conditions: pH = 6.8, setpoint temperature = 30 °C, atmospheric pressure as these conditions were most prominent in literature (Brewin *et al*, 1999; Barney *et al*, 2017; Bali *et al*, 1992; Romero-Perdomo *et al*, 2015). The magnetic stirrer speed was set to 105 rpm to allow for sufficient mixing. The recycle line was pumped at 40 rpm and the aeration pump was set to 10 rpm (0.143 mL/s). The reactor was inoculated after it had reached its required conditions and maintained steady-state for 20 min. Runs were allowed to continue until all glucose was depleted. Samples were taken every 2 h during mass-transfer limited growth and only periodically during the exponential growth and lag phase. Samples were taken in duplicate and analysed in the HPLC for carbon-compounds and acids. In addition, ammonia tests were performed on some of the samples. Absorbance readings were taken at 2 h intervals. Lastly, total nitrogen and total organic carbon were determined at the end of the run. All tests were performed as per manufacturer guidelines.

To investigate the effect of varying aeration feed compositions, three different compositions were tested: oxygen-rich air, atmospheric air, and oxygen-poor air. Each condition was tested in triplicate to ensure repeatability. Table 4 shows the experimental conditions. The oxygen-rich and oxygen-poor compositions were chosen such that they lay equal distances (14 percentage point) away from the atmospheric air condition and consequently the change in oxygen % compared to 21 % oxygen or ($\frac{2}{3}$ of 21 %) would be sufficiently different to ensure marked differences in the operational conditions

Table 4: Summary of utilised aeration feed compositions.

Experimental condition	Oxygen (%)	Nitrogen (%)
O2_21	21	79
O2_35	35	65
O2_7	7	93

3.3.3 Mass-transfer experiments

Mass-transfer experiments were conducted to determine the gas-liquid mass transfer, the reactor was set-up with a clean Burke's medium (not inoculated). The solution was sparged with nitrogen until a very low dissolved oxygen concentration was reached ($<$ 2 mg/L). Thereafter, the aeration of the reactor at a 21 % oxygen feed composition was done. The response of the system was recorded with a dissolved oxygen probe. The mass transfer coefficient (kla) was obtained by utilising Equation 11. The experiment was completed in triplicate.

$$kla = \frac{\ln\left(DO_{sat} - DO\right)}{\Delta t} \tag{11}$$

4 Results and discussion

4.1 Mass-transfer properties of the experimental setup

Mass-transfer experiments were performed to obtain the volume-based mass-transfer coefficient of the experimental setup. The natural logarithm of the difference in saturated dissolved oxygen and measured dissolved oxygen against time was plotted. Figure 5 shows the experimental data. A linear trend was fit against the three data sets, where all R^2-values > 0.93. The slope of the linear fit was the mass-transfer coefficient. At a 21 % oxygen aeration feed composition, the mass-transfer coefficient was found to be 0.0027 s^{-1}.

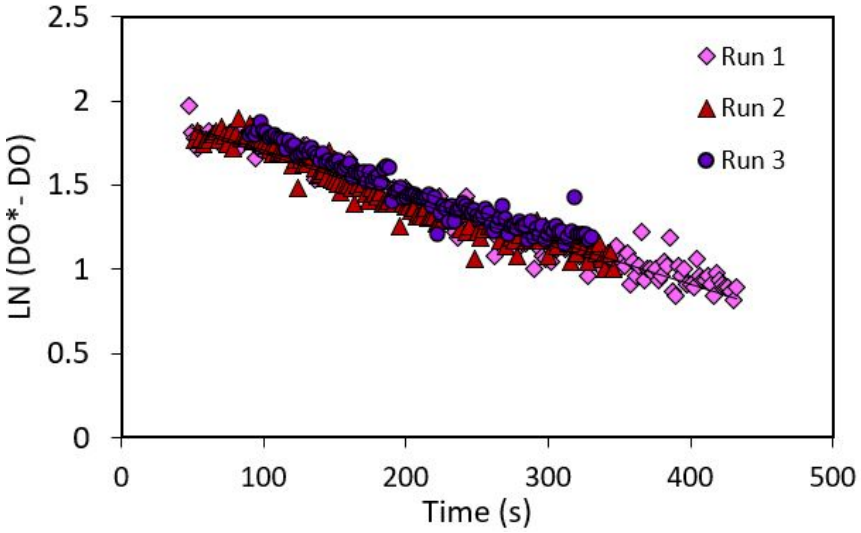

Figure 5: The volume-based mass-transfer coefficient for the experimental setup was tested at a 21 % oxygen aeration feed composition. Good repeatability among all three experiments was observed.

4.2 Aeration with atmospheric air

4.2.1 Dissolved oxygen and pH control

A set of experiments (O2_21) was completed with an aeration feed composition of 21% oxygen and 79% nitrogen. The dissolved oxygen behaviour was a notable variable during the runs as a mass-transfer limited regime was reached. An initial high dissolved oxygen was observed, this was considered the lag phase, as there was little oxygen demand. After the lag phase, a steep drop followed, rendering an anoxic environment. The anoxic environment was maintained for approximately 15 h, and then, a sudden increase was observed due to the depletion of glucose and thereby the sudden reduction in oxygen uptake by the microbes. To compare the various runs, the variance in lag phase had to be accounted for. Time shifts were applied to the data based on their dissolved oxygen profiles. The points in time where the dissolved oxygen reached below 0.10 mg/L for the first time were aligned for all three runs. The unshifted filtered data and time-shifted dissolved oxygen data are displayed in Figures 6 and 7. Slight variations in initial dissolved oxygen concentration were due to variations in environmental factors. The laboratory temperature fluctuated between 20 °C - 25 °C, which affected the starting temperature of the experimental runs.

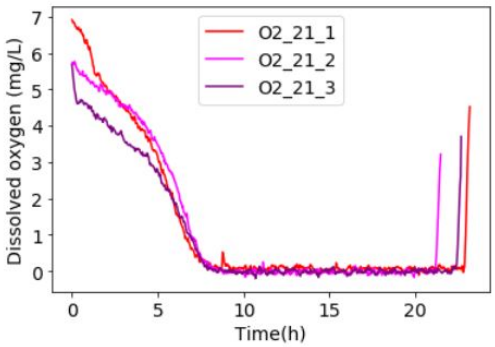

Figure 6: Filtered, unshifted dissolved oxygen data from 21 % oxygen aeration feed experiments. A steep drop is observed in all runs, followed by a period of low dissolved oxygen. This indicates and oxygen-controlled growth rate.

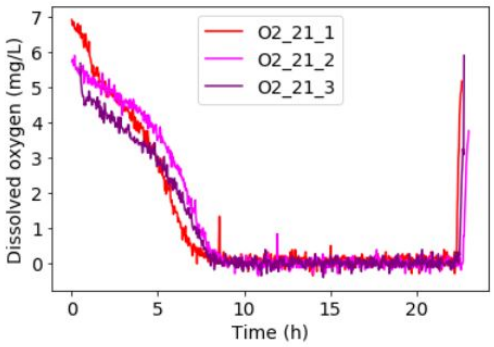

Figure 7: Time-shifted dissolved oxygen data from 21 % aeration feed experiments. The total growth phase is similar in length, variations were due to minor variations in glucose supply.

The pH was controlled at 6.8 for each run, deviations from the setpoint were mainly due to noisy readings and overshoot. As seen in Figure 8, some degree of overshoot was experienced in each run. This was likely due to the simple pH control system which only applied proportional control. The overshoot instances in Figure 8 coincide with the dosing instances (steps) in Figure 9. Overshoots up to a pH of 7.0 were assumed to have a negligible effect on the data acquired during the runs. At the end of each run, a rapid rise in pH was observed. This was attributed to the rapid increase in dissolved oxygen. Due to the carbon dioxide being pushed out of the medium, the pH of the solution would increase. Equation 12 shows the equilibrium between dissolved and gaseous carbon dioxide, where the ionic equilibrium constant, $K_H = 10^{-1.5}$ (Zang *et al*, 2011).

$$CO_2(g) \leftrightarrow CO_2(aq) \tag{12}$$

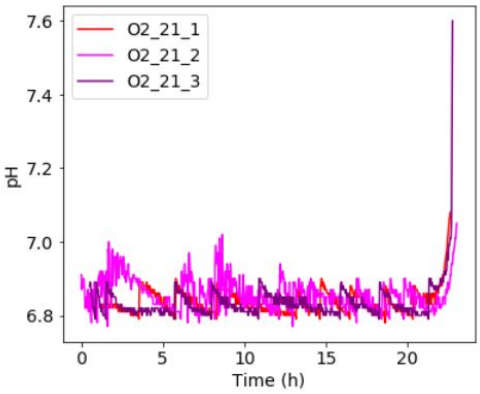

Figure 8: Raw pH data indicates sufficiently tight pH control

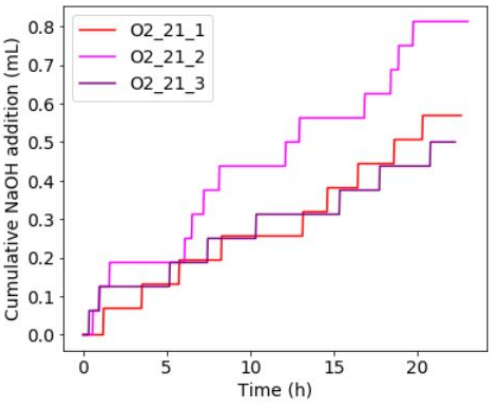

Figure 9: The cumulative 1M caustic solution addition shows little to no acid production took place.

4.2.2 Concentration profiles

One of the objectives of this study was to obtain a repeatable culture in a non-sterile environment. As seen in Figure 10, good repeatability was observed between runs from a process point of view. An average RSD of 15.7 % was calculated for the data points. The growth curve indicates different regimes were met during growth. The different growth-regimes coincided with the trends in the dissolved oxygen profiles. An initial lag phase was present to establish the culture, where the dissolved oxygen was high as there was a low oxygen demand. This was followed by a two-part growth phase. Initially, exponential growth occured causing an exponential decrease in dissolved oxygen. This was followed by mass-transfer limited growth at low dissolved oxygen concentrations. Once all the glucose was consumed, growth terminated and a sudden increase in dissolved oxygen took place as the oxygen demand reduced drastically.

Figure 11 shows the glucose concentration profiles for the various runs. Slight variations in starting glucose concentrations affected the total run time for each experiment. An overall straight line trend was observed during the mass-transfer limited regime and a decrease in consumption rate was present towards the glucose depletion point. During the lag phase, some glucose consumption was already observed. This, however, did not translate to the suspended microbial growth. The likely cause for this observation was biofilm formation, which was observed on the probes and inside the tubing during all experimental runs. Biofilm formation at the start of the run would be able to establish a favourable growth environment for the microbes to protect their nitrogenase enzyme from too much oxygen stress.

From acid analyses on a high-pressure liquid-chromatographer, it was clear that malic acid was the only byproduct. No other fermentation products were produced. Malic acid increased exponentially during the exponential growth-regime and had an average maximum concentration of 0.07 g/L. The malic acid concentration decreased when the point of glucose depletion was approached. This indicated that malic acid was utilised as a carbon source by the diazotrophic culture when glucose started depleting (Figure 12). The malic acid production was likely a tool for energy down-regulation. Since malic acid is ATP neutral, it was hypothesised to serve as a carbon sink to decrease the energy generation within the microbes. Section 4.4.3 elaborates on this concept.

The yield of biomass on glucose for each run was calculated, as well as, the productivity of each run. The lag phase was omitted during the productivity calculation. All values were based on suspended biomass readings and thus, would be a slight underestimation since there was a thin biofilm present. Table 5 shows the resulting values.

Table 5: Yield and productivity data for runs at 21 % oxygen aeration feed composition

Run	Yield (g/g)	Productivity (mg/L.h)
O2_21_1	0.22	6.56
O2_21_2	0.20	6.49
O2_21_3	0.17	5.05
Average	0.20	6.03

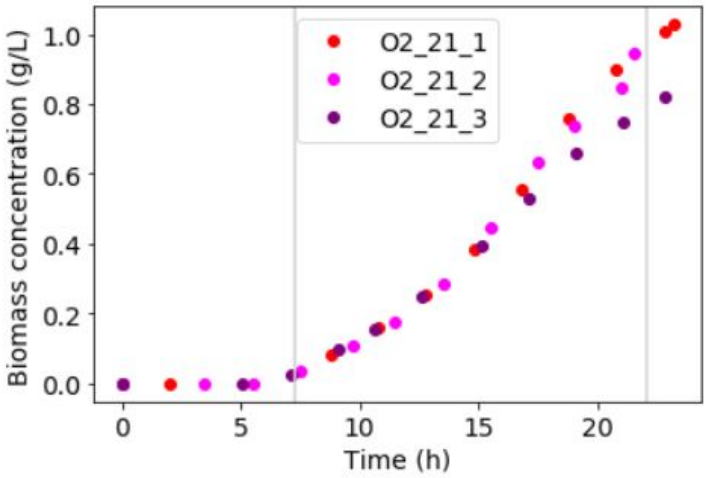

Figure 10: Several growth-regimes are clearly visible on the growth curve. An initial lag phase, exponential growth, and mass-transfer limited growth. The mass-transfer limited regime is indicated by the vertical lines.

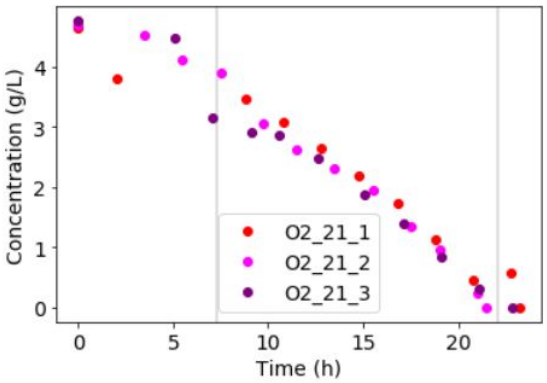

Figure 11: A steady-drop in glucose proportional to the growth curve was observed. The mass-transfer limited regime is indicated by the vertical lines.

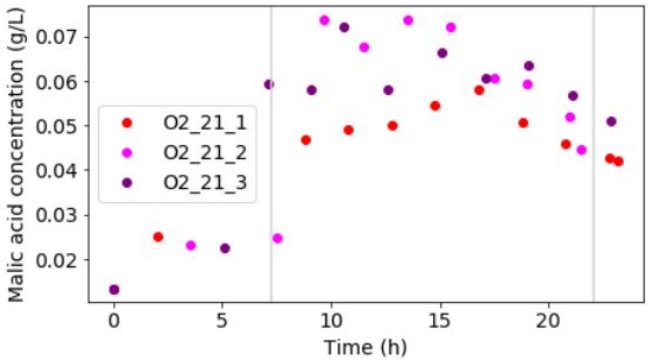

Figure 12: Malic acid was produced by the culture and later consumed. The mass-transfer limited regime is indicated by the vertical lines.

4.3 Aeration with oxygen-rich air

4.3.1 Dissolved oxygen and pH control

A set of experiments (O2_35) with an aeration feed composition of 35 % oxygen and 65 % nitrogen was completed. During the lag phase, the aeration oxygen composition was held at 21 % to ensure repeatable starting cultures. The conditions were changed as the dissolved oxygen approached 0.2 mg/L (the mass-transfer limited growth regime). At O2_35, similar trends to O2_21 were observed in the dissolved oxygen profiles. Filtered, unshifted dissolved oxygen data and its time-shifted equivalent are shown in Figures 20 and 21. Even though, the oxygen supply was significantly increased, the culture still attained an anoxic environment. Since the nitrogenase enzyme, responsible for nitrogen-fixation, is oxygen-sensitive, diazotrophs

utilise build-in mechanisms to protect the enzyme. It was hypothesised that the microbes promote an anoxic environment using two different mechanisms. The first being consumption of oxygen for oxidative phosphorylation and thus, ATP production. The second mechanism would be a protective mechanism of the microbe to shield the nitrogenase enzyme from the surplus of oxygen. One such mechanism, oxygen scavenging, where the microbes prevent oxygen diffusion at the peripheral cytoplasmic membrane level, was mentioned by Oelze (2000). It was assumed that this protection mechanism comes at an additional ATP cost. Another mechanism is substrate usage, which reduces the exposure of the nitrogenase enzyme to oxygen by increasing the consumption of oxygen (Smercina *et al*, 2019). Section 5 shows the investigation of this hypothesis through mass and energy balances based on experimental data.

When looking at the pH data and the cumulative base addition, clear peaks in pH are present at the dosing instances. The pH control was deemed sufficiently tight as slight deviations (pH $\pm$ 0.2) were assumed to have a negligible effect on the overall diazotrophic growth. As discussed in Section 2, diazotrophs have the ability to grow in a vast range of pH conditions. A surge in pH was observed at the glucose depletion instance. This corresponds with the trends observed at 21 % aeration feed compositions. The rapid climb in pH was attributed to a sudden decrease in dissolved carbon dioxide.

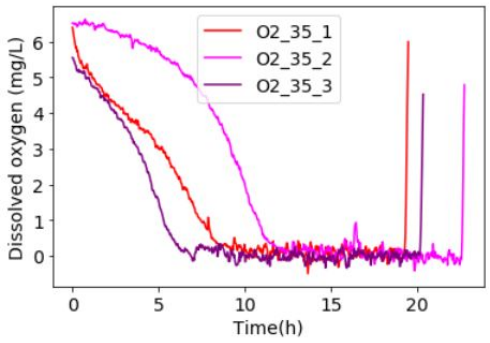

Figure 13: Filtered, unshifted dissolved oxygen data from 35% oxygen aeration feed experiments. An anoxic environment is reached which indicates mass-transfer limited growth.

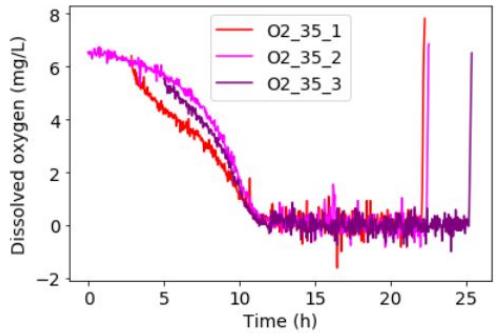

Figure 14: Time-shifted dissolved oxygen data from 35 % aeration feed experiments. Variations in total run time were due to variations in glucose supply.

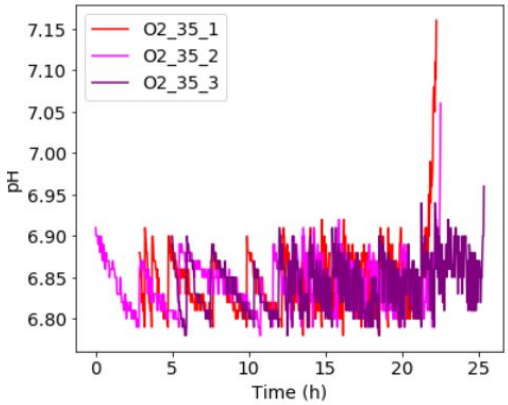

Figure 15: Raw pH data indicates sufficiently tight pH control.

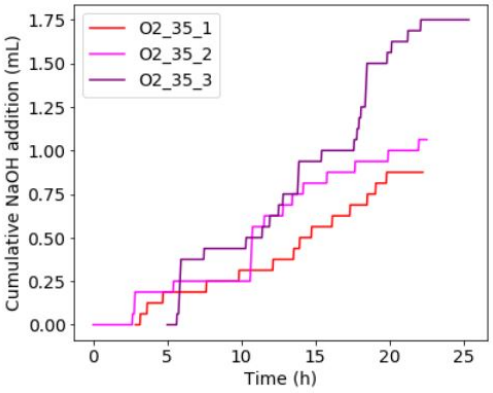

Figure 16: The cumulative 1M caustic solution addition shows little control was required.

4.3.2 Concentration profiles

A repeatable culture was obtained at oxygen-rich aeration conditions in a non-sterile environment with an average RSD of 8.1 %. The growth curve (based on suspended biomass) followed the same trend as the culture at condition O2_21: first the lag phase, then exponential growth, followed by mass-transfer limited growth (Figure 17). The slopes indicate a slight decrease in growth rate towards glucose depletion.

The final biomass concentration in run O2_35_1 was slightly lower due to a lower initial glucose concentration, as seen in Figure 18. The deviations in the glucose profiles stem from the variation in initial glucose concentration, as the slopes are very similar. Similarly to condition O2_21, an initial biofilm formation was suspected as there was a lag observed between glucose consumption and suspended microbial growth. The biofilm at condition O2_35 was visibly thicker than at O2_21, however, still relatively thin inside the recycle line tubing due to high turbulence.

Malic acid formation was observed during the mass transfer limited growth. An average final concentration of approximately 0.07 g/L was obtained. The malic acid was utilised in run O2_35_3 as an alternative carbon source at the point of glucose depletion. This was not observed in run O2_35_1 and O2_35_2 as their termination point occured before malic acid could start being consumed.

The yield of biomass on glucose for each run was calculated as shown in Table 6. The productivity for each run was calculated over the mass-transfer limited growth regime only. These values were based on suspended growth and thus, did not account for any sessile biomass. This would imply an underestimation of biomass concentration.

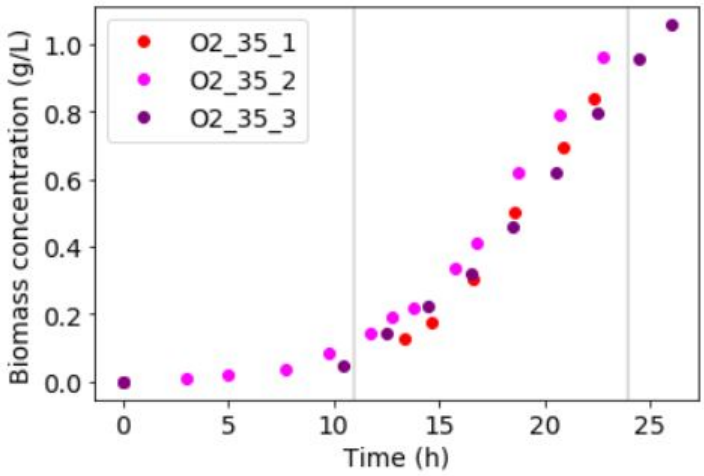

Figure 17: Vertical lines indicated the mass-transfer limited regime at 35 % aeration feed compositions.

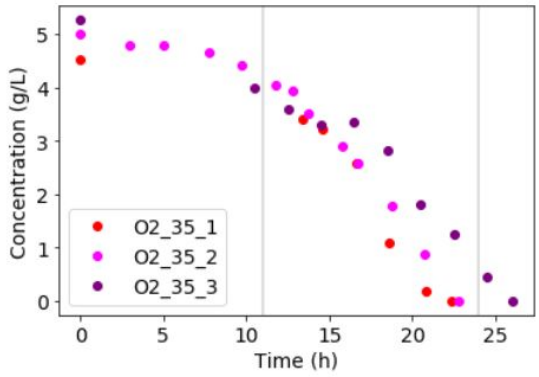

Figure 18: The initial glucose concentration varied slightly in the three runs, this caused Run O2_35_3 to take longer to reach its termination point. The mass-transfer limited regime is indicated by the vertical lines.

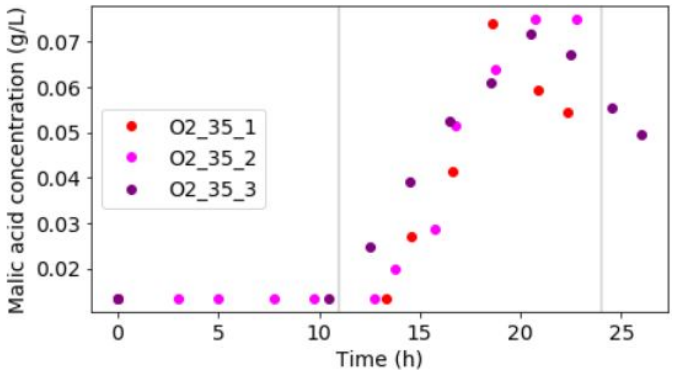

Figure 19: Malic acid was produced by the culture during the mass-transfer limited regime. A small amount was consumed towards the end of the run. The mass-transfer limited regime is indicated by the vertical lines.

Table 6: Yield and productivity data for runs at 35 % oxygen aeration feed composition

Run	Yield (g/g)	Productivity (mg/L.h)
O2_35_1	0.19	8.54
O2_35_2	0.19	7.45
O2_35_3	0.20	6.77
Average	0.19	7.59

4.4 Aeration with oxygen-poor air

4.4.1 Dissolved oxygen and pH control

In the experimental runs with oxygen-poor air (O2_7), with the composition of 7 % oxygen and 93 % nitrogen, the same dissolved oxygen trend was observed as in runs with O2_21 and O2_35. The mass-transfer limited regime was about 20 h for each run. This was much longer compared to the runs at O2_21 and O2_35. This indicated a slower growth rate at a 7 % oxygen aeration feed composition during the mass-transfer limited regime.

When looking at the pH profiles in Figure 22, run O2_7_1 and O2_7_2 show sufficient pH control. Run O2_7_3, however, had some pH control problems. This was due to the base addition line being blocked and thus, the controller was signalling to add drops of 1 M NaOH, but it was not physically being added. The blockage was removed at the 10 h mark, while the microbes were still in their lag phase. The malfunctioning base addition line was assumed to have little effect on the experimental results as the lowest pH reached was 6.5 and the malfunction did not occur during mass-transfer limited growth. A pH of 6.5 is still well in the survivable range for diazotrophs. Another blockage occurred towards the end of the run, where a drop in pH was observed. Here, the base addition line was fixed around 27 h. The base addition profiles shown in Figure 23 accounted for controller signaling during the malfunction.

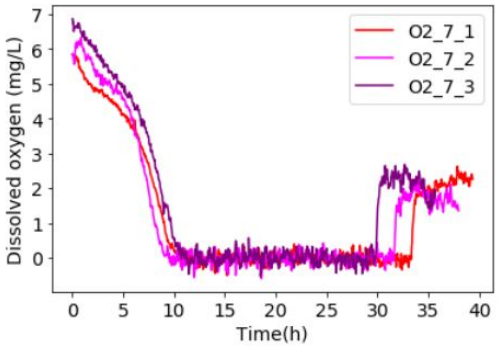

Figure 20: Filtered, unshifted dissolved oxygen data from 7% oxygen aeration feed experiments. The lag time was similar for all runs as well as the total duration of each run.

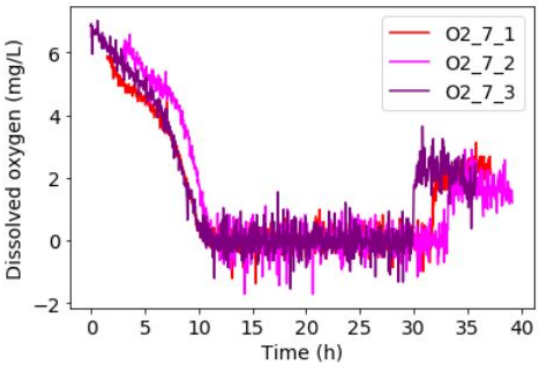

Figure 21: Time-shifted dissolved oxygen data from 7 % aeration feed experiments. Slight variations in mass-transfer limited regime duration were observed. This was due to glucose supply variations.

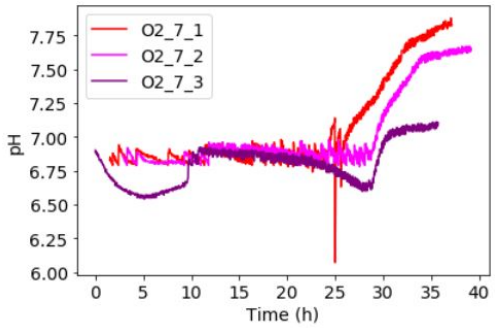

Figure 22: Raw pH data indicates sufficient pH control in run O2_7_1 and O2_7_2. Malfunctioning of the base addition line in run O2_7_3 resulted in two dips in pH.

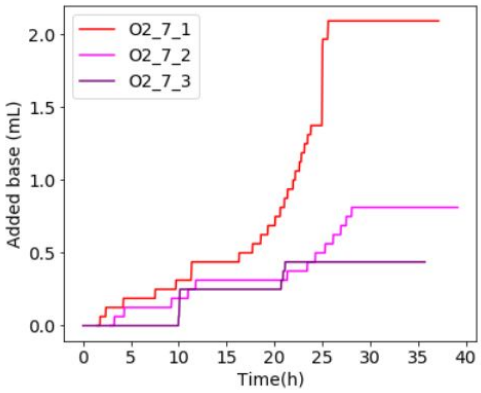

Figure 23: The cumulative 1M caustic solution addition shows most base addition occured during the mass-transfer limited regime.

4.4.2 Concentration profiles

Concentration profiles for experimental runs at O2_7 (oxygen-poor aeration feed) are shown in Figure 24 to 26. Similar to O2_21 and O2_35, O2_7 entered a mass-transfer limited regime where the oxygen supply controlled the growth rate. Glucose profiles in Figure 25 show a greater consumption rate towards the end of the experiment in run O2_7_1 compared to the other runs. This was due to byproduct formation, 0.25 g/L acetic acid and 0.45 g/L ethanol in addition to the malic acid formation. This translated into a slightly lower malic acid yield. Run O2_7_2 and O2_7_3, show almost identical trends as both did not show much byproduct formation (< 0.1 g/L). Malic acid profiles show a sharp increase in malic acid must have taken place during the lag phase and the exponential growth phase. This was likely due to excessive glucose

supply. The lag phase was held at a 21 % oxygen feed composition to obtain the same starting conditions as at conditions O2_21 and O2_35. The malic acid was formed during this higher oxygen supply, whereas malic acid consumption took place during the low oxygen supply in O2_7_2 and O2_7_3. Comparing the yield and productivity's among runs at O2_7 as shown in Table 7, the runs could be deemed repeatable. When comparing the results to the results under O2_21 and O2_35, there is a clear decrease in both yield and productivity. The productivity was decreased due to lower oxygen supply which resulted in slower growth rates. The yield in run O2_7_1 was significantly decreased due to byproduct formation. The yield in run O2_7_2 and O2_7_3 was similar to the yield in run O2_7_1, even though the byproduct formation in run O2_7_2 and O2_7_3 was much lower. This was likely due to increased biofilm formation. In general, lower yields at condition O2_7 could be observed. An average RSD of 12.9 % was calculated for O2_7

Table 7: Yield and productivity data for runs at 7 % oxygen aeration feed composition

Run	Yield (g/g)	Productivity (mg/L.h)
O2_7_1	0.12	2.87
O2_7_2	0.13	2.90
O2_7_3	0.12	2.36
Average	0.12	2.71

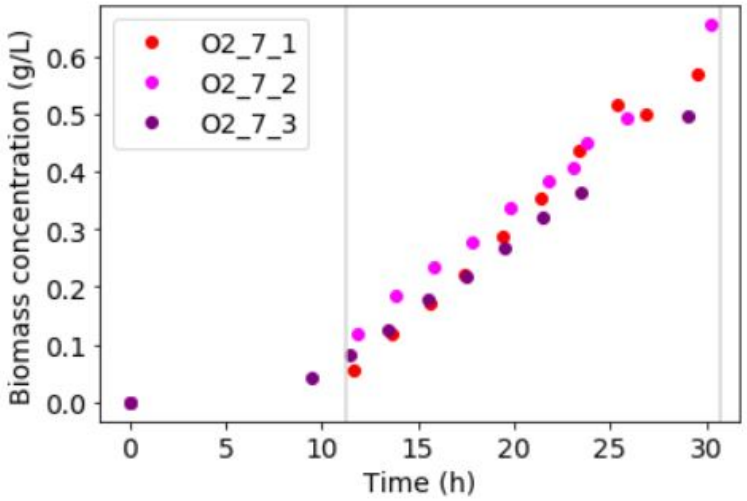

Figure 24: Biomass concentration profiles for each run at O2_7 show a straight line trend during the mass-transfer limited regime. Discrepancies in the final biomass concentrations was due to differences in glucose supply. The mass-transfer limited regime is indicated by the vertical lines.

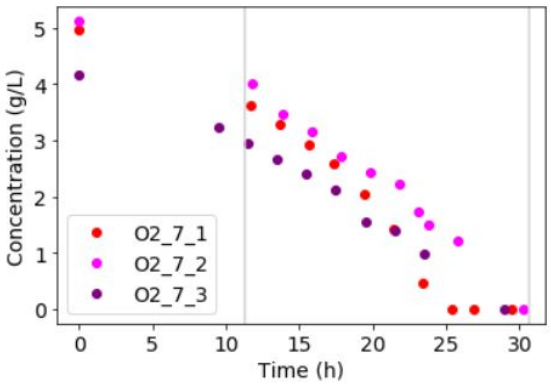

Figure 25: Glucose trends were in line with the biomass and byproduct production. Repeatable profiles were obtained. The mass-transfer limited regime is indicated by the vertical lines.

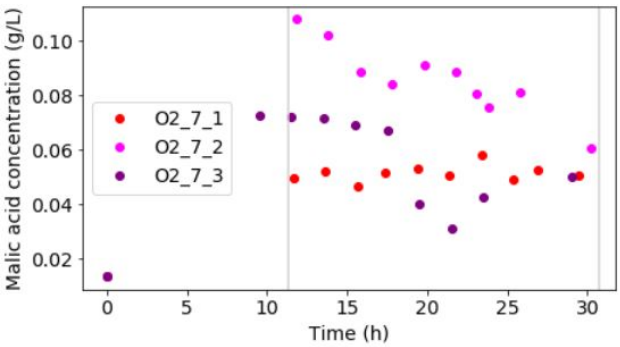

Figure 26: A large amount of malic acid was formed during runs at O2_7. The variance in malic acid concentrations in run O2_7_2 and O2_7_1 is likely due to byproduct formation in run O2_7_1. Run O2_7_3 was supplied with less glucose and shows a malic acid consumption towards the end of the run. The mass-transfer limited regime is indicated by the vertical lines.

4.4.3 Comparison of conditions

When comparing all experimental conditions, the most significant difference is the change in growth rate for different oxygen supply levels. The data for all conditions was normalized both horizontally and vertically. The lag phase for all conditions was made equal to have a better comparison. Figure 27 shows all three conditions and their varying slopes during the mass-transfer limited growth phase. The change in oxygen supply did not translate into a similar change in growth rate. This was likely due to down-regulation of the ATP complex at high oxygen availability as proposed by Oelze (2000). An overflow in oxygen would provide an excess in ATP, to prevent this, the diazotrophs can down-regulate their electron transport chain. This works by decreasing the amount of hydrogen ions released during the consumption of one oxygen atom. This would then decrease the chemical gradient over the ATP complex and thus, result in lower ATP production per oxygen atom. This theory was explored in a model on the experimental data in Section 5.2. In addition, varying amounts of oxygen affect biofilm thickness. At higher oxygen levels, biofilm thickness might be increased as a means to protect the microbes against the environmental stress. Similarly, when oxygen supply is too low, biofilm might form more readily (Bailey, 2011). The ratio between glucose uptake rates at condition O_2_35 and O_2_21 was 1.50 ± 0.10 (mean ± σ) ($\frac{r_s 35}{r_s 21}$), whereas the ratio of growth rates between the two conditions was 1.12 ± 0.09 ($\frac{r_x 35}{r_x 21}$). This shows that condition O_2_35 was less efficient in glucose consumption compared to condition O_2_21. For condition O_2_7 and O_2_21, a glucose consumption ratio of 1.29 ± 0.18 ($\frac{r_s 21}{r_s 7}$) was calculated, whereas the corresponding ratio of growth rates was 2.71 ± 0.34 ($\frac{r_x 21}{r_x 7}$). This indicates condition O_2_21 utilized significantly more glucose towards biomass formation than condition O_2_7. The lower efficiency at condition O_2_7 could be attributed to a less efficient metabolism. Some glucose was also spent on byproducts. These byproducts consisted of malic acid, some ethanol, and possibly intracellular polymeric substances (IPS) such as PHB.

When comparing the yield, productivity, and mass-transfer limited growth rate. The yields at O2_21 and O2_35 show similar results. The presented yields are, however, based on suspended biomass. As mentioned previously, the biofilm under O2_35 (35 % oxygen) might be thicker due to higher oxygen-stress and thus, hold more additional biomass. Productivity's were calculated from the exponential growth regime until the glucose depletion point, whereas the growth rate was only calculated over the mass-transfer limited regime. Table 8 shows averaged results for the experimental runs at all three conditions.

Table 8: The effect of aeration feed composition on yield, productivity, growth rate and glucose consumption rate. The standard deviation was calculated for each slope and shown in the slope data.

Run	Yield (g/g)	Productivity (mg/L.h)	Growth rate (g/L.h)	Glucose consumption rate (g/L.h)
O_2_21	0.20	6.03	0.0732 ± 0.003	0.262 ± 0.003
O_2_35	0.19	7.59	0.0820 ± 0.006	0.393 ± 0.031
O_2_7	0.12	2.75	0.0277 ± 0.003	0.207 ± 0.033

The malic acid formation in all runs could be due to a high glucose uptake rate during the lag phase. Due to the oxygen restriction during the mass-transfer limited growth, the additional energy from the overflow of glucose needed to be balanced out. Malic acid probably served as a glucose sink due to its net zero ATP production pathway. Figure 28 shows the cell-based glucose uptake to support this argument. The glucose uptake peaks are present during the exponential growth regime and during the mass-transfer limited growth. This coincides with malic acid production. A downward trend in glucose uptake is present during the mass-transfer limited growth as indicated by the vertical lines in Figure 28. Another contributing factor to the glucose profile could be biofilm formation. The establishment of a biofilm under environmental stress while carbon was readily available could be part of the consortium's survival strategy.

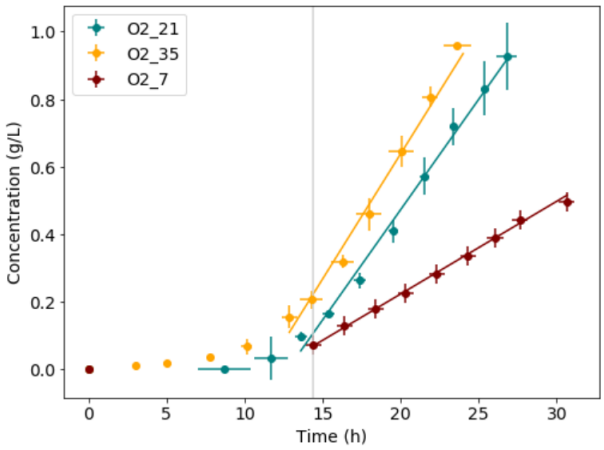

Figure 27: The microbial growth data for all experimental runs was averaged in x- and y-direction. Time-shifted to start their mass-transfer limited growth at the same point in time (vertical line).The error bars show the standard deviations in the results from the triplicate repeat runs.

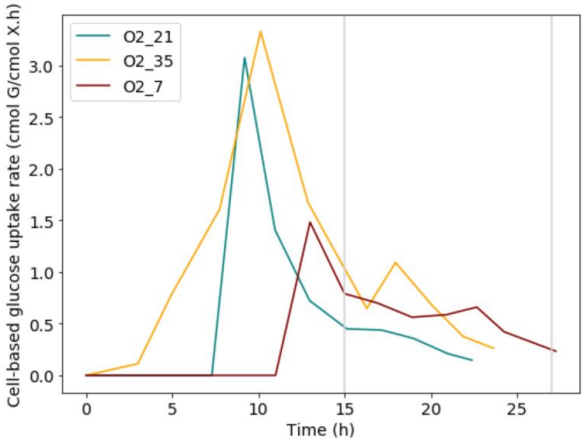

Figure 28: Distinct peaks in cell-based glucose uptake occur during the lag phase. As soon as mass-transfer limited growth initiates, the glucose uptake rate stabilises.

4.5 Culture properties

4.5.1 C:N ratio

Total organic carbon (TOC) was estimated to be roughly the same as the non-purgeable organic carbon (NPOC) content at the end of each run. The NPOC does not include the volatile organic carbon (VOC) in the sample and thus, it excludes ethanol, acetic acid, and acetone among others (Environmental Protection Agency, 2021). Table 9 shows the resulting NPOC of the aliquot at the end of each run. The carbon in the malic acid measured at the end of each run amounted to less carbon as the carbon measured through NPOC. This indicates other carbon-sources were present in the liquid. These could be EPS from the biofilm or small amounts of fermentation product.

Total nitrogen tests were completed at the end of each run. An unfiltered (UF) and a filtered (F) sample were used each time. The difference between the two samples indicated the total nitrogen in the suspended biomass (N in X). The mass percentage of nitrogen on suspended biomass was calculated by taking the total suspended biomass concentration (X) into account. The total nitrogen in the liquid (N in L) was also calculated. Since the cells were frozen at $-40\,^{\circ}\mathrm{C}$, some cells might have burst, which resulted in DNA and proteins from within the cells entering the liquid medium. In addition, proteins and DNA form part of the biofilm matrix which continuously grows and sheds into the supernatent (Bailey, 2011). Another source of nitrogen in the liquid was ammonia, however, very little ammonia (< 20 mg/L) was measured. The results of the total nitrogen test are shown in Table 10. When converting the mass% nitrogen in biomass to its mol% equivalent, and assuming all other ratios remain the same, the biomass formula was calculated to be $CH_{1.8}O_{0.5}N_{0.08}$. This means the nitrogen concentration in diazotrophic biomass was quite low.

Table 9: NPOC results at the end of each experimental run show little to no carbon was left in the medium. The carbon source was, therefore, either metabolized to biomass, biofilm (EPS), PHB, or released as carbon dioxide.

Sample	Biomass (g/L)	NPOC (mg/L)	NPOC (mmol/L)
O2_21_1	1.71	79.06	6.59
O2_21_2	1.58	361.35	30.11
O2_21_3	1.37	104.89	8.74
O2_35_1	1.40	122.04	10.17
O2_35_2	1.60	120.62	10.05
O2_35_3	1.76	91.70	7.64
O2_7_1	0.95	195.10	16.26
O2_7_2	1.09	94.61	7.88
O2_7_3	0.83	71.18	5.93

Table 10: Total nitrogen was measured at the end of each run. The distribution of nitrogen over biomass and liquid was obtained

Run	%O2	X (g/L)	N (F) (mg/L)	N (UF) (mg/L)	N in X	N in X (%)	N in L (%)
O2_21_1	21	0.82	125.31	141.65	16.34	1.99	88.46
O2_21_2	21	0.94	90.29	165	74.71	7.92	54.72
O2_21_3	21	1.02	115.97	141.65	25.68	2.51	81.87
Average						4.14	75.02
O2_35_1	35	1.06	80.96	150.99	70.03	6.63	53.62
O2_35_2	35	0.96	115.97	195.35	79.38	8.24	59.37
O2_35_3	35	0.83	101.97	127.64	25.67	3.08	79.89
Average						5.98	64.29
O2_7_1	7	0.78	106.63	136.98	30.35	3.89	77.84
O2_7_2	7	0.82	71.62	111.30	39.68	4.86	64.35
O2_7_3	7	0.68	80.96	118.31	37.35	5.51	68.43
Average						4.75	70.21

An estimate C:N ratio of the supernatent could be calculated based on NPOC and Total Nitrogen test results. Table 11 shows the results for each experimental condition.

Table 11: Estimated C:N ratios for liquid fraction of the culture broth based on experimental results. This does not include volatile byproducts, IPS, and EPS.

Sample	NPOC (mg/L)	N (F) (mg/L)	C:N
O2_21_1	79.06	125.31	0.63
O2_21_2	361.35	90.29	4.00
O2_21_3	104.89	115.95	0.90
Avg			2.04
O2_35_1	122.04	80.98	1.51
O2_35_2	120.62	115.97	1.04
O2_35_3	91.70	101.97	0.90
Avg			1.15
O2_7_1	195.10	106.63	1.83
O2_7_2	94.61	71.62	1.32
O2_7_3	71.18	80.96	0.88
Avg			1.34

Both TOC and TN showed low values of < 200 mg/L and < 20 mg/L, respectively. This was deemed excellent from a water treatment point of view and indicates a high selectivity towards biomass production. Figure 29 shows the resulting C:N ratios, where the C:N of O2_21_2 was deemed an outlier. These results confirm the hypothesis that much of the carbon was converted to sessile biomass, IPS or EPS.

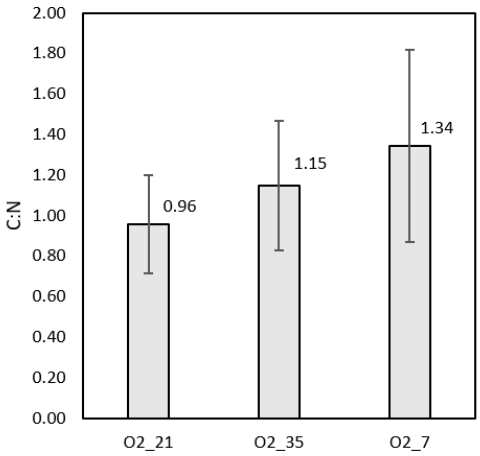

Figure 29: The C:N ratios at each condition were between 1 - 2. Differences between conditions could be attributed to varying malic acid concentrations and ETC down-regulation, which would increase carbon dioxide formation. The error bars indicated the standard deviations of each set of results.

4.5.2 Next-generation DNA sequencing results

Species identification was done through next-generation DNA sequencing. The cultures (from each experimental condition) were found to have no fungal infections. For each culture sample 50 to 100 different species were identified. There were, however, few species which dominated the microbial consortium. These species made up 60 % - 70 % of the cultures. The dominant species matched across experimental conditions, however, depending on oxygen-availability they were present in slightly different percentages. Table 12 shows a summary of the species that made up the largest part of the consortia.

From the read count in the metagenomic information, it was clear that *Chryseobacterium* ssp. and *Flavobacterium* ssp. made up approximately 50 % of the bacterial communities. This showed that the experimental conditions targeted nitrogen-fixing species successfully. In addition, the composition of the cultures showed that most of the dominating species were most commonly found in soil (Dhole, Shelat & Deepak, 2017; Giri & Pati, 2004; Naqqash *et al*, 2020; Kaminski *et al*, 1991) with intrinsic sensitivities to oxygen therefore negating the likelihood of air-borne contamination. This strongly indicated that the cultured bacteria were indeed retrieved from the soil samples. The Bary-Curtis dissimilarity index (Equation 10) was calculated over at least 84 % and 87 % of the total species count of the two aerobic culture data sets (O2_21 and O2_35), where counts of unknown species were omitted. The index was computed as 0.284 which implies there was a significant similarity (71.6 %) between the data sets. The high similarity indicates that the consortium was relatively stable at these conditions. Due to the low read count measured for the O2_7 run sample (supplementary material) the Bary-Curtis dissimilarity index could not be computed for this condition, however, the ngDNA report indicated very similar species were identified as the aerobic runs providing qualitative support for the stability of the consortium under low aeration conditions. The overall culture profile, however, was similar for all three conditions. Figure 30 to 32 show the results for each experimental condition. Full meta-genomic reports are included in Appendix C. Table 12 shows an overview of the characteristics of the most prevalent bacterial strains.

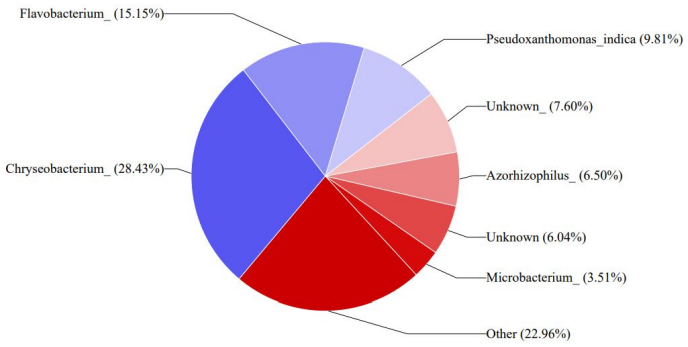

Figure 30: Overview of species under condition O2_21

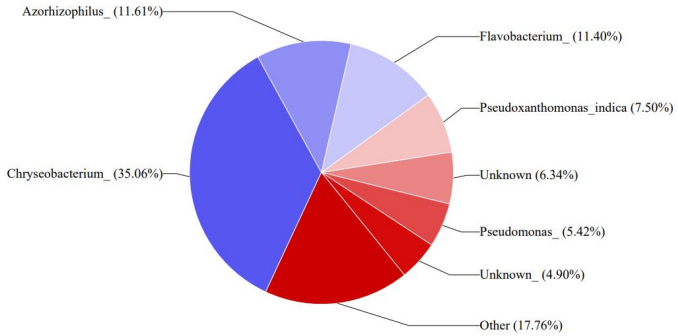

Figure 31: Overview of species under condition O2_35

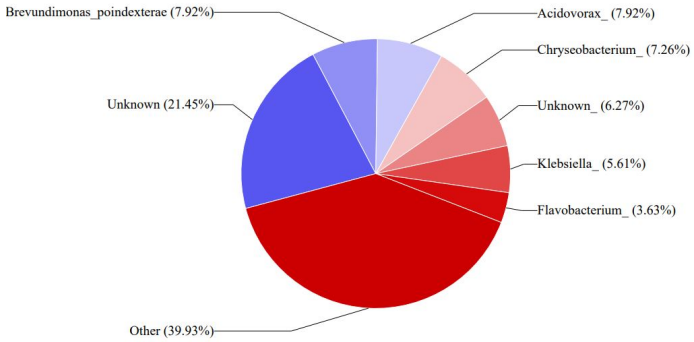

Figure 32: Overview of species under condition O2_7

The hypothesis of PHA/PHB production, as discussed in Section 5.2, was also re-enforced by the fact that at least 20 % - 30 % of each culture consisted of PHA/PHB producers. This number was likely higher, however, a large count of an unknown genus was reported for all three samples. The small amount of malic acid production could be attributed to the unknown species which might be known producers of this organic acid. Alternatively, it could be produced from an incomplete TCA-cycle in any of the species under glucose overflow conditions.

Table 12: Summary of most prominent bacteria species in the experimental cultures

Species	Description	Environment	N_2-fixing	PHA/PHB	References
Chryseobacterium	Gram-negative, yellow bacterium commonly found in soil. The bacterium also produces plant-promoting growth hormones.	Aerobic	Yes	-	(Dhole, Shelat & Deepak, 2017; Calderón *et al*, 2011)
Flavobacterium	Gram-negative, rod-shaped bacterium found in soil and fresh water.	Aerobic	Yes	-	(Giri & Pati, 2004)
Pseudoxanthomonas	Gram-negative, rod-shaped bacterium	Aerobic	No	Producing	(De Donno Novelli, Moreno & Rene, 2021)
Azorhizophilus	Rhizobial bacterium capable of fixing nitrogen both symbiotically and in free-living conditions.	Aerobic	Yes	Producing	(Kaminski *et al*, 1991; Jurat-Fuentes & Jackson, 2012)
Microbacterium	Gram-positive, heterotrophic bacterium	Aerobic	Yes	Producing	(Gtari *et al*, 2012; Osman, Elrazak & Khater, 2016; Orozco-Medina, López-Cortés & Maeda-Martínez, 2009)
Pseudomonas	Plant-growth promoting bacterium. Posseses adaptation strategy for anaerobic environments.	Aerobic	Yes	Producing	(Ali & Jamil, 2017; Jurat-Fuentes & Jackson, 2012)
Brevundimonas	Root colonizing bacterium which also facilitates effective phosphate solubization for enhanced plant growth.	Aerobic	Yes	Producing	(Naqqash *et al*, 2020; Bhuwal *et al*, 2013)
Agrobacterium	Gram-negative, rod-shaped bacterium	Aerobic	Yes	Degrading	(Nojima, Mineki & Iida, 1996; Van Montagu & Zambryski, 2017; Earth Observing System, 2021)
Acidovorax	Gram-negative with nitroaromatic degradation ability	Aerobic	Yes	Degrading	(Rai, Solanki & Anal, 2021; UniProt, 2021)
Klebsiella	Gram-negative, heterotrophic soil bacterium	Aerobic	Yes	Producing	(Feng, Feng & Shu, 2018; Apparao & Krishnaswamy, 2015)

5 Modelling

5.1 Mass balance

To investigate the trends in the experimental data more closely, a mass balance was performed for all three conditions. Two different approaches were used. The first approach assumed that all unaccounted for carbon was spent on biofilm formation. The second approach adjusted the biomass formation by a fudge factor of 1.2 to account for some biofilm, however, the unaccounted for carbon was attributed to PHB formation. The carbon-sink was chosen as PHB, since Oelze (2000) mentioned the storage of glucose as PHB in *A. vinellandi*. In addition, a large part of the active species within the culture, are capable of PHA/PHB production for energy storage. Both approaches were explored in an attempt to explain the observed growth behaviour. Section 5.3 elaborates on the purpose and limitations of the modelling approaches.

5.1.1 Approach 1: Biofilm as a carbon-sink

Equation 13 shows the overall reaction that was utilized for the mass transfer limited regime. The cmol equivalent of each carbon compound were utilized to solve the mass balance. The biofilm was modelled as cellulose ($CH_{5/3}O_{5/6}$).

$$CH_2O + O_2 + N_2 \rightarrow CH_{1.8}O_{0.5}N_{0.08} + CH_{3/2}O_{5/4} + CO_2 + H_2O + CH_{5/3}O_{5/6} \tag{13}$$

From this equation an 7x7-matrix (Equation 5.1.1) was set up and three specifications were used from the experimental data. The specifications included: the glucose consumption rate (r_s); the oxygen consumption rate (r_{O2}); and the biomass production rate(r_x). The biomass formation was based on suspended biomass measurements. It was assumed that malic acid rates played a negligible role during mass-transfer limited growth. Table 14 shows the solution to the mass balance for each condition in cmmol/L.h. Table 13 shows the specifications used in the mass balance calculation.

$$S = \begin{bmatrix} -1 & 0 & 0 & 1 & 1 & 0 & 1 \\ -2 & 0 & 0 & 1.8 & 0 & 2 & 5/3 \\ -1 & -2 & 0 & 0.5 & 2 & 1 & 5/6 \\ 0 & 0 & -2 & 0.08 & 0 & 0 & 0 \\ -1 & 0 & 0 & 0 & 0 & 0 & 0 \\ 0 & -1 & 0 & 0 & 0 & 0 & 0 \\ 0 & 0 & 0 & 1 & 0 & 0 & 0 \end{bmatrix} \times \begin{bmatrix} 0 \\ 0 \\ 0 \\ 0 \\ r_s \\ r_{O2} \\ r_x \end{bmatrix}$$

Table 13: Specifications utilized in the mass balance for approach 1. The suspended biomass readings were used for biomass growth rates.

Condition	r_s (cmol/L.h)	r_{O2} (cmol/L.h)	r_x (cmol/L.h)
O2_21	0.0087	0.0023	0.0032
O2_35	0.013	0.0038	0.0036
O2_7	0.0069	0.00082	0.0012

Table 14: Solution to the mass balance at various experimental conditions, assuming biofilm is the sole carbon sink at no additional ATP cost

Condition	O2_21 (cmol/L.h)	O2_35 (cmol/L.h)	O2_7 (cmol/L.h)
r_s	8.72	13.10	6.89
r_{O2}	2.31	3.82	0.82
r_{N2}	0.13	0.14	0.05
r_x	3.19	3.58	1.20
r_{CO2}	2.95	4.53	1.06
r_{H2O}	3.70	5.73	1.96
$r_{biofilm}$	2.57	4.98	4.61

5.1.2 Approach 2: PHB as a carbon-sink

Equation 14 shows the overall reaction that was utilized for the mass-transfer limited regime. The cmol equivalent of each carbon compound were utilized to solve the mass balance. The PHB was modelled as its monomer ($CH_{3/2}O_{1/2}$).

$$CH_2O + O_2 + N_2 \rightarrow CH_{1.8}O_{0.5}N_{0.08} + CH_{3/2}O_{5/4} + CO_2 + H_2O + CH_{3/2}O_{1/2} \tag{14}$$

A 7x7-matrix was set up where biomass production rate was taken as the average slope multiplied by 1.2. The multiplication was done to account for biofilm formation.Table 15 shows the numerical specifications utilized for each conditions. All values are in units of cmol/L.h. As in approach 1, malic acid rates found to be negledgible. The matrix shown in Equation 5.1.2 was utilized to solve the mass balance. Table 16 shows the solution to the mass balance for each condition in cmmol/L.h.

$$S = \begin{bmatrix} -1 & 0 & 0 & 1 & 1 & 0 & 1 \\ -2 & 0 & 0 & 1.8 & 0 & 2 & 3/2 \\ -1 & -2 & 0 & 0.5 & 2 & 1 & 1/2 \\ 0 & 0 & -2 & 0.08 & 0 & 0 & 0 \\ -1 & 0 & 0 & 0 & 0 & 0 & 0 \\ 0 & -1 & 0 & 0 & 0 & 0 & 0 \\ 0 & 0 & 0 & 1 & 0 & 0 & 0 \end{bmatrix} \times \begin{bmatrix} 0 \\ 0 \\ 0 \\ 0 \\ r_s \\ r_{O2} \\ r_x \end{bmatrix}$$

Table 15: Specifications utilized in the mass balance.

Condition	r_s (cmol/L.h)	r_{O2} (cmol/L.h)	r_x (cmol/L.h)
O2_21	0.0087	0.0023	0.0038
O2_35	0.013	0.0038	0.0043
O2_7	0.0069	0.00082	0.0015

Table 16: Solution to the mass balance at various experimental conditions, assuming PHB is the sole byproduct of significance.

Condition	O2_21 (cmol/L.h)	O2_35 (cmol/L.h)	O2_7 (cmol/L.h)
r_s	8.72	13.10	6.89
r_{O2}	2.31	3.82312	0.82
r_{N2}	0.15	0.17	0.06
r_x	3.83	4.29	1.45
r_{CO2}	3.28	5.14	1.59
r_{H2O}	4.07	6.48	2.70
r_{PHB}	1.61	3.67	3.85

5.1.3 Comparison between approaches

When looking at the results between the two approaches, it is clear that the composition of the carbon sink (biofilm in approach 1 and PHB in approach 2) affects the rates of consumption and production of both water and carbon-dioxide. This is due to the fact that the biofilm and PHB have different elemental compositions. PHB production consumes less oxygen than biofilm production. This means that in PHB production, oxygen must go towards other products such that the mass balance is balanced.

5.2 Energy balance

To support the argument of down-regulation of ATP in the microbes, the system was modelled using the results obtained from experimental work. The microbial culture was modelled as a whole for simplicity and thus, the behaviour of individual bacterial strains was neglected. The model assumed only biofilm (approach 1) or polyhydroxybutyrate (PHB) (approach 2) was produced as a significant byproduct during mass transfer limited growth and the following biomass formula was used: $CH_{1.8}O_{0.5}N_{0.08}$. The model was utilised to calculate the P/O-ratio for each condition. The oxygen uptake rate (OUR) in mol/L.h was calculated using Equation 15. The dissolved oxygen concentration in mol/L at saturation was adjusted for the various oxygen partial pressures. The gas-liquid mass transfer coefficient (kla) in h^{-1} was determined experimentally. The average OUR was calculated at each O2_21 and the mass transfer coefficient was adjusted proportionally to each oxygen composition. Figure 33 shows the OUR profiles at each condition.

$$OUR = kla \times (DO_{sat} - DO) - \frac{\delta DO}{\delta t} \tag{15}$$

All oxygen was assumed to be utilised in oxidative phosphorylation (OP). Thus, the oxygen uptake was assumed to be responsible for all ATP generation. To calculate the overall ATP requirement, Equation 16 was utilised. Where the ATP requirement for growth, γ, was assumed to be 2.5 ATP/cmol biomass. The energy cost of nitrogen fixation was assumed to be the theoretically reported value of 16 ATP/N_2. The rate of nitrogen fixation (r_{N_2}) was determined from the rate of biomass production (r_X) in the mass balance. The rate of biomass production was averaged for each O2_21 and utilized in the calculations. Since, ammonia excretion was very low in all runs (<20 mg/L), the nitrogen requirement for ammonia was omitted in the model.

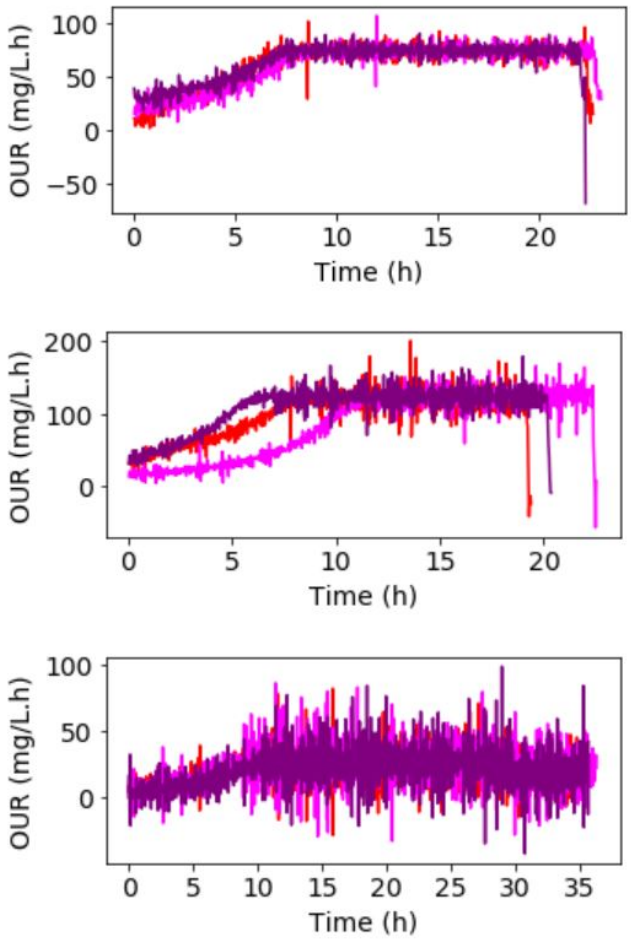

Figure 33: The oxygen uptake profiles for O2_21 (top), O2_35 (middle), and O2_7 (bottom) are shown. The OUR at the mass-transfer limited regime was utilized during the energy balance.

It was assumed that biofilm production came at no additional ATP cost, however, the production of PHB requires glycolysis. Thus, it releases 2 ATP for each glucose consumed. One monomer of PHB consists of two moles of condensed acetyl-CoA. This means that for each monomer of PHB produced, one mole of glucose is consumed. Since the monomer formula for PHB was taken as $C_4H_6O\_2$, there would be 0.5 ATP released for each cmol of PHB produced through the linear pathway of Acetyl-CoA condensation. The calculation of P/O was done for each condition over the mass-transfer limited regime.

$$2 \times P/O \times r_{O_2} - \gamma \times r_X - \beta \times r_{N_2} + 0.5 \times r_{PHB} = 0 \tag{16}$$

Table 17 shows the calculated P/O-ratios for each experimental condition. A clear distinction between high and low oxygen compositions is present. For approach 1, the expected result according to the theory presented by Oelze (2000) is found. The higher oxygen availability results in down-regulation. This shows that oxygen supply could be throttled and controlled to achieve optimal growth at the maximum energy efficiency. For approach 2, the significantly lower calculated P/O at O2_35 is supported by the down-regulation discussed by Oelze (2000) as well. Here, the reason for down-regulation under the low oxygen

condition is due to the supply of energy through PHB production, which would result in too much ATP if the ETC would not down-regulate. This still indicates that the oxygen availability should be controlled, as a high selectivity towards biomass is preferred.

Table 17: The calculates P/O-ratios at each condition show down-regulation occurred during both oxygen-rich and oxygen-poor aeration.

P/O	Approach 1	Approach 2
O2_21	2.16	2.43
O2_35	1.47	1.52
O2_7	2.30	1.94

5.3 Model limitations and intention

While two different approaches were followed for the mass and energy balance, the results are largely based on assumptions. Due to the observation of biofilm during all experimental runs, the first approach attributed lost carbon to biofilm. The second approach was based the mentioning of PHB by (Oelze, 2000) and the large amount of active species possessing a PHA/PHB storage mechanisms. The storage of glucose as PHB under the oxygen-limited conditions was viewed as a realistic condition as it is widely described in literature (Section 2).

There was a necessity for simplification due to the complex nature of the consortium. The main conclusion from the mass and energy balance was that if all carbon was channeled to biomass, with the same composition as suspended biomass, an unrealistically low energy requirement for biomass production would result. Thus, from the mass and energy balance, it was highly likely that a N-lean carbon sink was present. This carbon sink could be intracellular or extracellular in nature, however, its true composition remains unknown. In addition, the ATP cost of channelling glucose to a carbon sink was not estimated experimentally. In approach 2, PHB was modelled as an energy producing mechanism, whereas approach 1 contained an ATP-neutral carbon sink. In reality, the carbon sink might increase energy expenditure instead due to transporter costs and adjacent metabolic activities which were omitted by setting the cell maintenance term to zero. Therefore, the model should not be viewed as an explanation of the results, but rather a mathematical exploration into its possible causes of the observed behaviour. A myriad of mechanisms could be responsible for the observed results.

6 Conclusion and recommendations

In the current study a locally obtained soil diazotrophic microbial culture was successfully cultured in a non-sterile bench-scale bioreactor. This study provides one of the only known investigations evaluating the effect of operational conditions on BNF in this type of bioreactor. A repeatable culture was obtained and the effect of oxygen availability on the growth profile of the culture was investigated. From the experimental data, it was concluded that aeration feed composition had a significant effect on the growth profile of the diazotrophic culture studied. A mass-transfer limited regime was reached for all conditions, where oxygen availability directly controlled the growth rate. Increased oxygen availability, however, did not proportionally increase the growth rate as the energy requirements were affected. This was likely due to ETC down-regulation and nitrogenase protection mechanisms against oxygen-stress. Glucose was found to be less efficiently utilized towards biomass under oxygen-poor conditions. This was attributed a high production of IPS and EPS carbon sinks under oxygen-poor conditions. In conclusion, there was an optimal oxygen feed rate which ensured the most efficient metabolism for the diazotrophic culture. The most efficient growth occured at condition O2_21. The supernatent was found to be virtually clean, with little to no carbon and nitrogen-compounds present. This confirmed that part of the glucose was channeled to a carbon sink in the form of IPS or EPS. The metagenomic data showed that the largest portion of the microbial population were aerobic nitrogen-fixers. The dominating species were *Chryseobacterium* ssp. and *Flavobacterium* ssp..

The energy effect under varying operating conditions was explored through two modelling approaches. Both approaches showed a lower P/O-ratio for oxygen-rich conditions compared to atmospheric air under the assumption of a N-free carbon sink with no additional ATP cost.

In future experiments, a control and throttling of oxygen into the system could generate an optimal growth environment with high selectivity towards biomass and optimal energy usage. A controlled aeration system would optimize oxygen supply and thus, increase yield and productivity. In addition, fed-batch experiments should be performed in order to learn more about the diazotrophic culture behaviour and their response to byproduct build-up. Another opportunity is the symbiosis of diazotrophs with lignocellulolytic and cellulolytic micro-organisms. The co-inoculation of these micro-organisms would act as fertilizer, soil conditioner and bio-control agent. Diazotrophs can provide the nitrogen needed in lignocellulose breakdown while utilising the breakdown products as a carbon source. This could eliminate expensive carbon-sources from the diazotrophic growth process and thus, improve the sustainability of the process.

References

Ali, I and Jamil, N (2017) "Biosynthesis and genetics of polyhydroxyalkanoates by newly isolated Pseudomonas aeruginosa IFS and 30N using inexpensive carbon sources" *International journal of Environmental Science and Technology*, *14*, (9): 1–10.

Altieri, M and Nicholls, C (2012) "Agroecology Scaling Up for Food Sovereignty and Resiliency" *Sustainable agriculture reviews*, *11*, 1–29.

Apparao, A and Krishnaswamy, V (2015) "Production of Polyhydroxyalkanoate (PHA) by a Moderately Halotolerant Bacterium Klebsiella pneumoniae U1 Isolated from Rubber Plantation Area" *International Journal of Environmental Bioremediation Biodegradation*, *3*, (2): 54–61.

Arashida, H, Kugenuma, T, Watanabe, M and Maeda, I (2019) "Nitrogen fixation in Rhodopseudomonas palustris co-cultured with Bacillus subtilis in the presence of air" *Journal of Bioscience and Bioengineering*, *127*, (5): 589–593.

Augimeri, R, Varley, A and Strap, J (2015) *Establishing a Role for Bacterial Cellulose in Environmental Interactions: Lessons Learned from Diverse Biofilm-Producing Proteobacteria*.

Bailey, W (2011) *Biofilms: Formation, Development and Properties*, Nova Science Publishers, New York.

Bali, A, Blanco, G, Hill, S and Kennedy, C (1992) "Excretion of Ammonium by a nifL Mutant of Azotobacter vinelandii Fixing Nitrogen" *Applied and Environmental Microbiology*, *58*, (5): 1711–1718.

Balsanelli, E, Baura, V de, Oliveira Pedrosa, F de, Souza, E de and Monteiro, R (2014) "Exopolysaccharide Biosynthesis Enables Mature Biofilm Formation on Abiotic Surfaces by Herbaspirillum seropedicae" (9).

Barney, B, Plunkett, M, Natarajan, V, Mus, F, Knutson, C and Peters, J (2017) "Transcriptional Analysis of an AmmoniumExcreting Strain of Azotobacter vinelandii Deregulated for Nitrogen Fixation" *Applied and Environmental Microbiology*, *83*, (20): 1–22.

Bentzon-Tilia, M, Farnelid, H, Jurgens, K and € Riemann, L (2014) "Cultivation and isolation of N2-fixing bacteria from suboxic waters in the Baltic Sea" *FEMS Microbiology Ecology*, (88): 358–371.

Bhuwal, A, Singh, G, Aggarwal, K, Goyal, V and Yadav, A (2013) "Isolation and Screening of Polyhydroxyalkanoates Producing Bacteria from Pulp, Paper, and Cardboard Industry Wastes" *International journal of biomaterials*, *2013*, 1–10.

Brewin, B, Woodley, P and Drummond, M (1999) "The Basis of Ammonium Release in nifL Mutants of Azotobacter vinelandii" *Journal of Bacteriology*, *181*, (23): 7356–7362.

BYJU's (2021) *Nitrogen* URL: `https://byjus.com/chemistry/nitrogen/`.

Cacciari, M, Del Gallo, M, Ippoliti, S, Lippi, D, Pietrosanti, T and Pietrosanti, W (1986) "Growth and survival of Azospirillum brasilense and Arthrobacter giacomelloi inbinary continuous culture" *Plant and soil*, *90*, (1): 107–116.

Calderón, G, García, E, Rojas, P, García, E, Rosso, M and Losada, A (2011) "Chryseobacterium indologenes infection in a newborn: a case report" *Journal of Medical Case Reports*, *5*, (10): 1–3.

Cohen, G and Johnstone, D (1963) "Acid Production by Azotobacter vinelandii" *Nature*, *198*, 211.

De Donno Novelli, L, Moreno, S and Rene, E (2021) "Polyhydroxyalkanoate (PHA) production via resource recovery from industrial waste streams: A review of techniques and perspectives" *Bioresource Technology*, *331*,

Dedkova, E and Blatter, L (2014) "Role of β-hydroxybutyrate, its polymer poly-β-hydroxybutyrate and inorganic polyphosphate in mammalian health and disease" *Frontiers in Physiology*, *5*, 260.

Dhole, A, Shelat, H and Deepak, P (2017) "Chryseobacterium indologenes A Novel Root Nodule Endophyte in Vigna radiata" *International Journal of Current Microbiology and Applied Sciences*, *6*, (4): 836–844.

Díaz-Barrer, A, Rodrigo, A, Martíne, I and Peña, C (2016) "Poly-3-Hydroxybutyrate Production by Azotobacter Vinelandii Strains in Batch Cultures at Different Oxygen Transfer Rates" *Journal of Chemical Technology and Biotechnology*, *91*, 1063–1071.

Dreschel, T (2018) *Hydroponics* URL: https://www-accessscience-com.uplib.idm.oclc.org/content/hydroponics/330600.

Earth Observing System (2021) *Nitrogen Fixation: N-Fixing Plants And Bacteria* URL: https://eos.com/blog/nitrogen-fixation/.

Environmental Protection Agency (2021) *Technical Overview of Volatile Organic Compounds* URL: https://www.epa.gov/indoor-air-quality-iaq/technical-overview-volatile-organic-compounds#:~:text=Volatile%5C%20organic%5C%20compounds%5C%20%5C%28VOC%5C%29%5C%20means%5C%20any%5C%20compound%5C%20of,by%5C%20EPA%5C%20as%5C%20having%5C%20negligible%5C%20photochemical%5C%20reactivity%5C%202..

Evans, A, Gallon, J, Jones, A, Staal, M, Stal, L, Villbrandt, M and Walton, T (2000) "Nitrogen Fixation by Baltic cyanobacteria is adapted to the prevailing photon flux density" *New Phytologist*, (147): 285–295.

Feng, Y, Feng, J and Shu, Q (2018) "Isolation and characterization of heterotrophic nitrifying and aerobic denitrifying Klebsiella pneumoniae and Klebsiella variicola strains from various environments" *Journal of Applied Microbiology*, *124*, (5): 1195–1211.

Giri, S and Pati, B (2004) "A comparative study on phyllosphere nitrogen fixation by newly isolated Corynebacterium sp. Flavobacterium sp. and their potentialities as biofertilizer" *Acta Microbioly Immunoly Hungary*, *51*, (1): 47–56.

Gtari, M, Ghodhbane-Gtari, F, Nouioui, I, Beauchemin, N and Tisa, L (2012) "Phylogenetic perspectives of nitrogen-fixing actinobacteria" *Archibes of microbiology*, *194*, (1): 3–11.

Gupta, G, Panwar, J, Akhtar, M and Jha, P (2012) "Endophytic Nitrogen-Fixing Bacteria as Biofertilizer" *Sustainable agriculture reviews*, *11*, 183–221.

Gupta, R, Fletcher, D and Haynes, B (2010) "Taylor Flow in Microchannels: A Review of Experimental and Computational Work" *Journal of Computational Multiphase Flows*, *2*, (1): 1–31.

Haber Transport (2018) *Haber Bosch* URL: https://www.haber.co.za/haber-process/#:~:text=%5C%20Haber%5C%20Process%5C%20%5C%201%5C%20The%5C%20Haber%5C%20Process.,When%5C%20it%5C%20was%5C%20first%5C%20invented,%5C%20the...%5C%20More.

Halsall, D (1993) "Inoculation of wheat straw to enhance lignocellulose breakdown and associated nitrogenase activity" *25*, (4): 419–429.

Haury, J and Spillert, H (1981) "Fructose Uptake and Influence on Growth of and Nitrogen Fixation by Anabaena variabilis" *Journal of Bacteriology*, *147*, (1): 227–235.

Hester, R and Harrison, R (2012) *Soils and Food Security*, 1st ed. Royal Society of Chemistry, Cambridge: pp. i–vi.

Hill, N, Patriquin, D and Sircom, K (1990) "Increased oxygen consumption at warmer temperatures favours aerobic nitrogen fixation in plant litters" *Soil Biology and Biochemistry*, *22*, (3): 321–325.

Holl, C and Montoya, J (2008) "Diazotrophic growth of the marine cyanobacterium Trichodesmium IMS101 in continuous culture: effects of growth rate on N2-fixation rate, biomass, and C:N:P stoichiometry" *Journal of Phycology*, *44*, (1): 929–937.

Huang, B, Feng, H, Wang, M, Li, N, Cong, Y and Shen, D (2013) "The effect of C/N ratio on nitrogen removal in a bioelectrochemical system" *Bioresource technology*, (132): 91–98.

Iwata, K, Azlan, A, Yamakawa, H and Omori, T (2010) "Ammonia accumulation in culture broth by the novel nitrogen-fixing bacterium, Lysobacter sp. E4" *Journal of Bioscience and Bioengineering*, *110*, (4): 415–418.

Jurat-Fuentes, J and Jackson, T (2012) *Chapter 8 - Bacterial Entomopathogens*, 2nd ed. Academic Press: pp. 265–349.

Kaminski, P, Mandon, K, Arigoni, F, Desnoues, N and Elmerich, C (1991) "Regulation of nitrogen fixation in Azorhizobium caulinodans: identification of a fixK-like gene, a positive regulator of nifA." *Molecular Microbiology*, *5*, (8): 1983–1991.

Kennedy, I, Choudhury, A and Kecskes, M (2004) "Non-symbiotic bacterial diazotrophs in crop-farming systems: can their potential for plant growth promotion be better exploited?" *Soil biology biochemistry*, (36): 1229–1244.

Kloss, M, Imannek, K and Fendrick, I (1983) "Physiological properties of Azospirillium Brasilene Sp 7 in a malate limited chemostat" *Journal of General Applied Microbiology*, *29*, (1): 447–457.

Kozai, T, Niu, G and Takagaki, M (2015) *Plant Factory : An Indoor Vertical Farming System for Efficient Quality Food Production*, 1st ed. Elsevier Science and Technology, Amsterdam: pp. 1–10.

Kumar, R and Cho, J (2014) "Reuse of hydroponic waste solution" *Environmental Science and Pollution Research*, *21*, (16): 9569–9577.

Kuypers, M, Marchant, H and Kartal, B (2018) "The microbioal nitrogen-cycling network" *Nature reviews*, 1–14.

Lexow, W (2019) *Identifying Energy Extraction Optimisation Strategies for A. succinogenes* Department of Chemical Engineering, University of Pretoria, 26-27.

Li, S, Peng, C, Wang, C, Zheng, J, Hu, Y and Li, D (2017) "Microbial Succession and Nitrogen Cycling in Cultured Biofilms as Affected by the Inorganic Nitrogen Availability" *Microbial Ecology*, (73): 1–15.

Lynch, J and Harper, S (1985) "The Microbial Upgrading of Straw for Agricultural Use" *Philosophical Transactions of the Royal Society of London*, *310*, (1144): 221–226.

Mahanty, T, Bhattacharjee, S, Goswami, M, Bhattacharyya, P, Das, B, Ghosh, A and Tribedi, P (2018) "Biofertilizer: a potential approach for sustainable agricultural development" *Environmental Science Pollution Resolutions*, (24): 3315–3335.

McInnes, A, Shepard, A, Raes, E, Waite, A and Quigg, A (2014) "Simultaneous Quantification of Active Carbon- and Nitrogen-Fixing Communities and Estimation of Fixation Rates Using Fluorescence In Situ Hybridization and Flow Cytometry" *Applied and Environmental Microbiology*, *80*, (21): 6750–6759.

Merck KGaA (2021) *Nitrogen (total) Cell Test* data retrieved from https://www.sigmaaldrich.com/ZA/en/product/mm/10061

Mukhtar, H, Bashir, H, Nawaz, A and Haq, I (2018) "Optimization of growth conditions for Azotobacter species and their use as biofertilizer" *Journal of Bacteriology and Mycology*, *6*, (5): 274–278.

Nagai, S, Nishizawa, Y and Aiba, S (1969) "Energetics of Growth of Azotobacter vinelandii in a Glucose-limited Chemostat Culture" *Journal of General Microbiology*, *59*, (1): 163–169.

Naqqash, T, Imran, A, Hameed, S, Shahid, M, Majeed, A, Iqbal, J, Hanif, M and Ejaz S Malik, K (2020) "First report of diazotrophic Brevundimonas spp. as growth enhancer and root colonizer of potato" *Scientific reports*, *10*,

Nojima, S, Mineki, S and Iida, M (1996) "Purification and characterization of extracellular poly(3-hydroxybutyrate) depolymerases produced by Agrobacterium sp. K-03" *Journal of Fermentation and Bioengineering*, *81*, (1): 72–75.

OECD, OfECoD (2018) *Human acceleration of the nitrogen cycle : managing risks and uncertainty*, IWA Publishing, London.

Oelze, J (2000) "Respiratory protection of nitrogenase in Azotobacter species: is a widely held hypothesis unequivocally supported by experimental evidence?" *FEMS Microbiology reviews*, *24*, 321–333.

Orozco-Medina, C, López-Cortés, A and Maeda-Martínez, A (2009) "Aerobic Gram-positive heterotrophic bacteria Exiguobacterium mexicanum and Microbacterium sp. in the gut lumen of Artemia franciscana larvae under gnotobiotic conditions" *Current Science*, *96*, (1): 120–129.

Osman, Y, Elrazak, A and Khater, W (2016) "ioprocess Optimization of Microbial Biopolymer Production" *Journal of Biobased Materials and Bioenergy*, *10*, 1–10.

PacBio (2018) *Procedure Checklist - Full-Length 16S Amplification, SMRTbell^R Library Preparation and Sequencing* data retrieved at https://dnatech.genomecenter.ucdavis.edu/wp-content/uploads/2018/07/PacBio-Full-Length-16S-Sequencing-Protocol-June2018.pdf.

Padilla-Córdova, C, Mongili, B, Contreras, P, Fino, D, Tommasi, T and Díaz-Barrera, A (2020) "Productivity and scale-up of poly03-hydroxybutyrate production under different oxygen transfer conditions in cultures of Azotobacter vinelandii" *Journal of Chemical Technology and Biotechnology*, *95*, 3034–3040.

Pankievicz, V, Irving, T, Maia, L and Ané, J (2019) "Are we there yet? The long walk towards the development of efficient symbiotic associations between nitrogen-fixing bacteria and non-leguminous crops" *BMC Biology*, *17*, (99): 1–17.

Pappu, A, Bhattacharjee, A, Dasgupta, S and Goel, R (2017) "Nitrogen Cycle in Engineered and Natural Ecosystems—Past and Current" *Current Pollution Reports*, (3): 120–140.

Pedersen, J, Bombar, D, Paerl, R and Riemann, L (2018) *Diazotrophs and N2-fixation associated with particles in coastal eustarine waters.*

Population Action International (2011) "Why population matters to food security" *Population Action International*, 1–4.

Prashad, J, Suneja, S, Kukreja, K and Lakshminarayana, K (2001) "Poly-3-hydroxybutyrate production by Azotobacter chroococcum" *Folia microbiologica*, *46*, 315–320.

Rago, L, Zecchin, S, Villa, F, Goglio, A, Corsini, A, Cavalca, L and Schievano, A (2019) "Bioelectrochemical Nitrogen fixation (e-BNF): Electro-stimulation of enriched biofilm communities drives autotrophic nitrogen and carbon fixation" *Bioelectrochemistry*, (125): 105–115.

Rai, S, Solanki, A and Anal, A (2021) *Modern biotechnological tools: an opportunity to discover complex phytobiomes of horticulture crops*, Academic Press: pp. 85–124.

Rice, W and Paul, E (1971) "The acetylene reduction assay for measuring nitrogen fixation in waterlogged soil1" *Canadian Journal of Microbiology*, *17*, 1049–1056.

Romero-Perdomo, F, Camelo-Rusinque, M, Criollo-Campos, P and Bonilla-Buitrago, R (2015) "Effect of temperature and pH on the biomass production of Azospirillum brasilense C16 isolated from Guinea grass" *Pastos y Forraje*, *38*, (3): 231–233.

Serra, D and Hengge, R (2019) *Cellulose in Bacterial Biofilms*, vol. 12 Springer.

Smercina, D, Evans, S, Friesen, M and Tiemanna, L (2019) "To Fix or Not To Fix: Controls on Free-Living Nitrogen Fixation in the Rhizosphere" *Applied and environmental microbiology*, *86*, (6): 1–14.

Somerfield, P (2008) "Identification of the Bray-Curtis similarity index: Comment on Yoshioka" *Marine Ecology Progress Series*, *372*, 303–306.

Terpolilli, J, Hood, G and Poole, P (2012) "What Determines the Efficiency of N2-Fixing Rhizobium-Legume Symbioses?" *Advances in Microbial Physiology*, (60): 325–389.

Ullah, A, Mushtaq, H, Ali, H, Munis, M, Javed, M and Chaudhary, H (2015) "Diazotrophs-assisted phytoremediation of heavy metals: a novel approach" *Environmental Science and Pollution Research*, *22*, 2505–2514.

UniProt (2021) *Proteomes - Acidovorax sp. (strain JS42)* URL: `https://www.uniprot.org/proteomes/UP000000645`.

Van Montagu, M and Zambryski, P (2017) *Agrobacterium and Ti Plasmids*, Elsevier.

Wang, D, Xu, A, Elmerich, C and Ma, L (2017) "Biofilm formation enables free-living nitrogen-fixing rhizobacteria to fix nitrogen under aerobic conditions" *The ISME journal*, (11): 1602–1613.

Welz, P, Ramond, J, Braun, L, Vikram, S and Le Roes-Hill, M (2018) "Bacterial nitrogen fixation in sand bioreactors treating winery wastewater with high carbon to nitrogen ratio" *Journal of Environmental Management*, (207): 192–202.

Yu, S, Kyaw, E, Lynn, T mar, Latt, Z, Aung, A, Sev, T, Nwe, M and Mon, W (n.d.) "The correlation of carbon source and ammonium accumulation in culture broth by nitrogen-fixing bacterial isolates" *Journal of Scientific and Innovative Research*, *6*, (2): 63–67.

Zang, C, Huang, S, Wu, M, Du, S, Scholz, M, Gao, F, Lin, C, Guo, Y and Dong, Y (2011) "Comparison of Relationships Between pH, Dissolved Oxygen and Chlorophyll a for Aquaculture and Non-aquaculture Waters" *Water, Air Soil Pollution*, *219*, 157–174.

Zhou, L, Wang, X, Ren, W, Xu, Y, Zhao, L, Zhang, Y and Teng, Y (2020) "Contribution of autochthonous diazotrophs to polycyclic aromatic hydrocarbon dissipation in contaminated soils" *Science of the Total Environment*, *719*, 137410.

A Appendix A: Test kit and instrument calibration

To calibrate the N-compound test kits, known amounts of ammonia and nitrogen were dissolved in distilled water and tested with the ammonia and total nitrogen test kits. The results were used to set up a calibration curve. The calibration curve for the ammonia test kit is seen in Figure A.34. Equation 17 shows the equation to convert the absorbance reading (A) of the total nitrogen tests to nitrogen concentration (X_n).

$$X_n = 233.45 \times (A - 0.177) + 15 \tag{17}$$

To calibrate the Brooks instruments for gas flow rates, a simple burette test was used. The input signal to the Brookes instruments was controlled through a potentiometer which was manually adjusted to alter the current to the Brooks instruments. The Brooks instruments would then read out different signals to the Arduino MEGA 2650 which were used for calibration. These signals varied from 14.00 to 102.00. A burette was filled with water and submerged. For each input signal to the Brooks instruments, the displacement of water in the burette was timed. This showed a linear relationship between input signal to the Brooks instrument and the gas flow rate. Figure A.35 and A.36 show the resulting calibration curves for the Brooks flow regulators for nitrogen and oxygen gas, respectively. The nitrogen flow rate calibration was based on a nitrogen pressure of 200 kPa, whereas the oxygen pressure for which the Brooks controller was calibrated was 500 kPa.

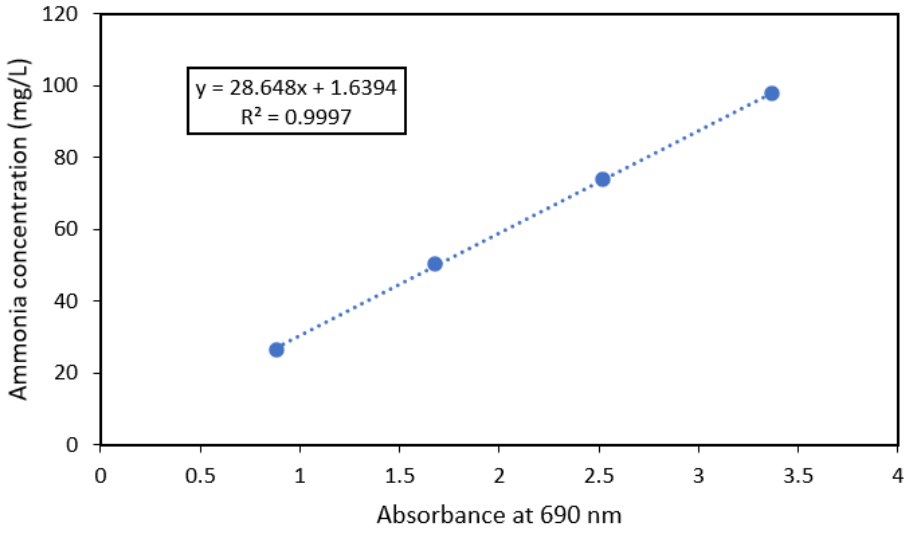

Figure A.34: A linear relationship was found between ammonia concentration and absorbance readings at 690 nm.

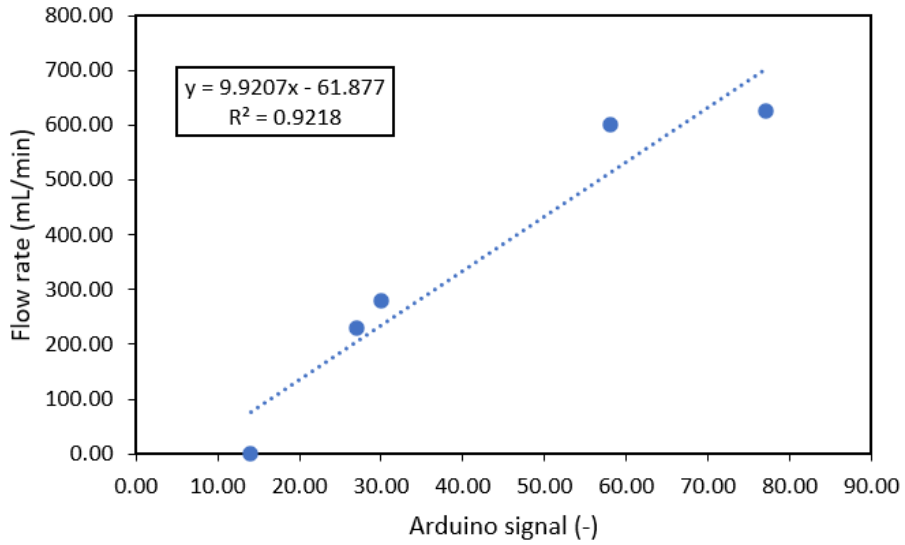

Figure A.35: The calibration curve of pure nitrogen through the the Brooks flow controller was found to be fairly linear.

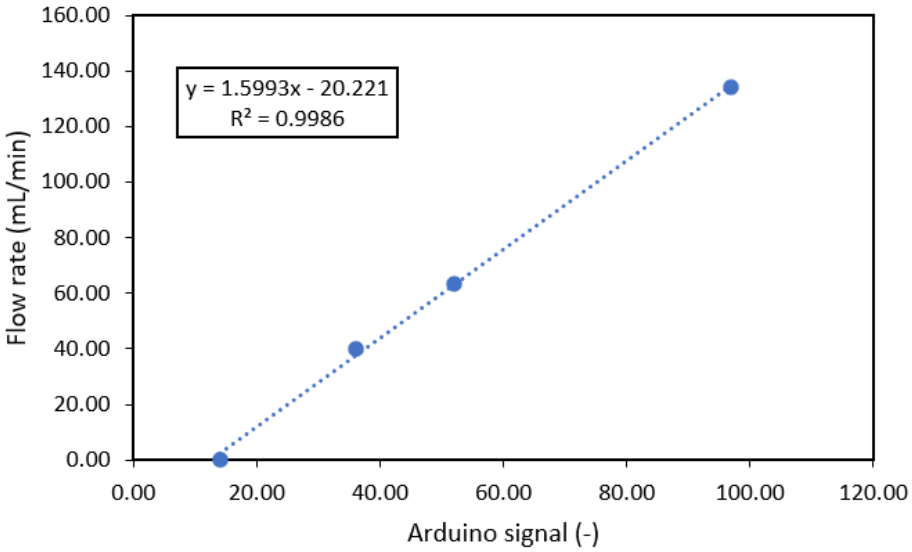

Figure A.36: The calibration curve of oxygen flow through the Brooks flow controller was found to be linear.

B Appendix B: Carbon analysis verification

During the course of experiments, several carbon analyses were performed. Organic acids and glucose were measured on a high-pressure liquid chromatographer (HPLC) and the total organic carbon (TOC) was determined on TOC analysis equipment using non-volatile organic carbon as an approximation for total organic carbon. Due to a contradiction in results, these methods were observed more closely.

B.1 HPLC analysis

To verify the accuracy of the HPLC in measuring malic acid (MA), several calibration solutions were made up. This was done by dissolving a known amount of malic acid in Burke's medium (5 g/L glucose). Two different methods were used on the HPLC during experiments, method A and method C. Method A was calibrated for acids specifically, whereas method C was calibrated for accurate glucose measurements. Table 18 shows the resulting readings of malic acid for the two methods. The Burke's medium contains phosphorus which might have interfered with the readings.

Table 18: Malic acid readings on the HPLC deviated significantly from the theoretical amounts under method A and C.

MA (g/L)	A method (g/L)	C method (g/L)	A method error (%)	C method error (%)
1.00	2.08	1.60	108.00	60.00
0.70	1.76	1.29	151.43	84.29
0.50	1.55	1.08	210.00	116.00
0.30	1.29	0.81	330.00	169.33
0.10	1.10	0.00	1000.00	-100.00

Method A overestimated the quantity of malic at each point. Method C did not pick up on malic acid at low concentrations as there was glucose in the system and the peaks overlap. Only at higher concentrations does malic acid show in the results. Thus, when looking at the experimental data, method A should rather be used for malic acid even if a correction needs to be implemented. The true malic acid values for the experimental conditions are likely only 0.05 – 0.1 g/L. An exponential calibration curve was fit to the data points. The curve has a satisfactory R^2-value and was thus, deemed good enough for conversion of measured data to actual concentrations. All malic acid concentrations from HPLC analysis were converted using the calibration curve. Figure B.37 shows the calibration curve.

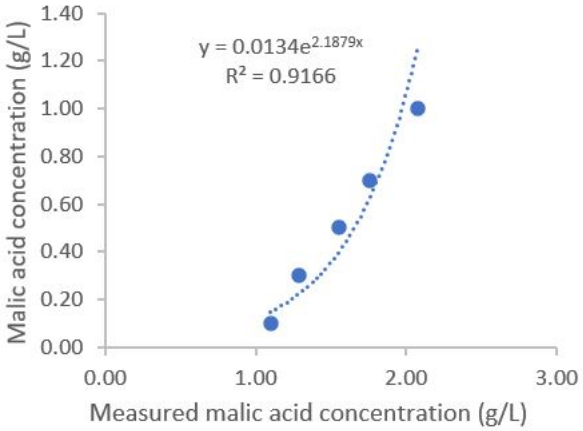

Figure B.37: An exponential curve was fit against the HPLC measured data and the theoretical malic acid values.

B.2 TOC analysis

When testing the accuracy of the TOC in reading malic acid, three different solutions were tested for NPOC (g/L). There was an underestimation of malic acid, which became more prevalent as malic acid concentrations increased. To cross-check this method, solution O2_7_3 (4.5.1) was spiked (O2_7_3*) with a known amount of malic acid. The theoretical difference (Th.) between the untouched O2_7_3 solution and the newly tested solution was compared to the difference in TOC readings. This confirmed the suspicion of inaccurate malic acid readings at higher concentrations. Table 19 and

Table 19: Three calibration solutions of malic acid were tested on the TOC analyzer. The error increased at higher concentrations. At low concentrations, the TOC was deemed sufficiently accurate.

Sample	MA (g/L)	C in MA (g/L)	NPOC (g/L)	Error (%)
1	1.00	0.36	0.17	-52.96
2	0.50	0.18	0.12	-30.60
3	0.10	0.04	0.04	0.00

Table 20: The final solution of run O2_7_3 was spiked with a known amount of malic acid to verify the TOC analysis

	MA added (g/L)	C in MA (g/L)	NPOC O2_7_3 (g/L)	Th. (g/L)	TOC (g/L)	Error (%)
O2_7_3*	10.00	3.58	2.14	190.58	98.86	48.13

B.3 Conclusion

To conclude, there was some malic acid in the system, however, less than previously assumed from HPLC readings. Values around 0.05-0.1 g/L were deemed more reasonable rather than readings close to 1.0 g/L. For the TOC readings, the error increases at higher malic acid concentrations. At low values the underestimation is likely up to 20 %.

C Appendix C: ngDNA sequencing reports

The full meta-genomic reports as generated by Inqaba biotec are attached below. The sample reports are labelled A, B, and C. The first report (A) is that of the 21 % oxygen condition. The second report (B) contains the data for the oxygen-rich condition. The last report (C) reflects the culture characteristics for the oxygen-poor environment. Section 4.5.2 contains a summary of the most prevalent species and their nitrogen-fixing abilities. The ability to produce PHA/PHB was also included.

inqaba biotec metagenomic report

Sample Information

Index:	M13_bc1002_F--M13_bc1052
Sample Name:	A
Run Name:	210827_Cell2
Report Date:	Mon Aug 30 10:43:31 2021

This report contains the summarized metagenomic analysis of full length 16s gene amplicons. Samples were sequenced on the Sequel system by PacBio (www.pacb.com). Raw subreads were processed through the SMRTlink (v9.0) Circular Consensus Sequences (CCS) algorithm to produce highly accurate reads (>QV40). These highly accurate reads were then processed through vsearch (https://github.com/torognes/vsearch) and taxonomic information was determined based on QIMME2. Report generation command used :$create_vsearch_single_sample_pdf_report_pacbio.py create_vsearch_single_sample_pdf_report_pacbio.py demultiplex.M13_bc1002_F--M13_bc1052_R.hifi_reads_otu_table.tsv M13_bc1002_F--M13_bc1052 A 210827_Cell2 16s

Taxanomical Classification

Kingdom Classification

Kingdom	Read Count	%
Bacteria	6985.0	100.00

Top Kingdom Classification

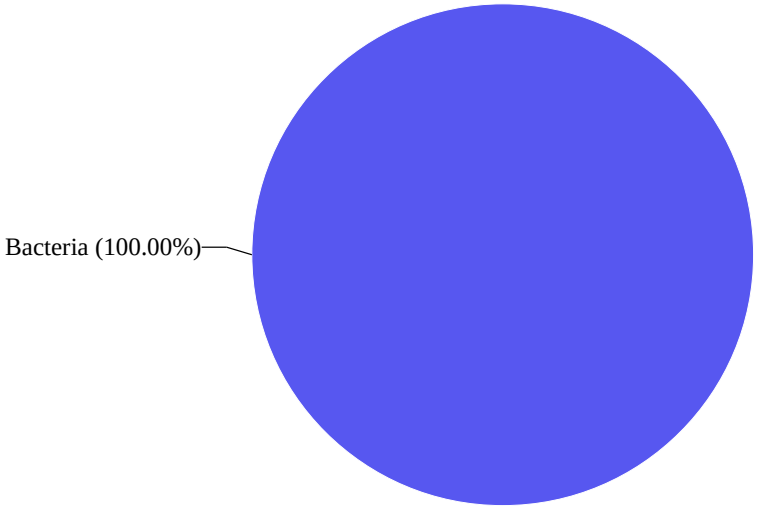

Phylum Classification

Phyla Classification	Read Count	%
Bacteroidetes	3696.0	52.91
Proteobacteria	2845.0	40.73
Actinobacteria	335.0	4.80
Planctomycetes	37.0	0.53
Firmicutes	29.0	0.42
Verrucomicrobia	23.0	0.33
Cyanobacteria	11.0	0.16
Unknown	6.0	0.09
Acidobacteria	1.0	0.01
Armatimonadetes	1.0	0.01
Gemmatimonadetes	1.0	0.01

Top Phylum Classification

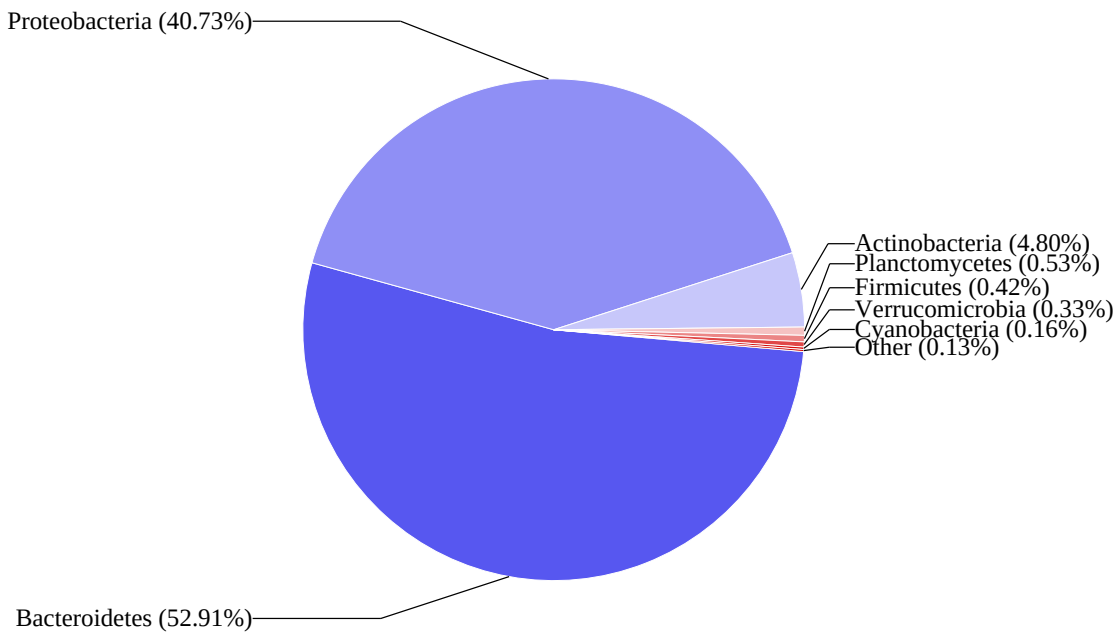

Class Classification

Class	Read Count	%
Flavobacteriia	3514.0	50.31
Gammaproteobacteria	1764.0	25.25
Alphaproteobacteria	879.0	12.58
Actinobacteria	335.0	4.80
Betaproteobacteria	198.0	2.83
VC2_1_Bac22	78.0	1.12
Sphingobacteriia	62.0	0.89
Planctomycetia	37.0	0.53
	25.0	0.36
Cytophagia	21.0	0.30
Clostridia	16.0	0.23
Verrucomicrobiae	15.0	0.21
Unknown	13.0	0.19
Bacilli	13.0	0.19
ML635J	11.0	0.16
Bacteroidia	1.0	0.01
Acidobacteria	1.0	0.01
Deltaproteobacteria	1.0	0.01
Gemmatimonadetes	1.0	0.01

Top Class Classification

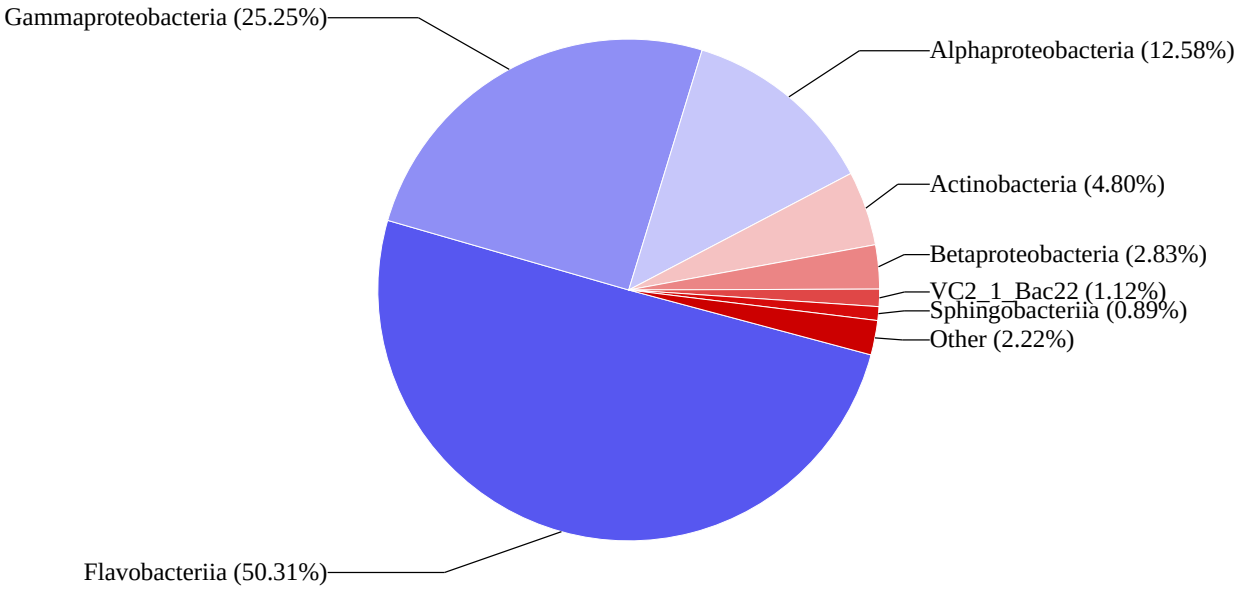

Order Classification

Order	Read Count	%
Flavobacteriales	3514.0	50.31
Xanthomonadales	865.0	12.38
Pseudomonadales	783.0	11.21
Caulobacterales	485.0	6.94
Rhizobiales	343.0	4.91
Actinomycetales	335.0	4.80
Burkholderiales	198.0	2.83
	114.0	1.63
Enterobacteriales	109.0	1.56
Sphingobacteriales	62.0	0.89
Gemmatales	37.0	0.53
Unknown	28.0	0.40
Sphingomonadales	25.0	0.36
Cytophagales	21.0	0.30
Clostridiales	16.0	0.23
Verrucomicrobiales	15.0	0.21
Rickettsiales	15.0	0.21
Lactobacillales	11.0	0.16
Rhodospirillales	4.0	0.06
Bacteroidales	1.0	0.01
iii1	1.0	0.01
Bacillales	1.0	0.01
Desulfuromonadales	1.0	0.01
Gemmatimonadales	1.0	0.01

Top Order Classification

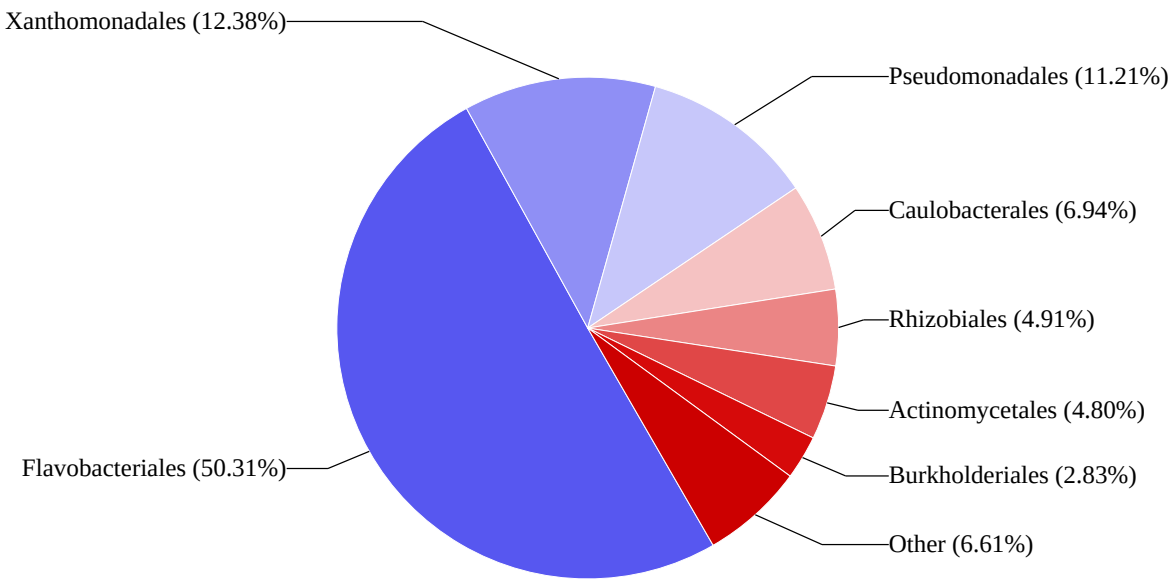

Family Classification

Family	Read Count	%
Unknown	2523.0	36.12
Flavobacteriaceae	1164.0	16.66
Xanthomonadaceae	864.0	12.37
Pseudomonadaceae	783.0	11.21
Caulobacteraceae	473.0	6.77
Microbacteriaceae	325.0	4.65
Rhizobiaceae	313.0	4.48
Comamonadaceae	193.0	2.76
Enterobacteriaceae	109.0	1.56
Sphingobacteriaceae	62.0	0.89
Isosphaeraceae	36.0	0.52
Sphingomonadaceae	24.0	0.34
Cytophagaceae	21.0	0.30
Clostridiaceae	16.0	0.23
Chitinophagaceae	16.0	0.23
Verrucomicrobiaceae	15.0	0.21
Hyphomicrobiaceae	12.0	0.17
Cellulomonadaceae	8.0	0.11
Streptococcaceae	8.0	0.11
Oxalobacteraceae	4.0	0.06
Rhodospirillaceae	3.0	0.04
Phyllobacteriaceae	3.0	0.04
Beijerinckiaceae	2.0	0.03
Sinobacteraceae	1.0	0.01
Paenibacillaceae	1.0	0.01
Desulfuromonadaceae	1.0	0.01
Gemmatimonadaceae	1.0	0.01
Acetobacteraceae	1.0	0.01
Gemmataceae	1.0	0.01
Alcaligenaceae	1.0	0.01
Enterococcaceae	1.0	0.01

Top Family Classification

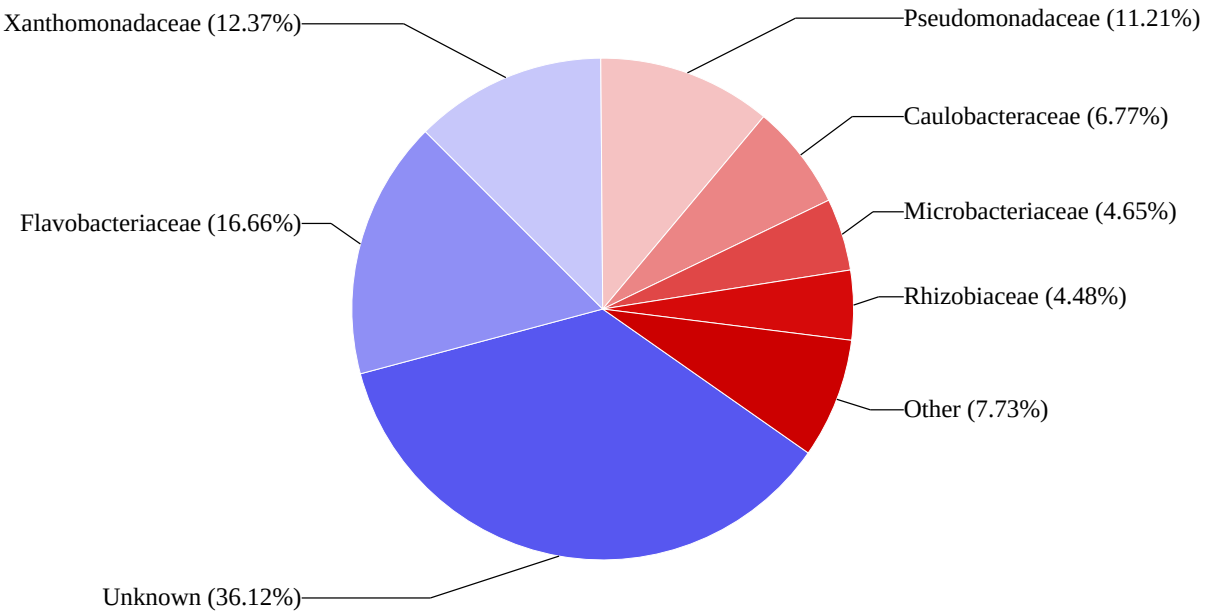

Genus Classification

Genus	Read Count	%
Chryseobacterium	1986.0	28.43
Flavobacterium	1097.0	15.71
Unknown	878.0	12.57
Pseudoxanthomonas	855.0	12.24
Azorhizophilus	454.0	6.50
Microbacterium	325.0	4.65
Pseudomonas	279.0	3.99
Agrobacterium	204.0	2.92
Caulobacter	162.0	2.32
Acidovorax	151.0	2.16
Brevundimonas	106.0	1.52
Elizabethkingia	83.0	1.19
Klebsiella	79.0	1.13
Mycoplana	53.0	0.76
Pedobacter	50.0	0.72
Riemerella	34.0	0.49
Flectobacillus	17.0	0.24
Clostridium	16.0	0.23
Sphingopyxis	14.0	0.20
Amorphomonas	11.0	0.16
Arthrospira	11.0	0.16
Azotobacter	10.0	0.14
Devosia	10.0	0.14
Cellulomonas	8.0	0.11
Candidatus	8.0	0.11
Shinella	7.0	0.10
Limnohabitans	7.0	0.10
Lactococcus	7.0	0.10
Kaistia	6.0	0.09
Imtechella	6.0	0.09
Salmonella	5.0	0.07
Novosphingobium	4.0	0.06
Sphingobium	4.0	0.06
Herbaspirillum	4.0	0.06
Azospirillum	3.0	0.04
Azomonas	3.0	0.04
Stenotrophomonas	3.0	0.04
Nitrobacteria	3.0	0.04
Variovorax	3.0	0.04
Xylophilus	2.0	0.03
Spirosoma	2.0	0.03

Pedomicrobium	2.0	0.03
Terrimonas	1.0	0.01
Mucilaginibacter	1.0	0.01
Hydrocarboniphaga	1.0	0.01
Dyella	1.0	0.01
Paenibacillus	1.0	0.01
Fimbriimonas	1.0	0.01
Gemmatimonas	1.0	0.01
Streptococcus	1.0	0.01
Gemmata	1.0	0.01
Phenylobacterium	1.0	0.01
Xenorhabdus	1.0	0.01
Vagococcus	1.0	0.01
Curvibacter	1.0	0.01

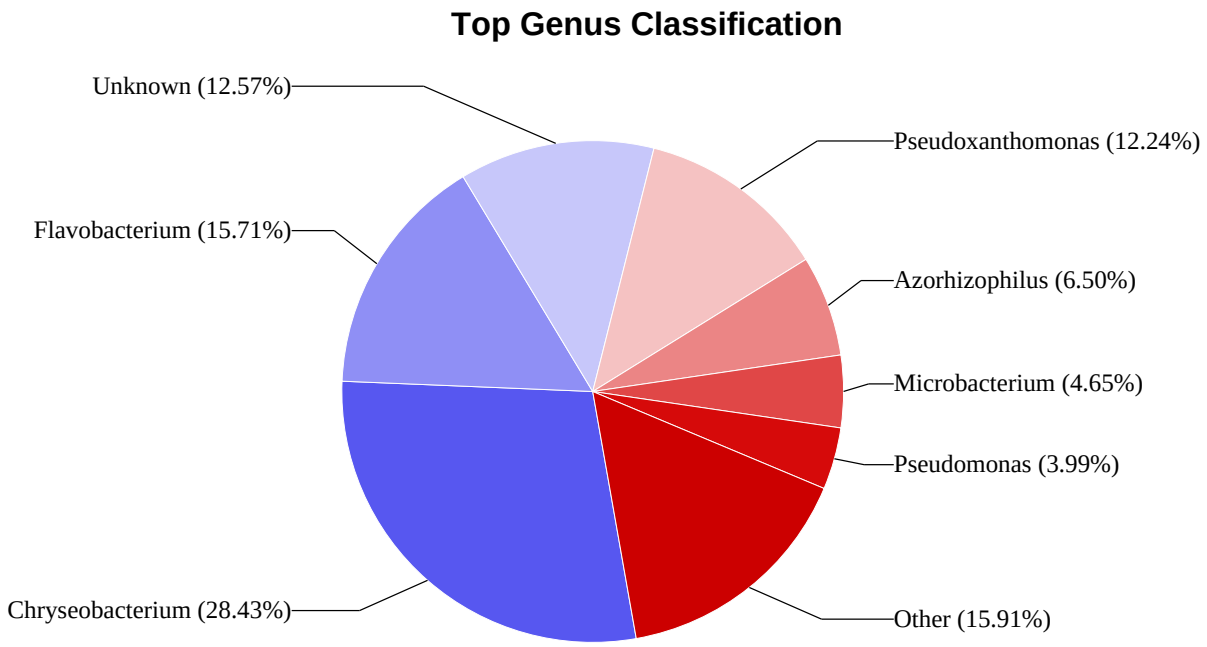

Species Classification

Species	Read Count	%
Chryseobacterium_	1986.0	28.43
Flavobacterium_	1058.0	15.15
Pseudoxanthomonas_indica	685.0	9.81
Unknown_	531.0	7.60
Azorhizophilus_	454.0	6.50
Unknown	422.0	6.04
Microbacterium_	245.0	3.51
Agrobacterium_	203.0	2.91
Pseudomonas_veronii	167.0	2.39
Pseudoxanthomonas_mexicana	161.0	2.30
Caulobacter_	161.0	2.30
Acidovorax_	137.0	1.96
Brevundimonas_poindexterae	103.0	1.47
Elizabethkingia_	82.0	1.17
Klebsiella_	79.0	1.13
Pseudomonas_	76.0	1.09
Mycoplana_	53.0	0.76
Microbacterium_aurum	37.0	0.53
Pedobacter_	37.0	0.53
Riemerella_	34.0	0.49
Pseudomonas_umsongensis	23.0	0.33
Microbacterium_chocolatum	23.0	0.33
Flectobacillus_	17.0	0.24
Clostridium_pasteurianum	16.0	0.23
Flavobacterium_gelidilacus	15.0	0.21
Sphingopyxis_	14.0	0.20
Amorphomonas_oryzae	11.0	0.16
Arthrospira_	11.0	0.16
Azotobacter_armeniacus	10.0	0.14
Devosia_	10.0	0.14
Cellulomonas_	8.0	0.11
Acidovorax_delafieldii	8.0	0.11
Candidatus_	8.0	0.11
Limnohabitans_	7.0	0.10
Kaistia_	6.0	0.09
Shinella_	6.0	0.09
Imtechella_halotolerans	6.0	0.09
Pseudoxanthomonas_	5.0	0.07
Salmonella_	5.0	0.07

Herbaspirillum_	4.0	0.06
Lactococcus_garvieae	4.0	0.06
Flavobacterium_succinicans	4.0	0.06
Pseudomonas_thermotolerans	3.0	0.04
Acidovorax_wohlfahrtii	3.0	0.04
Novosphingobium_	3.0	0.04
Azospirillum_	3.0	0.04
Sphingobium_yanoikuyae	3.0	0.04
Nitrobacteria_hamadaniensis	3.0	0.04
Variovorax_	3.0	0.04
Lactococcus_	3.0	0.04
Xylophilus_ampelinus	2.0	0.03
Spirosoma_	2.0	0.03
Stenotrophomonas_acidaminiphila	2.0	0.03
Microbacterium_lacticum	2.0	0.03
Pedomicrobium_australicum	2.0	0.03
Sphingobium_	1.0	0.01
Agrobacterium_undicola	1.0	0.01
Hydrocarboniphaga_effusa	1.0	0.01
Azomonas_agilis	1.0	0.01
Stenotrophomonas_panacihumi	1.0	0.01
Microbacterium_maritypicum	1.0	0.01
Dyella_	1.0	0.01
Fimbriimonas_	1.0	0.01
Gemmatimonas_	1.0	0.01
Novosphingobium_stygium	1.0	0.01
Streptococcus_alactolyticus	1.0	0.01
Gemmata_obscuriglobus	1.0	0.01
Flavobacterium_frigidarium	1.0	0.01
Phenylobacterium_	1.0	0.01
Xenorhabdus_bovienii	1.0	0.01
Vagococcus_	1.0	0.01
Caulobacter_henricii	1.0	0.01
Azomonas_	1.0	0.01
Curvibacter_	1.0	0.01

Top Species Classification

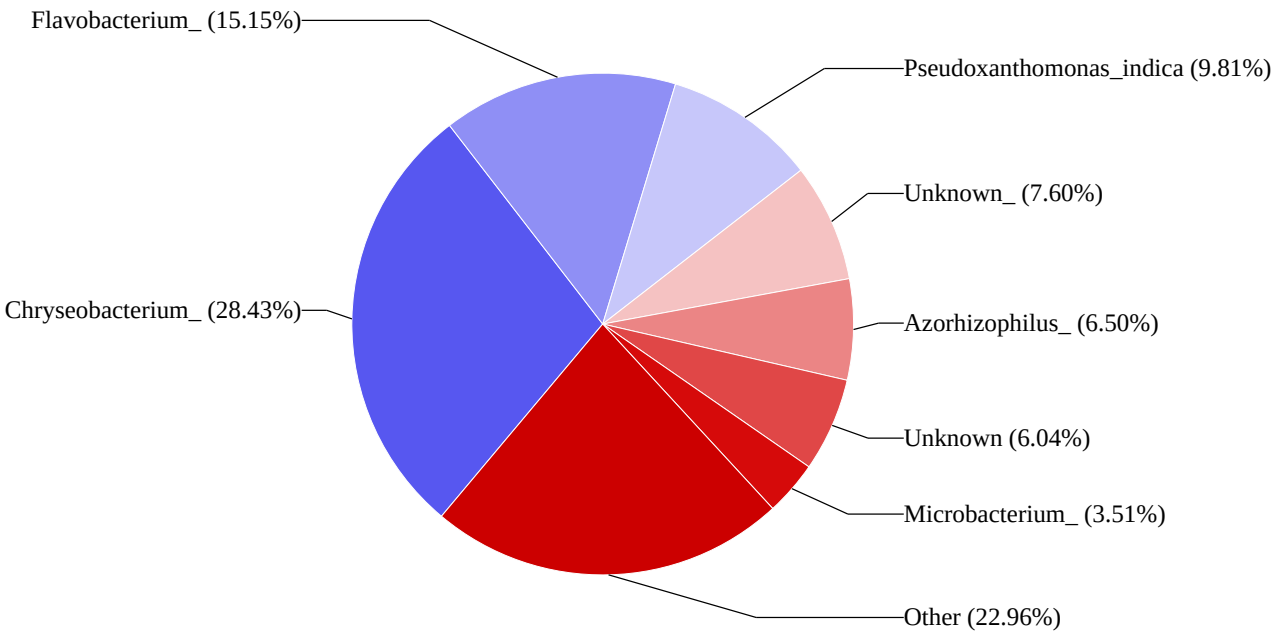

---------- End of report ----------

inqaba biotec metagenomic report

Sample Information

Index:	M13_bc1002_F--M13_bc1053
Sample Name:	B
Run Name:	210827_Cell2
Report Date:	Mon Aug 30 10:45:28 2021

This report contains the summarized metagenomic analysis of full length 16s gene amplicons. Samples were sequenced on the Sequel system by PacBio (www.pacb.com). Raw subreads were processed through the SMRTlink (v9.0) Circular Consensus Sequences (CCS) algorithm to produce highly accurate reads (>QV40). These highly accurate reads were then processed through vsearch (https://github.com/torognes/vsearch) and taxonomic information was determined based on QIMME2. Report generation command used :$create_vsearch_single_sample_pdf_report_pacbio.py create_vsearch_single_sample_pdf_report_pacbio.py demultiplex.M13_bc1002_F--M13_bc1053_R.hifi_reads_otu_table.tsv M13_bc1002_F--M13_bc1053 B 210827_Cell2 16s

Taxanomical Classification

Kingdom Classification

Kingdom	Read Count	%
Bacteria	8343.0	100.00

Top Kingdom Classification

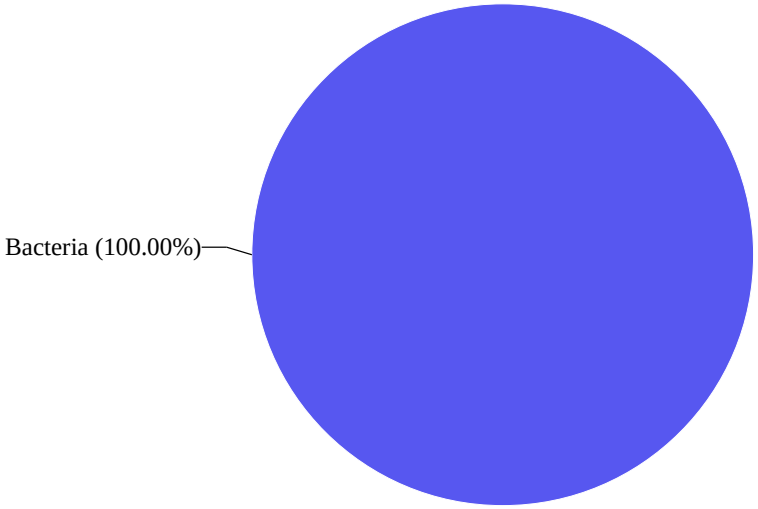

Phylum Classification

Phyla Classification	Read Count	%
Bacteroidetes	4634.0	55.54
Proteobacteria	3432.0	41.14
Actinobacteria	207.0	2.48
Firmicutes	21.0	0.25
Planctomycetes	14.0	0.17
Verrucomicrobia	11.0	0.13
Gemmatimonadetes	10.0	0.12
Unknown	9.0	0.11
Chloroflexi	2.0	0.02
Acidobacteria	2.0	0.02
Cyanobacteria	1.0	0.01

Top Phylum Classification

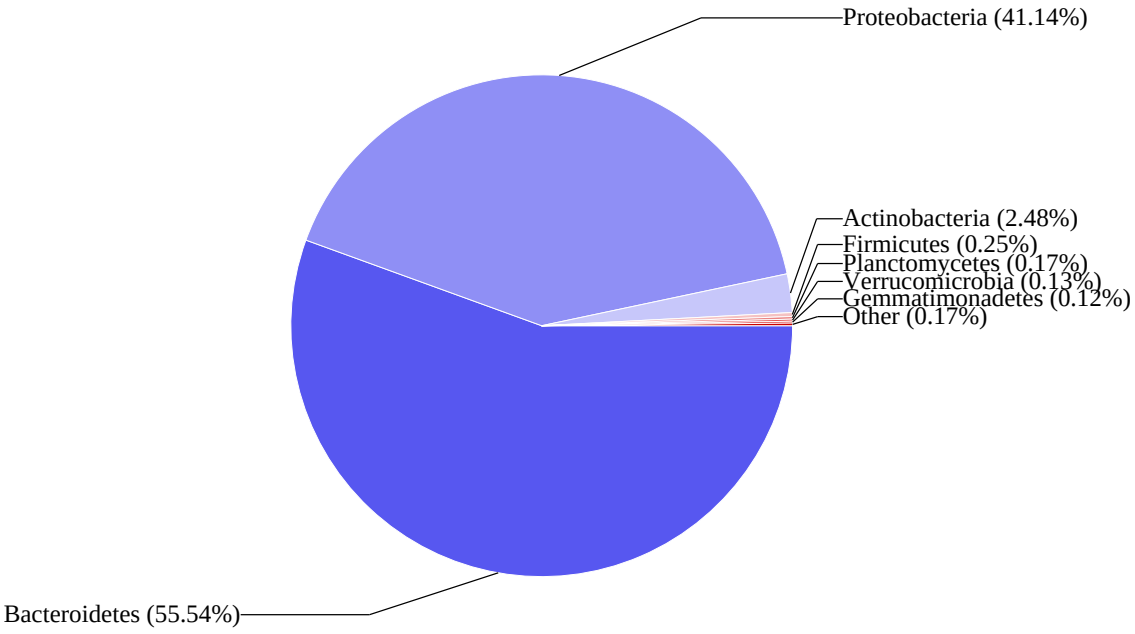

Class Classification

Class	Read Count	%
Flavobacteriia	4566.0	54.73
Gammaproteobacteria	2458.0	29.46
Alphaproteobacteria	903.0	10.82
Actinobacteria	206.0	2.47
Betaproteobacteria	61.0	0.73
Sphingobacteriia	38.0	0.46
Unknown	17.0	0.20
Bacilli	17.0	0.20
Planctomycetia	14.0	0.17
Cytophagia	13.0	0.16
	11.0	0.13
VC2_1_Bac22	11.0	0.13
Gemmatimonadetes	10.0	0.12
Verrucomicrobiae	6.0	0.07
Clostridia	4.0	0.05
Deltaproteobacteria	2.0	0.02
C0119	1.0	0.01
Ellin6529	1.0	0.01
Thermoleophilia	1.0	0.01
ML635J	1.0	0.01
Acidobacteriia	1.0	0.01
Acidobacteria	1.0	0.01

Top Class Classification

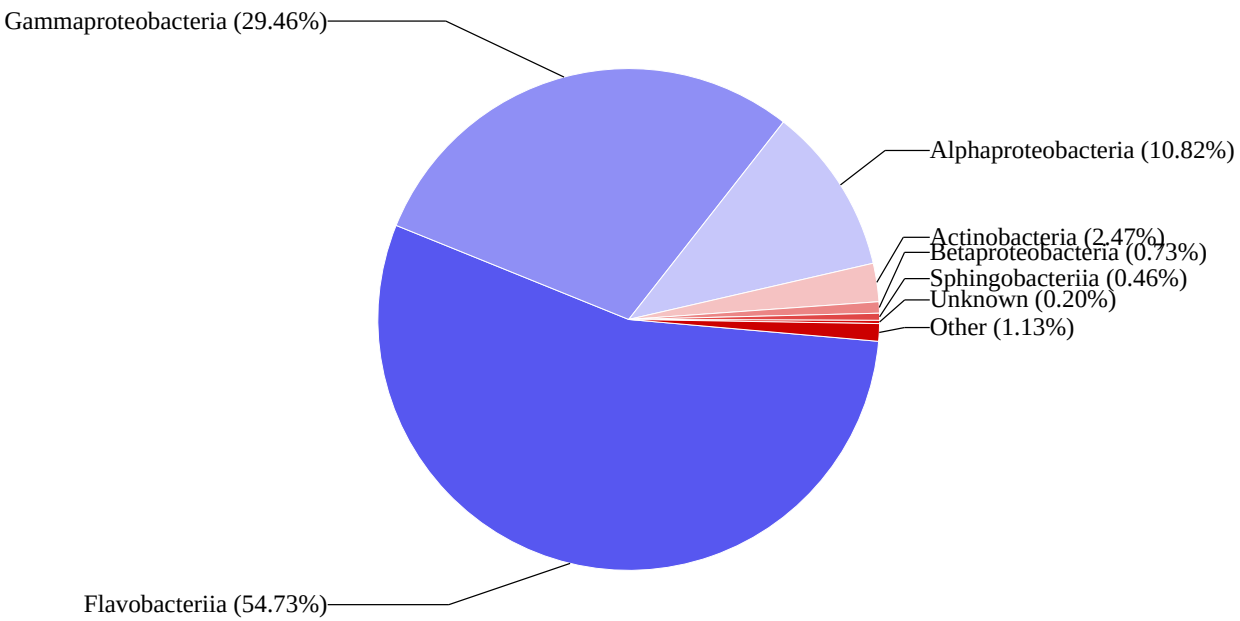

Order Classification

Order	Read Count	%
Flavobacteriales	4566.0	54.73
Pseudomonadales	1727.0	20.70
Caulobacterales	726.0	8.70
Xanthomonadales	705.0	8.45
Actinomycetales	206.0	2.47
Rhizobiales	138.0	1.65
Burkholderiales	61.0	0.73
Unknown	40.0	0.48
Sphingobacteriales	38.0	0.46
	25.0	0.30
Enterobacteriales	18.0	0.22
Lactobacillales	15.0	0.18
Sphingomonadales	15.0	0.18
Gemmatales	14.0	0.17
Cytophagales	13.0	0.16
Gemmatimonadales	10.0	0.12
Verrucomicrobiales	6.0	0.07
Rhodospirillales	5.0	0.06
Clostridiales	4.0	0.05
Rickettsiales	4.0	0.05
Bacillales	2.0	0.02
S	1.0	0.01
Gaiellales	1.0	0.01
Acidobacteriales	1.0	0.01
CCU21	1.0	0.01
Myxococcales	1.0	0.01

Top Order Classification

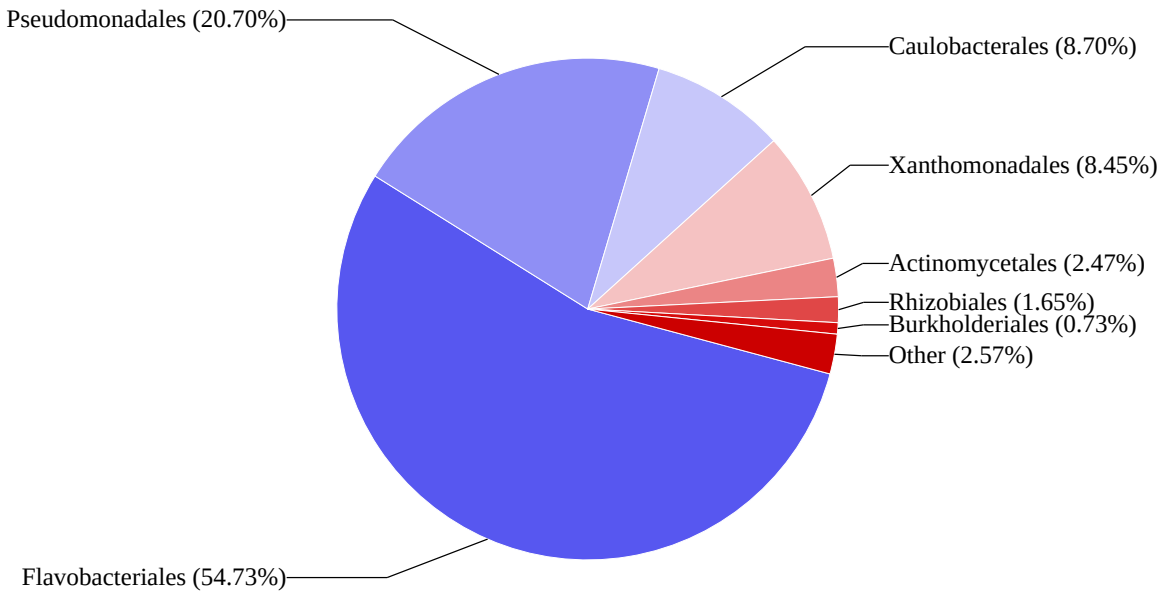

Family Classification

Family	Read Count	%
Unknown	3412.0	40.90
Pseudomonadaceae	1724.0	20.66
Flavobacteriaceae	1237.0	14.83
Caulobacteraceae	724.0	8.68
Xanthomonadaceae	705.0	8.45
Microbacteriaceae	200.0	2.40
Rhizobiaceae	108.0	1.29
Comamonadaceae	56.0	0.67
Sphingobacteriaceae	38.0	0.46
Enterobacteriaceae	18.0	0.22
Cytophagaceae	13.0	0.16
Sphingomonadaceae	13.0	0.16
Streptococcaceae	12.0	0.14
Isosphaeraceae	12.0	0.14
Hyphomicrobiaceae	11.0	0.13
Gemmatimonadaceae	8.0	0.10
Verrucomicrobiaceae	6.0	0.07
Chitinophagaceae	6.0	0.07
Cellulomonadaceae	5.0	0.06
Alcaligenaceae	5.0	0.06
Rhodospirillaceae	4.0	0.05
Clostridiaceae	4.0	0.05
Phyllobacteriaceae	4.0	0.05
Beijerinckiaceae	3.0	0.04
Moraxellaceae	3.0	0.04
Gemmataceae	2.0	0.02
Ellin5301	1.0	0.01
Gaiellaceae	1.0	0.01
Carnobacteriaceae	1.0	0.01
Acetobacteraceae	1.0	0.01
Acidobacteriaceae	1.0	0.01
Paenibacillaceae	1.0	0.01
Mycobacteriaceae	1.0	0.01
Erythrobacteraceae	1.0	0.01
Staphylococcaceae	1.0	0.01
Cystobacteraceae	1.0	0.01

Top Family Classification

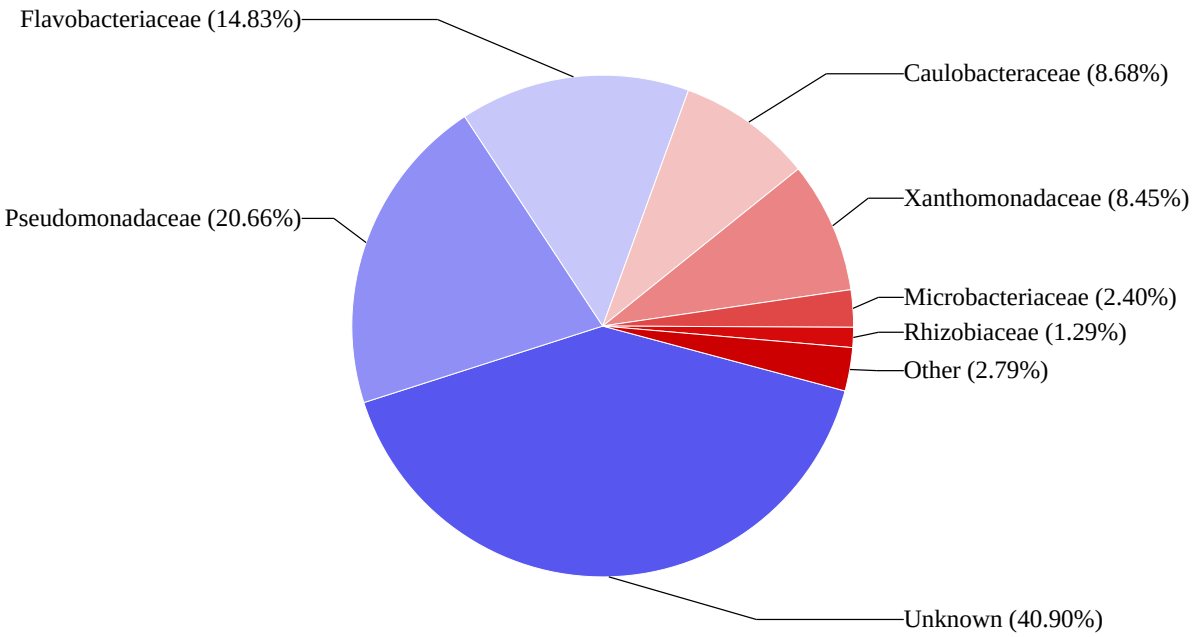

Genus Classification

Genus	Read Count	%
Chryseobacterium	2925.0	35.06
Flavobacterium	1137.0	13.63
Azorhizophilus	969.0	11.61
Unknown	843.0	10.10
Pseudoxanthomonas	686.0	8.22
Pseudomonas	578.0	6.93
Brevundimonas	320.0	3.84
Microbacterium	200.0	2.40
Mycoplana	153.0	1.83
Elizabethkingia	104.0	1.25
Agrobacterium	59.0	0.71
Riemerella	45.0	0.54
Caulobacter	40.0	0.48
Azotobacter	39.0	0.47
Pedobacter	36.0	0.43
Acidovorax	35.0	0.42
Azomonas	16.0	0.19
Stenotrophomonas	15.0	0.18
Flectobacillus	13.0	0.16
Lactococcus	12.0	0.14
Devosia	11.0	0.13
Shinella	10.0	0.12
Gemmatimonas	8.0	0.10
Amorphomonas	7.0	0.08
Novosphingobium	6.0	0.07
Kaistia	6.0	0.07
Cellulomonas	5.0	0.06
Arthrospira	5.0	0.06
Klebsiella	4.0	0.05
Achromobacter	4.0	0.05
Sphingopyxis	4.0	0.05
Candidatus	4.0	0.05
Variovorax	4.0	0.05
Clostridium	4.0	0.05
Xylophilus	3.0	0.04
Imtechella	3.0	0.04
Acinetobacter	3.0	0.04
Aminobacter	3.0	0.04
Enterobacter	2.0	0.02
Azospirillum	2.0	0.02
Nitrobacteria	2.0	0.02

Gemmata	1.0	0.01
Kerstersia	1.0	0.01
Chitinophaga	1.0	0.01
Limnohabitans	1.0	0.01
Chelatococcus	1.0	0.01
Sphingobium	1.0	0.01
Nostocoida	1.0	0.01
Curvibacter	1.0	0.01
Phaeospirillum	1.0	0.01
Luteimonas	1.0	0.01
Haloferula	1.0	0.01
Isobaculum	1.0	0.01
Paenibacillus	1.0	0.01
Mitsuaria	1.0	0.01
Mycobacterium	1.0	0.01
Erythromicrobium	1.0	0.01
Macrococcus	1.0	0.01
Salmonella	1.0	0.01

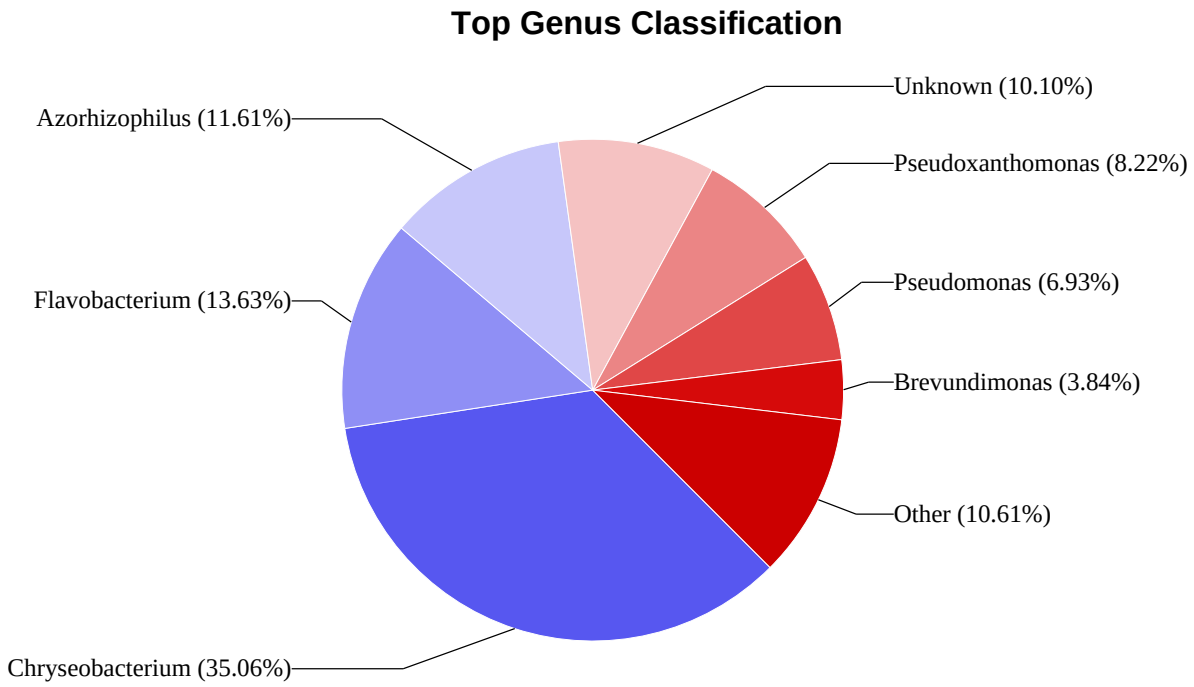

Species Classification

Species	Read Count	%
Chryseobacterium_	2925.0	35.06
Azorhizophilus_	969.0	11.61
Flavobacterium_	951.0	11.40
Pseudoxanthomonas_indica	626.0	7.50
Unknown	529.0	6.34
Pseudomonas_	452.0	5.42
Unknown_	409.0	4.90
Brevundimonas_poindexterae	312.0	3.74
Mycoplana_	153.0	1.83
Microbacterium_	145.0	1.74
Flavobacterium_succinicans	108.0	1.29
Elizabethkingia_	101.0	1.21
Pseudomonas_umsongensis	90.0	1.08
Agrobacterium_	58.0	0.70
Pseudoxanthomonas_mexicana	51.0	0.61
Riemerella_	45.0	0.54
Caulobacter_	40.0	0.48
Flavobacterium_gelidilacus	40.0	0.48
Azotobacter_armeniacus	39.0	0.47
Microbacterium_aurum	33.0	0.40
Pedobacter_	33.0	0.40
Acidovorax_	22.0	0.26
Microbacterium_chocolatum	14.0	0.17
Flectobacillus_	13.0	0.16
Devosia_	11.0	0.13
Azomonas_	9.0	0.11
Pseudomonas_viridiflava	9.0	0.11
Gemmatimonas_	8.0	0.10
Lactococcus_	8.0	0.10
Flavobacterium_frigidarium	7.0	0.08
Shinella_granuli	7.0	0.08
Amorphomonas_oryzae	7.0	0.08
Acidovorax_delafieldii	7.0	0.08
Stenotrophomonas_maltophilia	6.0	0.07
Kaistia_	6.0	0.07
Azomonas_agilis	5.0	0.06
Pseudoxanthomonas_	5.0	0.06
Arthrospira_	5.0	0.06
Stenotrophomonas_acidaminiphila	4.0	0.05

Lactococcus_garvieae	4.0	0.05
Klebsiella_	4.0	0.05
Cellulomonas_	4.0	0.05
Achromobacter_	4.0	0.05
Sphingopyxis_	4.0	0.05
Candidatus_	4.0	0.05
Variovorax_	4.0	0.05
Xylophilus_ampelinus	3.0	0.04
Novosphingobium_	3.0	0.04
Imtechella_halotolerans	3.0	0.04
Shinella_	3.0	0.04
Clostridium_pasteurianum	3.0	0.04
Aminobacter_	3.0	0.04
Stenotrophomonas_panacihumi	2.0	0.02
Acinetobacter_	2.0	0.02
Nitrobacteria_hamadaniensis	2.0	0.02
Acidovorax_wohlfahrtii	2.0	0.02
Enterobacter_cowanii	1.0	0.01
Gemmata_obscuriglobus	1.0	0.01
Kerstersia_gyiorum	1.0	0.01
Chitinophaga_	1.0	0.01
Limnohabitans_curvus	1.0	0.01
Chelatococcus_	1.0	0.01
Sphingobium_	1.0	0.01
Nostocoida_limicola	1.0	0.01
Curvibacter_	1.0	0.01
Microbacterium_maritypicum	1.0	0.01
Phaeospirillum_	1.0	0.01
Pseudomonas_thermotolerans	1.0	0.01
Pseudomonas_veronii	1.0	0.01
Azospirillum_	1.0	0.01
Novosphingobium_stygium	1.0	0.01
Cellulomonas_uda	1.0	0.01
Luteimonas_mephitis	1.0	0.01
Stenotrophomonas_	1.0	0.01
Acinetobacter_venetianus	1.0	0.01
Isobaculum_melis	1.0	0.01
Paenibacillus_	1.0	0.01
Mitsuaria_chitosanitabida	1.0	0.01
Mycobacterium_	1.0	0.01
Brevundimonas_intermedia	1.0	0.01
Erythromicrobium_ramosum	1.0	0.01
Macrococcus_	1.0	0.01

Salmonella_	1.0	0.01

Top Species Classification

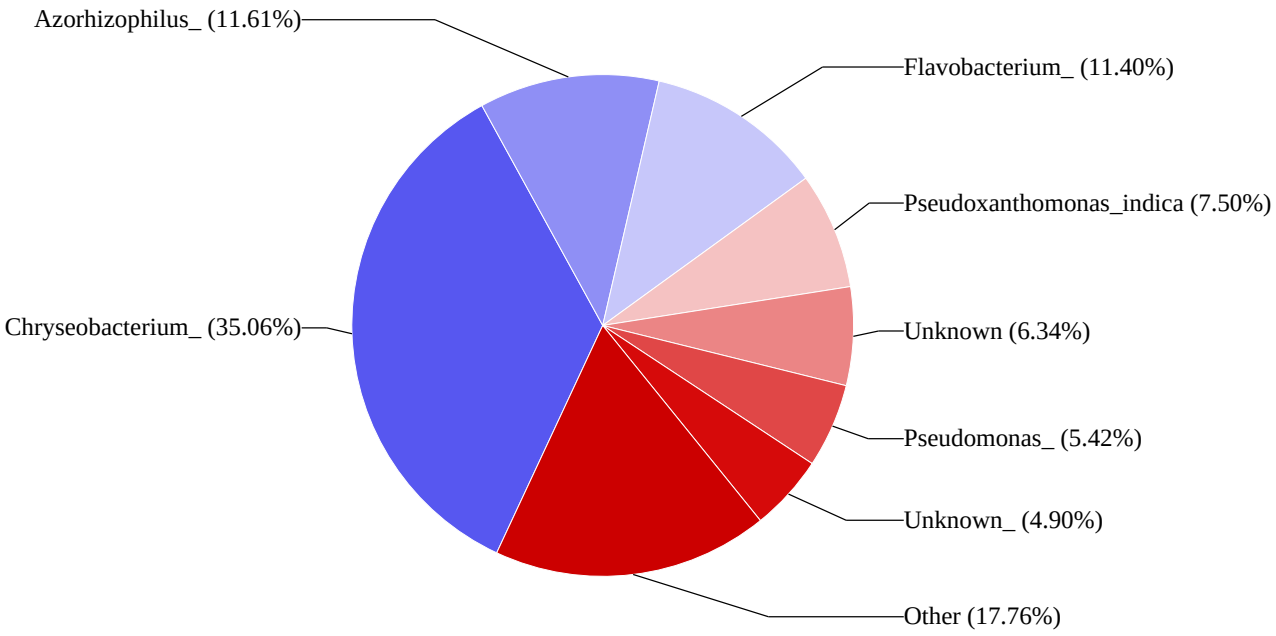

---------- End of report ----------

inqaba biotec metagenomic report

Sample Information

Index:	M13_bc1002_F--M13_bc1054
Sample Name:	C
Run Name:	210827_Cell2
Report Date:	Mon Aug 30 10:45:56 2021

This report contains the summarized metagenomic analysis of full length 16s gene amplicons. Samples were sequenced on the Sequel system by PacBio (www.pacb.com). Raw subreads were processed through the SMRTlink (v9.0) Circular Consensus Sequences (CCS) algorithm to produce highly accurate reads (>QV40). These highly accurate reads were then processed through vsearch (https://github.com/torognes/vsearch) and taxonomic information was determined based on QIMME2. Report generation command used :$create_vsearch_single_sample_pdf_report_pacbio.py create_vsearch_single_sample_pdf_report_pacbio.py demultiplex.M13_bc1002_F--M13_bc1054_R.hifi_reads_otu_table.tsv M13_bc1002_F--M13_bc1054 C 210827_Cell2 16s

Taxanomical Classification

Kingdom Classification

Kingdom	Read Count	%
Bacteria	303.0	100.00

Top Kingdom Classification

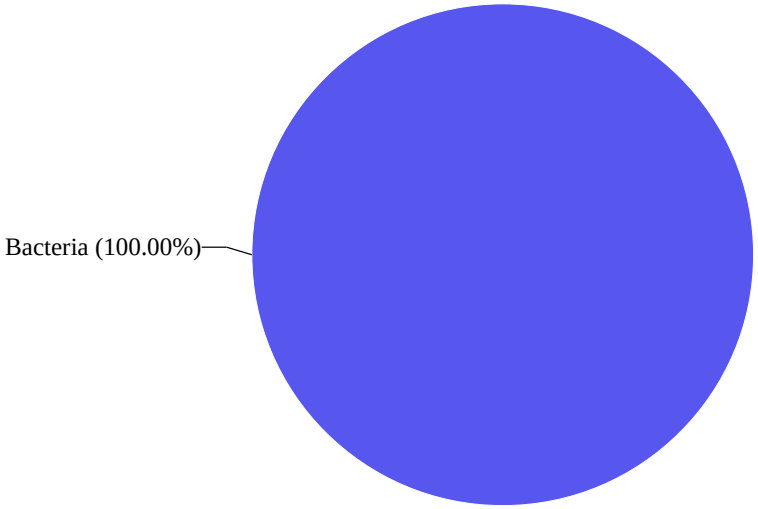

Phylum Classification

Phyla Classification	Read Count	%
Proteobacteria	179.0	59.08
Bacteroidetes	58.0	19.14
Actinobacteria	27.0	8.91
Firmicutes	23.0	7.59
Planctomycetes	3.0	0.99
Cyanobacteria	3.0	0.99
Unknown	3.0	0.99
Acidobacteria	2.0	0.66
Verrucomicrobia	2.0	0.66
Chloroflexi	2.0	0.66
GAL15	1.0	0.33

Top Phylum Classification

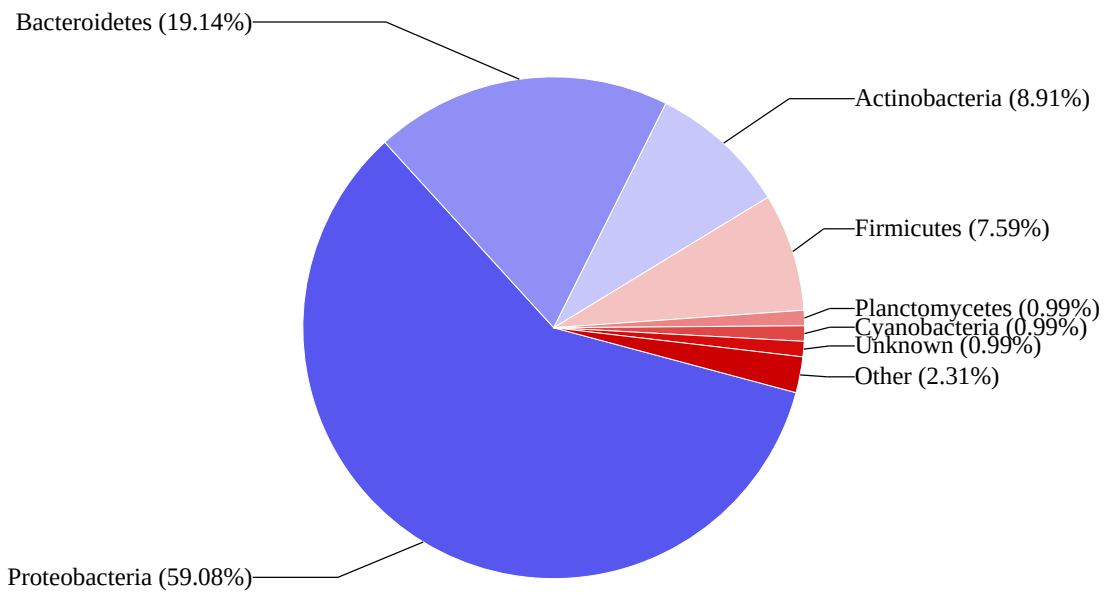

Class Classification

Class	Read Count	%
Alphaproteobacteria	71.0	23.43
Betaproteobacteria	51.0	16.83
Gammaproteobacteria	49.0	16.17
Flavobacteriia	42.0	13.86
Actinobacteria	22.0	7.26
Bacilli	21.0	6.93
Unknown	11.0	3.63
Sphingobacteriia	11.0	3.63
	4.0	1.32
Thermoleophilia	3.0	0.99
Planctomycetia	3.0	0.99
Deltaproteobacteria	2.0	0.66
Acidobacteria	2.0	0.66
Cytophagia	2.0	0.66
Clostridia	2.0	0.66
Verrucomicrobiae	1.0	0.33
Rubrobacteria	1.0	0.33
Oscillatoriophycideae	1.0	0.33
Chloroflexi	1.0	0.33
Anaerolineae	1.0	0.33
Chloroplast	1.0	0.33
VC2_1_Bac22	1.0	0.33

Top Class Classification

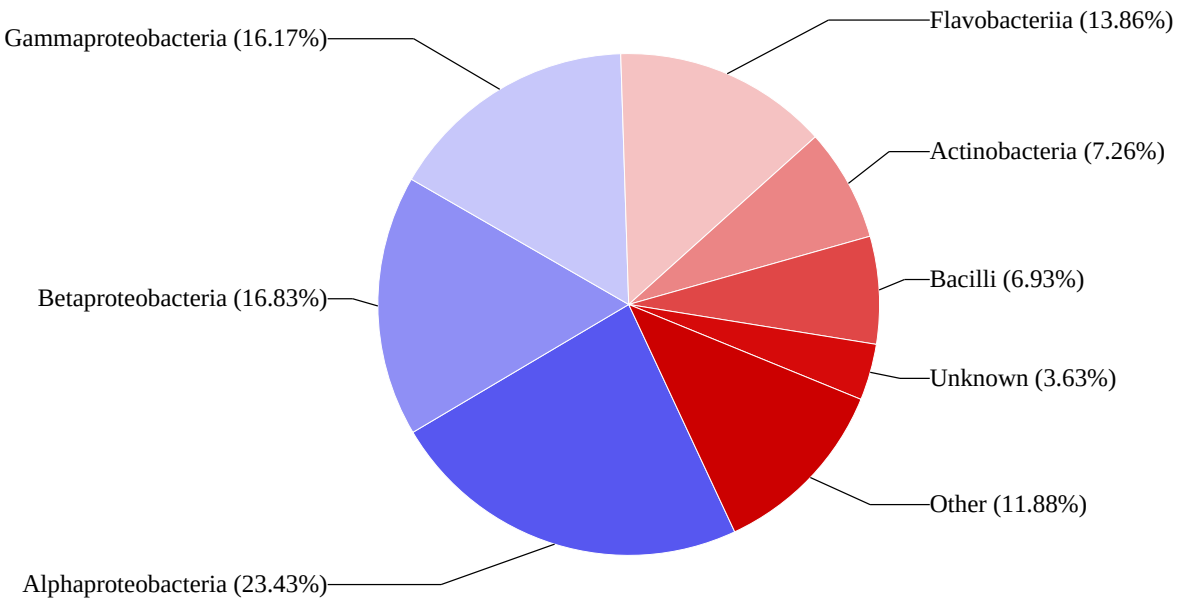

Order Classification

Order	Read Count	%
Caulobacterales	49.0	16.17
Burkholderiales	49.0	16.17
Flavobacteriales	42.0	13.86
Enterobacteriales	30.0	9.90
Actinomycetales	22.0	7.26
Unknown	18.0	5.94
Rhizobiales	14.0	4.62
Xanthomonadales	13.0	4.29
Lactobacillales	12.0	3.96
Sphingobacteriales	11.0	3.63
Bacillales	8.0	2.64
	6.0	1.98
Pseudomonadales	5.0	1.65
Rhodospirillales	3.0	0.99
Sphingomonadales	3.0	0.99
Solirubrobacterales	2.0	0.66
iii1	2.0	0.66
Gemmatales	2.0	0.66
Cytophagales	2.0	0.66
Clostridiales	2.0	0.66
Myxococcales	1.0	0.33
Legionellales	1.0	0.33
Verrucomicrobiales	1.0	0.33
Rubrobacterales	1.0	0.33
Gaiellales	1.0	0.33
SBR1031	1.0	0.33
Stramenopiles	1.0	0.33
MKC10	1.0	0.33

Top Order Classification

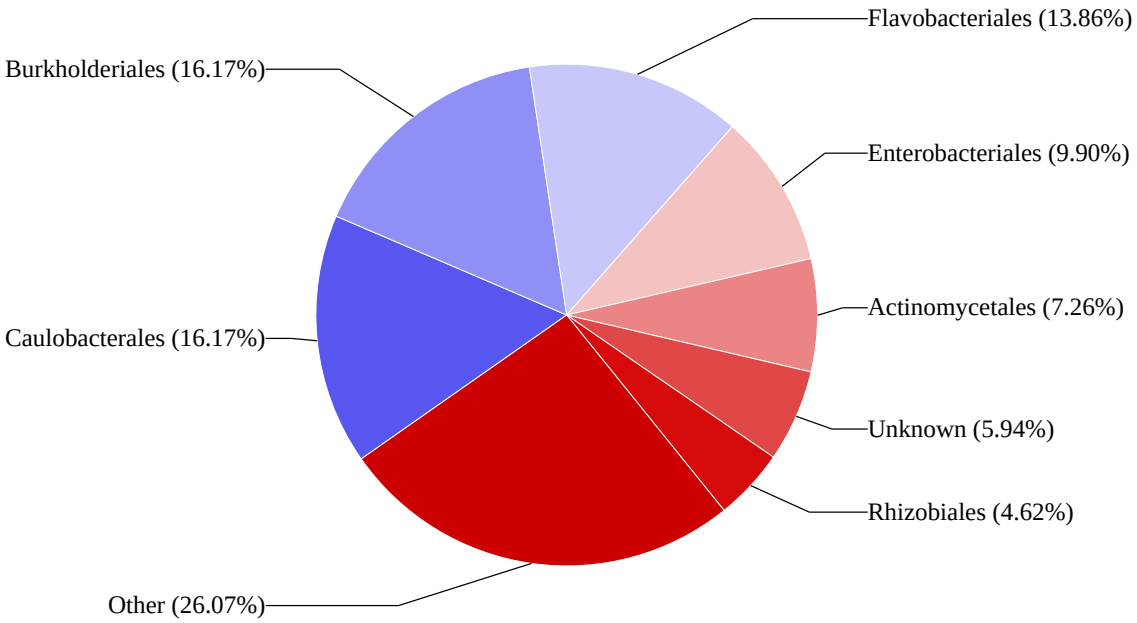

Family Classification

Family	Read Count	%
Unknown	58.0	19.14
Caulobacteraceae	49.0	16.17
Comamonadaceae	48.0	15.84
Enterobacteriaceae	30.0	9.90
Flavobacteriaceae	16.0	5.28
Microbacteriaceae	14.0	4.62
Xanthomonadaceae	13.0	4.29
Sphingobacteriaceae	11.0	3.63
Rhizobiaceae	10.0	3.30
Streptococcaceae	10.0	3.30
Staphylococcaceae	4.0	1.32
Pseudomonadaceae	4.0	1.32
Paenibacillaceae	3.0	0.99
Sphingomonadaceae	3.0	0.99
Rhodospirillaceae	2.0	0.66
Leuconostocaceae	2.0	0.66
Chitinophagaceae	2.0	0.66
Cytophagaceae	2.0	0.66
Geodermatophilaceae	2.0	0.66
Clostridiaceae	2.0	0.66
Alcaligenaceae	1.0	0.33
Polyangiaceae	1.0	0.33
Legionellaceae	1.0	0.33
Verrucomicrobiaceae	1.0	0.33
Streptomycetaceae	1.0	0.33
Isosphaeraceae	1.0	0.33
Rubrobacteraceae	1.0	0.33
Acetobacteraceae	1.0	0.33
Hyphomicrobiaceae	1.0	0.33
Gaiellaceae	1.0	0.33
Bradyrhizobiaceae	1.0	0.33
A4b	1.0	0.33
Bacillaceae	1.0	0.33
Gemmataceae	1.0	0.33
Cellulomonadaceae	1.0	0.33
Nocardioidaceae	1.0	0.33
Micromonosporaceae	1.0	0.33
Moraxellaceae	1.0	0.33

Top Family Classification

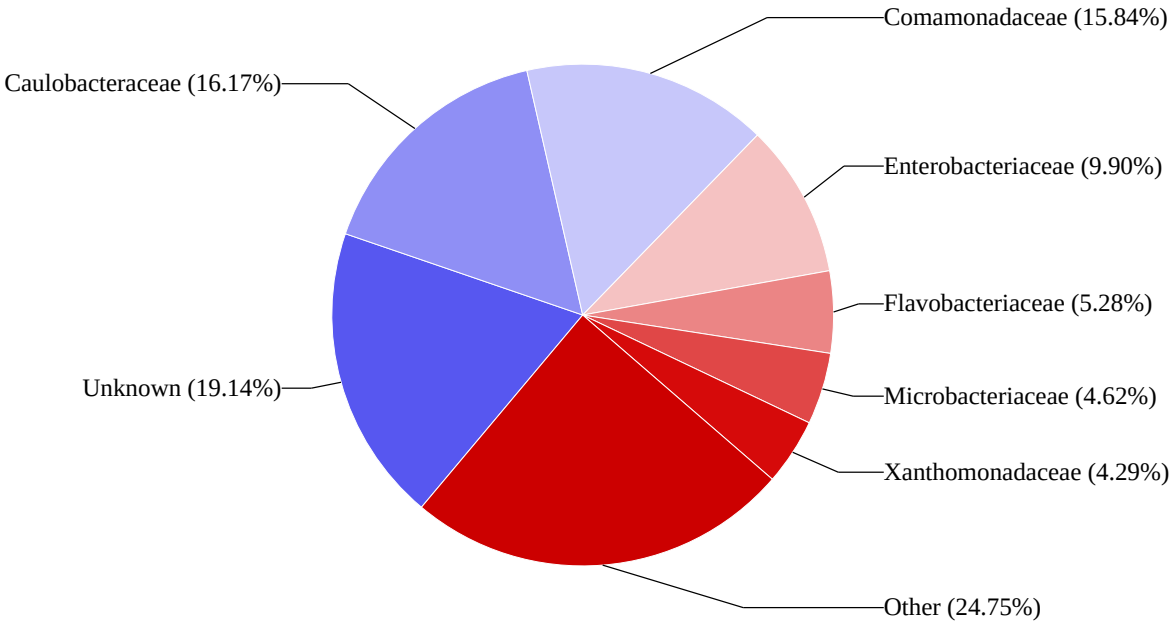

Genus Classification

Genus	Read Count	%
Unknown	76.0	25.08
Acidovorax	35.0	11.55
Brevundimonas	24.0	7.92
Chryseobacterium	22.0	7.26
Klebsiella	17.0	5.61
Microbacterium	14.0	4.62
Flavobacterium	12.0	3.96
Pseudoxanthomonas	10.0	3.30
Pedobacter	10.0	3.30
Mycoplana	10.0	3.30
Lactococcus	8.0	2.64
Variovorax	6.0	1.98
Agrobacterium	6.0	1.98
Salmonella	4.0	1.32
Macrococcus	4.0	1.32
Stenotrophomonas	3.0	0.99
Limnohabitans	3.0	0.99
Enterobacter	2.0	0.66
Paenibacillus	2.0	0.66
Azorhizophilus	2.0	0.66
Pseudomonas	2.0	0.66
Flectobacillus	2.0	0.66
Clostridium	2.0	0.66
Legionella	1.0	0.33
Phaeospirillum	1.0	0.33
Terrimonas	1.0	0.33
Azospirillum	1.0	0.33
Streptomyces	1.0	0.33
Singulisphaera	1.0	0.33
Rubrobacter	1.0	0.33
Ammoniphilus	1.0	0.33
Hydrogenophaga	1.0	0.33
Schlegelella	1.0	0.33
Amorphomonas	1.0	0.33
Modestobacter	1.0	0.33
Novosphingobium	1.0	0.33
Craurococcus	1.0	0.33
Pedomicrobium	1.0	0.33
Blastococcus	1.0	0.33
Streptococcus	1.0	0.33
Bacillus	1.0	0.33

Parasegitibacter	1.0	0.33
Leptothrix	1.0	0.33
Sphingosinicella	1.0	0.33
Caulobacter	1.0	0.33
Mucilaginibacter	1.0	0.33
Cellulomonas	1.0	0.33
Nocardioides	1.0	0.33
Imtechella	1.0	0.33
Agitococcus	1.0	0.33

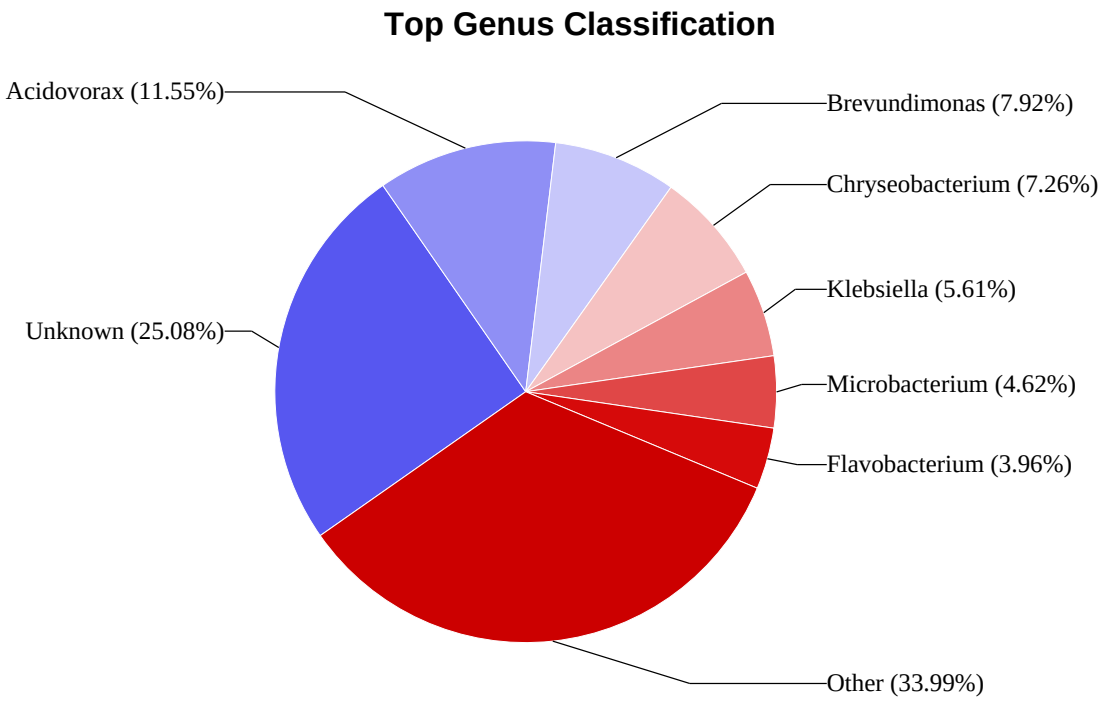

Species Classification

Species	Read Count	%
Unknown	65.0	21.45
Brevundimonas_poindexterae	24.0	7.92
Acidovorax_	24.0	7.92
Chryseobacterium_	22.0	7.26
Unknown_	19.0	6.27
Klebsiella_	17.0	5.61
Flavobacterium_	11.0	3.63
Acidovorax_delafieldii	10.0	3.30
Pseudoxanthomonas_indica	10.0	3.30
Mycoplana_	10.0	3.30
Microbacterium_	9.0	2.97
Pedobacter_	9.0	2.97
Variovorax_	6.0	1.98
Agrobacterium_	6.0	1.98
Lactococcus_	5.0	1.65
Microbacterium_aurum	4.0	1.32
Salmonella_	4.0	1.32
Lactococcus_garvieae	3.0	0.99
Macrococcus_caseolyticus	2.0	0.66
Azorhizophilus_	2.0	0.66
Macrococcus_	2.0	0.66
Flectobacillus_	2.0	0.66
Limnohabitans_	2.0	0.66
Clostridium_pasteurianum	2.0	0.66
Paenibacillus_illinoisensis	1.0	0.33
Legionella_	1.0	0.33
Phaeospirillum_	1.0	0.33
Terrimonas_ferruginea	1.0	0.33
Azospirillum_	1.0	0.33
Pseudomonas_umsongensis	1.0	0.33
Singulisphaera_rosea	1.0	0.33
Rubrobacter_	1.0	0.33
Paenibacillus_	1.0	0.33
Ammoniphilus_oxalaticus	1.0	0.33
Hydrogenophaga_palleronii	1.0	0.33
Schlegelella_	1.0	0.33
Amorphomonas_oryzae	1.0	0.33
Modestobacter_	1.0	0.33
Stenotrophomonas_maltophilia	1.0	0.33

Novosphingobium_stygium	1.0	0.33
Craurococcus_roseus	1.0	0.33
Pedomicrobium_	1.0	0.33
Blastococcus_aggregatus	1.0	0.33
Pseudomonas_carboxydohydrogena	1.0	0.33
Streptococcus_alactolyticus	1.0	0.33
Bacillus_badius	1.0	0.33
Parasegitibacter_luojiensis	1.0	0.33
Leptothrix_	1.0	0.33
Limnohabitans_curvus	1.0	0.33
Stenotrophomonas_	1.0	0.33
Sphingosinicella_microcystinivorans	1.0	0.33
Caulobacter_	1.0	0.33
Cellulomonas_	1.0	0.33
Imtechella_halotolerans	1.0	0.33
Flavobacterium_gelidilacus	1.0	0.33
Acidovorax_konjaci	1.0	0.33
Agitococcus_lubricus	1.0	0.33

Top Species Classification

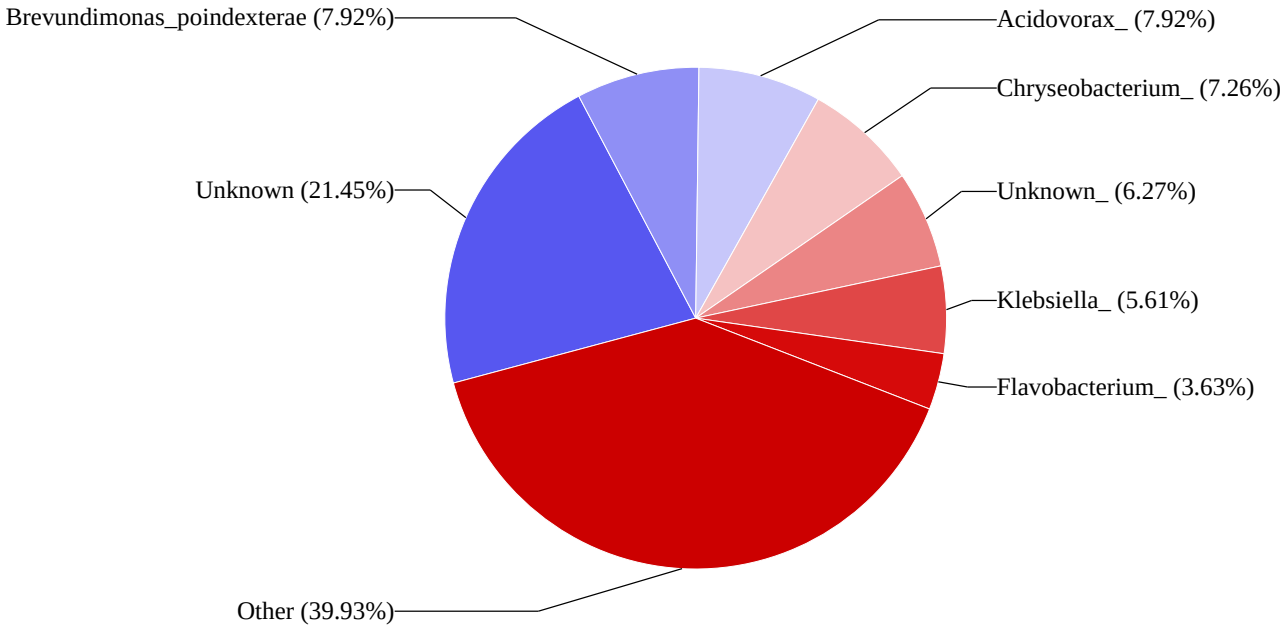

---------- End of report ----------